Department of Environment, Land, and Infrastructure Engineering

Master of Science in Environmental and Land Engineering

Master's degree thesis

EVALUATION OF SEISMIC BEHAVIOR OF A CIRCULAR TUNNEL IN HETEROGENEOUS SOIL BY USING DIFFERENT APPROACHES

Supervisor: Prof. Sebastiano Foti

Co-supervisor: Eng. Michele Palomba

Candidate: Mert Maral (S314039)

March 2024

Acknowledgments

I would like to express my deep gratitude to the numerous individuals and institutions who have played an invaluable role in the completion of this thesis. This endeavor would not have been possible without their unwavering support, guidance, and contributions.

I want to express my profound gratitude to Professor Sebastiano Foti, my academic mentor. His availability, unwavering support, and profound expertise have guided me through this research endeavor. His valuable counsel has been instrumental in ensuring the successful conclusion of this work.

I want to extend my appreciation to my co-advisors, Eng. Michele Palomba, and my colleagues, Dr. Reza Osgoui and Eng. Osman Murat Sarsilmaz. The meaningful contributions, constructive feedback, and collaborative efforts from each of you have greatly enhanced the quality of this research. Your expertise and dedicated contributions have played a vital role in shaping this academic pursuit.

Also, I would like to express immense appreciation to all my colleagues in the SYSTRA SWS and SYSTRA SWS Türkiye. They shared knowledge as well as provided a helping hand. Studying for this master's thesis would be far more difficult without their assistance.

My heartfelt thanks go out to my family, and, to my mom, for their unwavering emotional support during these two years. Her encouragement and understanding have been my pillars of strength throughout this challenging journey.

In conclusion, I extend my gratitude to all those who have been part of this academic journey. Your contributions and support have been vital to the attainment of my master's degree.

Abstract

From the past to today, Underground structures constitute a crucial element of modern life, serving diverse purposes such as transportation, storing materials, and managing sewage and water transportation. The most widely used type of these underground structures are tunnels used for transportation in subways, railways, and highways.

Unlike different fields in the construction sector, the tunnel industry has followed the age of mechanization. Tunnel Boring Machines (TBM) machines are used for faster and safer excavation. These machines enable tunnels to be excavated in a circular and pre-casted tunnel permanent lining is installed during excavation. The segmental lining must withstand both seismic and static loadings in the active seismic zone to give serviceability to the post-earthquake. The assessment of seismic performance in underground structures is currently a highly relevant research area within geotechnical earthquake and structural engineering.

This thesis explains and compares several approaches used by design engineers in quantifying the seismic effect on the tunnel with a real case study in heterogeneous formation. While analytical solution or free-field simplified analysis is generally used in homogeneous soil formation and the preliminary design phase, seismic response analysis or dynamic analysis is used in the soil heterogeneity and detail design phase.

The thesis is structured into five chapters, the first two of which are introductory and descriptive, in which the approaches used, based on existing literature, are explained, while the other chapters present the studies about the selected case project.

In the first chapter, which has an introductory purpose, the reasons why it was considered interesting to develop a thesis on this topic are explained, found in the literature, that shows earthquake damage in underground works.

The second chapter aims to describe the different procedures and methodologies used to date for the seismic design of tunnels, going on to highlight what are the substantial particularities between the different types of analysis. In particular, it focused on the differences between simplified analyses, sometimes even analytical, and somewhat more complex analyses, carried out through numerical modeling software.

In the third chapter, the general project properties are described, site investigations and laboratory test results are listed, and the critical analysis section is determined. The critical section's hydrogeological, geological, and geotechnical parameters are presented.

In the fourth chapter, seismic hazard analyses and site response analyses are carried out for the project location. Determined ground motion parameters and selected earthquake records are presented.

The final section presents and compares the results obtained using the methods described in the second section. The applicability of the simplified method in complex geological and geotechnical environments has been evaluated and it has been stated that it may lead to overdesign. A proportional relationship was established between the methods under the conditions of the case study.

Abstract

Dal passato a oggi, le strutture sotterranee costituiscono un elemento cruciale della vita moderna e servono a diversi scopi, come il trasporto, lo stoccaggio di materiali, la gestione delle acque reflue e del trasporto idrico. Il tipo più diffuso di queste strutture sotterranee sono le gallerie, utilizzate per il trasporto in metropolitane, ferrovie e autostrade.

A differenza di altre opere civili, l'industria delle gallerie ha seguito un processo di progressiva automatizzazione. Le macchine TBM (Tunnel Boring Machines) sono utilizzate per uno scavo più rapido e sicuro. Queste macchine consentono di scavare gallerie con sagoma circolare e di installare un rivestimento permanente prefabbricato durante lo scavo. Il rivestimento con conci deve resistere sia ai carichi sismici che carichi statici per garantire la funzionalità dell'opera anche dopo il terremoto. La valutazione delle prestazioni sismiche delle opere sotterranee è attualmente un'area di ricerca molto rilevante nell'ambito dell'ingegneria geotecnica sismica e strutturale.

Questa tesi illustra e confronta diversi approcci utilizzati in fase di progettazione per quantificare l'effetto sismico in una galleria in formazione eterogenea con un caso di studio reale. Mentre la soluzione analitica o l'analisi semplificata in campo libero sono generalmente utilizzate nella formazione omogenea del terreno e nella fase di progettazione preliminare, l'analisi della risposta sismica o l'analisi dinamica sono utilizzate nella caso di terreni eterogeni e in fasi di progettazione più avanzate.

La tesi è strutturata in cinque capitoli, di cui i primi due sono introduttivi e descrittivi, in cui vengono illustrati gli approcci utilizzati, basati sulla letteratura esistente, mentre gli altri capitoli presentano lo studio del caso progettuale selezionato.

Nel primo capitolo, che ha uno scopo introduttivo, vengono spiegate le ragioni per cui si è ritenuto interessante sviluppare una tesi su questo argomento, reperite nella letteratura che riporta i danni da terremoto nelle opere in sotterraneo.

Il secondo capitolo si propone di descrivere le diverse procedure e metodologie finora utilizzate per la progettazione sismica delle gallerie, andando a evidenziare quali siano le sostanziali particolarità tra i diversi tipi di analisi. In particolare, ci si è soffermati sulle differenze tra analisi semplificate, talvolta anche analitiche, e analisi più complesse, realizzate attraverso software di modellazione numerica.

Nel terzo capitolo si descrivono le caratteristiche generali del progetto, si elencano le indagini in sito e i risultati delle prove di laboratorio e si determina la sezione critica di analisi. Vengono presentati i parametri idrogeologici, geologici e geotecnici del modello.

Nel quarto capitolo vengono effettuate le analisi di pericolosità sismica e di risposta in sito del progetto. Vengono presentati i parametri di moto del suolo e i campioni sismici selezionati.

L'ultima sezione presenta e confronta i risultati ottenuti con i metodi descritti nei capitoli introduttivi. È stata valutata l'applicabilità del metodo semplificato in ambienti geologici e geotecnici complessi ed è stato affermato sì è evidenziato che può portare a ad una sovra dimensionato. È stata stabilita una relazione proporzionale tra lo stato di sollecitazione calcolato con i diversi metodi nel caso di studio.

List of symbols and abbreviations

a	Acceleration
a_g	Ground Acceleration
A	area
All	Alluvial soil
Agm-Agml	Sandy silty clays
L1669	Lava 1669
c'	Cohesion
cu	Undrained cohesion
C	Compressibility ratio
$[C]$	Damping matrix
Cc	Soil factor controls the shape of the spectra by enlarging the plateau at higher periods concerning rock conditions
CU	Class of use of a building according to the Italian Technical Code
d	Tunnel diameter
D_s, $D_s(\gamma)$	Soil damping ratio at the current shear strain, operative soil damping ratio
$D_{s,0}$	Soil damping ratio of soil at small strains, initial soil damping ratio
D_l	Tunnel lining damping ratio
EPB	Earth pressure balance
E_s	Soil Young modulus
$E_{s,0}$	Soil Young modulus at small strains
E_l	Tunnel lining Young modulus
f	frequency
f_{max}	Maximum frequency of the system
F	Flexibility ratio
F_0	Seismic parameter for the evaluation of the response spectrum, according to the Italian Technical Code (NTC 2018)
FEM	Finite Element Method
G_s, $G_s(\gamma)$	Soil shear modulus at the current shear strain, operative soil shear modulus
G_0	Soil shear modulus at small strains, initial soil shear modulus
h	Mesh element size
H	Soil deposit height
HVSR	Horizontal-to-Vertical Spectral Ratio
I	Impedance ratio
Il	Tunnel lining moment of inertia
k	Permeability
$[K]$	Stiffness matrix
$[M]$	Mass matrix
M	Dynamic bending moment
M_{ANAL}	Analytical dynamic bending moment
M_{MAX}	Maximum dynamic bending moment
M_{NUM}	Numerical dynamic bending moment
M_w	Moment magnitude
N	Dynamic axial force
N_{ANAL}	Analytical dynamic axial force
N_{MAX}	Maximum dynamic axial force
N_{NUM}	Numerical dynamic axial force
PGA	Peak ground acceleration

P_{VR}	Probability of exceeding for the evaluation of the seismic action, according to the Italian Technical Code
r	The radius of the tunnel lining
Sbl	Volcanic sand
SLO	Operating Limit State according to the Italian Technical Code (NTC 2018)
SLD	Damage Limit State according to the Italian Technical Code (NTC 2018)
SLV	Life-safety Limit State according to the Italian Technical Code (NTC 2018)
SLC	Collapse Prevention Limit State according to the Italian Technical Code (NTC 2018)
TBM	Tunnel boring machine
TR	Return period
T^*c	Seismic parameter for the evaluation of the response spectrum, according to the Italian Technical Code (NTC 2018)
VN	Nominal duration of a building
Vs	Soil shear waves velocity at the current shear strain, operative soil shear waves velocity Average Shear waves velocity
$Vs, z = 0$	Soil shear waves velocity at the soil surface (z = 0)
Vs,av	Average Shear waves velocity
y	Horizontal direction
z	Vertical depth
αr	First Rayleigh damping factor
βr	Second Rayleigh damping factor
γs	Soil unit weight
γ	shear strain
γmax	Soil maximum shear strain
ΔM	Percentage difference between MNUM-MAX and the MANAL MAX
ΔN	Percentage difference between NNUM-MAX and the NANAL MAX
Δz	Thickness of the soil cover above the tunnel, name
θ	centre angle of the tunnel
θr	centre angle of the tunnel crossing the soil discontinuity on the right of the tunnel
θl	centre angle of the tunnel crossing the soil discontinuity on the left of the tunnel
μ	friction coefficient
vs	Soil Poisson's ratio
vl	Tunnel Lining Poisson's ratio
ρ	soil density
φ	Shear strength angle
ω	Angular frequency

Table of Contents

Acknowledgments 2
Abstract 3
Abstract 5
List of symbols and abbreviations 7
Table of Contents 9
List of Figures 11
List of Tables 13
Chapter1 14
1 Introduction 14
5.1 Problem Statement 16
5.2 Objectives of the Thesis 17
5.3 Litterateur Review 17
5.4 Structure of Thesis 19
Chapter 2 20
2 Tunnel Seismic Analysis and Design Methodologies 20
2.1 Static and Seismic Site Characterization 21
2.2 Definition of the Site Soil Class 27
2.3 Numerical Modelling of The Excavation Tunnel - Static Model 28
2.4 Definition of the seismic environment 30
2.5 Definition of the Ground Response and Shaking 35
2.6 Seismic Design Approaches 50
Chapter3 58
3 Case Study: Metropolitana di Catania Lotto 1 58
3.1 Project Definition 58
3.2 Site Characterization and Critic Section 60
Chapter4 72
4 Seismic Hazard Assessment and Site Response Analysis 72
4.1 Seismic Hazard Assessment 72
4.2 Free Field Shear Deformation at the Critical Section 90
4.3 Simplified Method at the Analysis Section 90

4.4 Seismic Site Response Analysis (SSR).....92
Chapter 5.....101
5 Analysis, Results and Discussion.....101
5.1 Static and Seismic Analysis.....101
5.2 Results and Discussion.....124
Chapter 6.....126
6 Conclusions.....126
Bibliography.....129

List of Figures

Figure 1-1 A schematic representation of surface structures and different types of subsurface structures in urban areas.(Rashiddel et al., 2024) 14
Figure 2-1 Underground Structure Seismic Analysis and Design Procedure (Hashash et al., 2001) 20
Figure 2-2 Frequency response obtained from a resonant column test (Cosentini, 2 C.E.) 23
Figure 2-3 Stress-strain curve obtained from a cyclic torsional shear test (Cosentini, 2 C.E.) 23
Figure 2-4 Typical configuration used in down-hole seismic testing and Site Application 25
Figure 2-5 Reading H/V graphs in the amplitude-frequency and amplitude-depth domains. (from case site investigation 27
Figure 2-6 Intial Lithostatic Stress Field – Plaxis 2D Model 29
Figure 2-7 Real (a) and Simplified geometry of the segmental lining (Fabozzi & Bilotta, 2016) 30
Figure 2-8 Seismic Impacts on the tunnel depends on the condition.(Do et al., 2014) 35
Figure 2-9 Ground Shaking and Deformation (Tsinidis et al., 2020) 36
Figure 2-10 Non-linear model diagram 42
Figure 2-11 Schematic Soil Profile Definition 45
Figure 2-12 Schematic Soil Layer Definition(Cosentini, 2 C.E.) 45
Figure 2-13 Definition of the Bedrock (Cosentini, 2 C.E.) 46
Figure 2-14 Seismic Input 46
Figure 2-15 DeepSoil Output 47
Figure 2-16 Design Approaches 50
Figure 2-17 Simplified Numerical Model 54
Figure 2-18 *Simplified Plaxis Model and Output* 54
Figure 2-19 *Uncoupled Approach Plaxis Model and Output* 55
Figure 2-20 Time history acceleration 56
Figure 2-21 Plaxis 2D Numerical Model 56
Figure 2-22 Plaxis 2D Input 57
Figure 3-1 Spatial localization of the Stesicoro-Aeroporto route (section in light blue) 58
Figure 3-2 Schematic diagram of the shield tunnelling machine 59
Figure 3-3: Schematic Soil Profile 61
Figure 3-4 Borehole Si17 - Sampling 64
Figure 3-5 Down-Hole Test Result 65
Figure 3-6 HSRV Test Results 65
Figure 3-7 Seismic input for the scenario earthquake in Catania: a transects; b graphs related to the first point(P1) of transect t01: Vs profile, position of the receivers, accelerograms (in the radial, transverse and vertical components), spectral ratios ((Abate & Massimino, 2017) 66
Figure 3-8 Vs-Depth Graph 67
Figure 3-9 Critical Section and Test Point 5 and 6 69
Figure 3-10 Decay curves of modulus and damping factor 71
Figure 4-1 Schematic Map of Central Mediterranean Tectonics (Catalan et al., 2008) 73
Figure 4-2 : Database “Individual Seismogenic Sources” (FONTE INGV - DISS 3.3.0) 75
Figure 4-3Figure 4-4 : Excerpt of capable faults of the western portion of eastern sicily- ithaca working group (a database of active capable faults of the Italian territory. version december 2019) 75
Figure 4-5 Faults Kinematics a) San Caogero and b) Scapata di Malta_01 76
Figure 4-6 Epicentres of major earthquakes in the period 1125-1990 that caused damage or were felt in Catania (from Carbone et alii, 2010) 76
Figure 4-7 Fonte Database Macrosismico Italiano DBMI15 (https://emidius.mi.ingv.it)) 78
Figure 4-8 Catalog of strong earthquakes in Italy from 461 BC to 1997 - Source CFTI med from INGV 78
Figure 4-9Seismic Hazard Model INGV 79
Figure 4-10 Seismicity map for the city of Catania - Seismic hazard model MPS04-S1 (Source Web Application Developed by F. Martinelli & C. Meletti, INGV) 80
Figure 4-11 Acceleration values for annual frequency of exceedance - Graphic Elaboration form UNGV 80
Figure 4-12 4-13 Seismic hazard estimation for a 2% exceedance probability in 50 years: ag values. DPC-INGV Project S1, Deliverable D2, http://esse1.mi.ingv.it/d2.html (Meletti C., Montaldo V., 2007) 81

Figure 4-14 Disaggregation of PGA with probability of exceedance of 10% in 50 years 82
Figure 4-15 Identification of the site hazard (based on the results of the S1 - INGV project);.... 84
Figure 4-16 Choice of design strategy,..... 85
Figure 4-17 Determination of the design action 86
Figure 4-18 Design Target Spectrum 87
Figure 4-19 Step1: Refine Search Screen..... 87
Figure 4-20 Step2: Design Target Spectrum Definition..... 88
Figure 4-21 Step3: Preliminary Search..... 88
Figure 4-22 7 Accelerograms and Design Target Spectrum..... 89
Figure 4-23 Average of 7 accelerograms and Design Target Spectrum..... 89
Figure 4-24 Analysis Settings..... 92
Figure 4-25 Rp – Topsoil (Riporto)..... 93
Figure 4-26 L1669 – Lave 93
Figure 4-27 Sbl – Silty Sand..... 94
Figure 4-28: Agm- Clays..... 94
Figure 4-29 Bedrock Parameters 95
Figure 4-30 Ground Motion Definition 95
Figure 4-31 Analysis Control Definition..... 96
Figure 4-32 Output from Deepsoil 96
Figure 4-33 Depth vs PGA 97
Figure 4-34 Depth vs Shear Strain..... 97
Figure 4-35 Horizontal Displacement vs Depth 97
Figure 4-36 $G_{(\Upsilon)}/G_o$ vs Depth 98
Figure 4-37 Schematic Representation of the Cases and Their Vs Profiles 99
Figure 4-38 Comparison Horizontal Displacement and $G_{(\Upsilon)}/G_0$ in Cases 99
Figure 4-39 4.2 Comparison Free Field Shear Deformation – Each Methods and Cases.... 100
Figure 5-1 Plaxis 2D FE numerical static excavation model..... 102
Figure 5-2 Static internal forces in the tunnel lining. 103
Figure 5-3 Seismic Bending Moment in the tunnel lining – Wang , 1993 – Analytical Approach 104
Figure 5-4 Seismic Axial forces in the tunnel lining – Wang , 1993 – Analytical Approach 105
Figure 5-5 Figure 5-6 Seismic bending moment in the tunnel lining – Penzien, 1993- – Analytical Approach..... 105
Figure 5-7 Seismic axial forces in the tunnel lining – Penzien, 1993- – Analytical Approach.. 105
Figure 5-8 Seismic shear forces in the tunnel lining – Penzien, 1993- – Analytical Approach . 106
Figure 5-9 Mesh and boundary conditions of the FEM model – Simplified Approach 106
Figure 5-10 Envelope Bending Moment – Non-Slip Condition – Simplified Approach 107
Figure 5-11 Envelope Bending Axial Force – Non-Slip Condition – Simplified Approach..... 107
Figure 5-12 Envelope Shear Force – Non-Slip Condition – Simplified Approach 107
Figure 5-13 Envelope Bending Moment – Full-Slip Condition – Simplified Approach..... 108
Figure 5-14 Envelope Axial Force – Full-Slip Condition – Simplified Approach..... 108
Figure 5-15 Envelope Shear Force – Full-Slip Condition – Simplified Approach..... 108
Figure 5-16 Comparison the action at the Full Slip and Non-Slip Condition a)Bending Moment kN.m/m , b) Axial Force kN/m and c)Shear Force kN/m..... 109
Figure 5-17 Mesh and boundary conditions of the FEM model – Uncoupled Approach..... 110
Figure 5-18 Envelope Bending Moment – Non -Slip Condition – Uncoupled Approach..... 110
Figure 5-19 Envelope Axial Forces – Non-Slip Condition – Uncoupled Approach 111
Figure 5-20 Envelope Shear Forces – Non-Slip Condition – Uncoupled Approach..... 111
Figure 5-21 Envelope Bending Moment – Full -Slip Condition – Uncoupled Approach..... 111
Figure 5-22 Envelope Axial Force – Full -Slip Condition – Uncoupled Approach 112
Figure 5-23 Envelope Shear Force – Full -Slip Condition – Uncoupled Approach..... 112
Figure 5-24 Comparison the action at the Full Slip and Non-Slip Condition a)Bending Moment kN.m/m , b) Axial Force kN/m and c)Shear Force kN/m..... 113
Figure 5-25 Mesh and boundary conditions of the FEM model of the Each Cases – Uncoupled Approach 114
Figure 5-26 Envelope Bending Momen kNm/m – Full-Slip Condition 114
Figure 5-27 Envelope Axial Force kN /m – Full-Slip Condition 114
Figure 5-28 Envelope Bending Momen kNm/m – Non-Slip Condition..... 115
Figure 5-29 Envelope Axial Force kN /m – Non -Slip Condition..... 115

Figure 5-30 Mesh and boundary conditions of the numerical model for full-dynamic analysis of the tunnel 116
Figure 5-31 Bedrock Geotechnical Parameter – Linear Elastic 116
Figure 5-32 L1669 – Lava geotechnical Parameters – Mohr Coulomb..... 117
Figure 5-33 Sbl – Volcanic Sand Geotechnical Parameters – HS Small Strain 117
Figure 5-34 Agm – Sandy Silty Clay – HS Small Strain..... 118
Figure 5-35 Bending Moment kNm/m of the Earthquakes – Coupled Approach 120
Figure 5-36 Normal Force kN/m of the Earthquakes – Coupled Approach 120
Figure 5-37 Shear Force kN/m of the Earthquakes – Coupled Approach 121
Figure 5-38 – Bending Moment kNm/m – Coupled Approach 121
Figure 5-39 Axial Force kN/m – Coupled Approach 122
Figure 5-40 Shear Force kN/m – Coupled Approach 122
Figure 5-41 Mesh and boundary conditions of the FEM model of the Each Cases – Coupled Approach 123
Figure 5-42 Bending Momens kNm/m – Non-Slip Condition – Coupled Approach 123
Figure 5-43 Axial Force kNm/m – Non-Slip Condition – Coupled Approach..... 124

List of Tables

Table 2-1 Soil Categories, TAB. 3.2.II NTC 18..... 28
Table 2-2 Nominal design life values (NTC2018) 31
Table 2-3 Values of the serviceability coefficient Cu (NTC2018)..... 32
Table 2-4 Exceedance Probability (NTC2018) 32
Table 2-5 Expressions of S_S - TAB. 3.2.IV NTC 18 33
Table 2-6 TOPOGRAPHIC CATEGORIES - TAB. 3.2.III NTC 18..... 33
Table 2-7 Maximum values of the topographic amplification coefficient S_T..... 33
Table 2-8 Ratios of peak ground velocity to peak ground acceleration at surface 38
Table 2-9 Ground Motion Attenuation with Depth (Hung et al., 2009) 38
Table 2-10 Damping ratios and average reduction factors (± one standard deviation) of the normalized shear modulus G/G0 within 20 m depth (Eurocode8, 2022) 40
Table 3-1 Summary table of subsurface categories for each survey in Seismic Tomographs..... 60
Table 3-2 Summary table of subsurface categories for each survey in Down-Hole Test..... 60
Table 3-3 Geologic Profile and Critic Section 61
Table 3-4-Formation, Thickness and $V_{s,design}$ values 67
Table 3-5 Test site location (Cavallaro et al., n.d.)..... 68
Table 3-6 Test Site – Sample Formation 68
Table 3-7 Soil constant values for evaluation of$G(\gamma)$ and $\xi(\gamma)$: sites No. 1, 2 and 12clayey soil in the Catania plain; site No.3 silica sandy soil; sites No. 5 and 11clayey soil in the central area; site No. 6volcanic sand; sites No. 7 and No. 9scoriaceous lava; site No. 8 clayey soilin the central area. 70
Table 3-8 Geotechnical Parameters at the pk 3+700 71
Table 4-1 Acceleration values for annual frequency of exceedance 80
Table 4-2 Selected Natural 7 Accelerograms 88
Table 4-3 Layer Thickness in Deepsoil 92
Table 5-1 Tunnel Lining Characteristic..... 101
Table 5-2 Resutl of the Analytical Solution Wang,1993 and Penzien,2000 104
Table 5-3 Input motions, scale, and Duration..... 118
Table 5-4 Rayleigh Damping Coefficient in Plaxis 2D..... 119
Table 5-5 Internal Forces in Tunnel Lining due to Seismic Action Summary Table..... 124

Chapter1

1 Introduction

In modern world, the usage areas of underground structures are rapidly increasing due to various needs. Especially in developing metropolises, the importance of underground structures has been better understood. As a result, underground structures have become an important part of infrastructure in an increasingly urbanized world. In general, underground structures include subways, underground roads, material depots, shopping centers, parking lots, clean wastewater facilities and data centers. (Figure 1-1) In addition, nuclear power plants are built underground for safety reasons. Among the underground structures, underground subway structures are undoubtedly the most prominent. The provision of transportation by subways has emerged as an inevitable result for big cities.

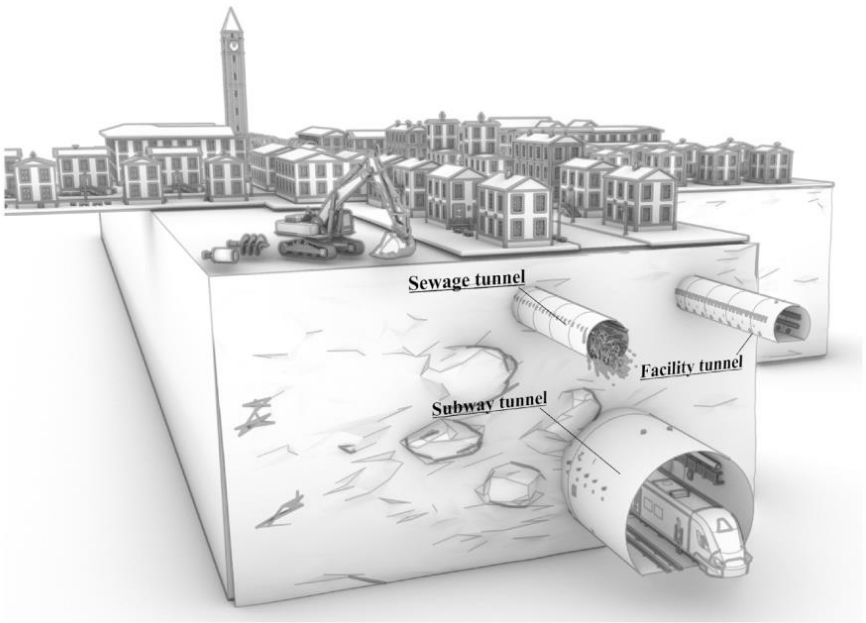

Figure 1-1 A schematic representation of surface structures and different types of subsurface structures in urban areas.(Rashiddel et al., 2024)

Throughout the history of tunneling, various methods have been explored; however, mechanized tunneling systems have emerged as the industry's forefront due to their advantages and high-performance rates. The Tunnel Boring Machine (TBM) has significantly contributed to tunnel construction, playing an essential role in mechanized tunneling. TBM's adaptability to different tunnel diameters, effectiveness in diverse geological environments, safety, speed, continuous tunneling capabilities, and notably, its minimal workforce requirements, distinguish it as a unique and pivotal technology in the

field.

Precast concrete segments (Segmental Lining) replaced steel or cast-iron segments as the main structural element for lining tunnels excavated by Tunnel Boring Machines (TBMs) in soft ground from 1960s to now. The segmental lining exceptional seismic performance due to their circular and predominantly symmetrical shape. Additionally, their jointed structure provides significant flexibility, contributing to their resilience during earthquakes (Dean et al., 2006).

The response of tunnels to seismic forces is intricate, and until approximately two decades ago, it was not typically regarded as a primary design concern. Only in recent times has both experimental and numerical research taken substantial strides in understanding the mechanisms that dictate soil-structure interaction for such structures during seismic events (Fabozzi et al., 2017).

The tunnel behavior under the seismic actions is complex and it doesn't consider as a main design issue. But recent experimental and numerical research have made some significant steps towards the comprehension of the mechanisms governing soil-structure interaction. Also, this consideration has been changed after some of them suffered serious damages caused by recent earthquakes, including the 1995 Kobe (Japan), the 1999 Chi-Chi (Taiwan) and the 1999 Kocaeli (Turkey) earthquakes (Hashash et al., 2001). The Pazarcik eartquakes (Mw:7.7). The earthquake of magnitude 7.7 in Pazarcik (Turkey) in 2023 caused cracks in the segments of railway tunnels under construction and caused some existing tunnels to give way.(Gokceoglu, 2023)

Precise seismic design holds significant importance, particularly in regions known for high seismic intensity such as Turkey, Italy, Japan, the United States, and Greece. Achieving accurate seismic design necessitates a profound understanding of the behavior of tunnel structures and soil under seismic loads. However, variations in seismic response tied to surface constructions and the intricate soil-structure interaction phenomena introduce uncertainty in assessing their seismic performance (Eng. Marco Zucca, n.d.). In recent years, regulatory authorities in different countries, including the publication of new national codes like NTC2018 in Italy and TBDY 2018 in Turkey, have responded by issuing regulations specifically addressing structures embedded underground in the face of seismic activity or earthquake-induced ground failures.

In this thesis, the behavior of a circular tunnel under seismic events will be evaluated by using simplified methods and precise methods which recommended by the new specifications. Then, a correlation between these methods will be tried to be established.

5.1 Problem Statement

Tunnels are multi-disciplinary projects requiring the collaboration of specialists in many different fields. In the seismic design of tunnels, geotechnical earthquake design engineers and tunnel design engineers should work together from the field investigation phase of the project to the detailed design phase. Current national specifications require site-specific analyses to be carried out, especially weak ground conditions and in active seismic zones. However, these specifications are not specifically for embedded structures and contain some deficiencies. Tunnel design engineers in design firms generally use analytical or simplified numerical methods in seismic analyses and perform their designs with the highest earthquake accelerations of the project location. In addition, this method assumes that the tunnel is in a homogeneous soil environment and analyses are performed only according to the formation in which the tunnel is located. It may not reflect the correct results for a tunnel in a heterogeneous soil environment. The use of these methods is due to the lack of sufficient field data or the lack of competence of the tunnel design engineer. Specific analyses have not yet been adopted by engineers.

5.2 Objectives of the Thesis

The effects induced by a seismic event in the lining of a tunnel can in fact be predicted using various methodologies, at an increasing level of complexity, either by calculating the load increments from the seismic response of the subsurface under examination in free-field conditions, or based on the solution of a soil-structure interaction problem in dynamic conditions. The aim of this paper is therefore to illustrate the different procedures and compare the results, varying both the type of 2D numerical analysis, but also the characteristics of the site under examination (presence or absence of a stratigraphic transition).

Within the scope of this thesis, in-depth bibliographic research was therefore conducted, to analyze the different causes and types of damage and to improve the approach to the seismic design of such works, highlighting procedures for analyzing and solving the problems present in this area.

These methodologies were applied to the case study considered, represented by a natural railway tunnel in the Metropolitan Catania, to which various analytical and numerical analyses were carried out using Plaxis 2D software.

5.3 Litterateur Review

Numerous sources have been thoroughly reviewed throughout the thesis. The primary literature reviews for tunnel seismic design are(Owen, 1981) Earthquake engineering of large underground structure and Wang, 1993, Seismic Design of -Tunnels a Simple State of the Art Design Approach, and Penzien, 2000, Stress in Linings of Bored Tunnels.

Wang and Penzien is used for analytical solution and hand calculation to validate numerical models. After that Hashash et al., 2001, Seismic Design and Analysis of Underground Sturcutres, which is the most known and is suggested paper by International Tunnelling Association as guide for tunnel design, is reviewed to construct structure of the thesis In addition to this article , Hung, 2009, FHWA Technical Manual for Design and Construction Manual of Road Tunnel Civil Elements is examined to find some lack knowledge about shallow tunnel seismic design.

After that it is focused on research, which is carried out in Italain territory, Firstly.

Fabozzi & Bilotta, 2016, Behaviour of the Segmental Lining under Seismic Action was reviewed to understand segmental lining vulnerability, Italian codes adn Italian seismicity. Then, (Bilotta et al., 2007, Pseudo static and Dynamic analyses of Tunnels in Transversal and Longitudinal Directions) article is used as guidelines to carry out numerical analysis for applying uncoupled and coupled approaches.

A similar study, study Abate et al., 2023, Effect of soil heterogeneity on seismic tunnel lining forces, on the effect of soil heterogeneity on the tunnel in the region where the case study was carried out, was examined, and used to check the work carried out in this thesis.

Then, for finite element analysis, International Association for the Engineering Modelling, Analysis, and Simulation Community: NAFEMS, Plaxis Manuals, and for site response analysis DeepSoil Manuals were used as references. Several papers were relied on, mainly those accepted and published by the World Tunnelling Congress and ISRM international Society for Rock Mechanics and Rock Engineering and, in addition to textbooks and national and international standards.

.

5.4 Structure of Thesis

The current thesis is designed to provide a logical sequence for reviewing issues and developing solutions. The first chapter encompasses a brief introduction to tunnel seismic design, the importance of considered research topic.

Chapter 2 described the tunnel seismic analysis and design procedures, then explain different approaches.

Chapter 3 covers the project details include ground investigation activities, chosen critical section, and chosen parameters.

Chapter 4 present both seismic hazard analysis, ground motion selection ,free field shear deformation and site response analysis processes

Chapter 5 present the obtained results comes from different approach, and to present impact of the lava sub-layer effect, finally evaluate result to define precise approach.

Chapter 2

2 Tunnel Seismic Analysis and Design Methodologies

The design process of the tunnel in seismic active zone concludes 6 phases:

1. Static and seismic site characterization
2. Definition of the Site Soil Class
3. Numerical Modelling of The Excavation Tunnel - Static Model
4. Definition of the seismic environment
5. Evaluation of the Ground Response to Shaking and to Ground Deformation
6. Seismic Design Approaches

The response of the tunnel to a seismic action depends on variables such as the shape, size and depth of the structure. the characteristics of the soil and/or rock mass, the intensity of the seismic event (parameters such as maximum acceleration, magnitude, epicentral distance and duration are important) and the mechanical characteristics of the structure and its lining.(Dowding & Rozan, 1978)

Schema which represents underground structure analysis and design procedure, in below is suggested for general overview all type underground structure by the (Hashash et al., 2001).

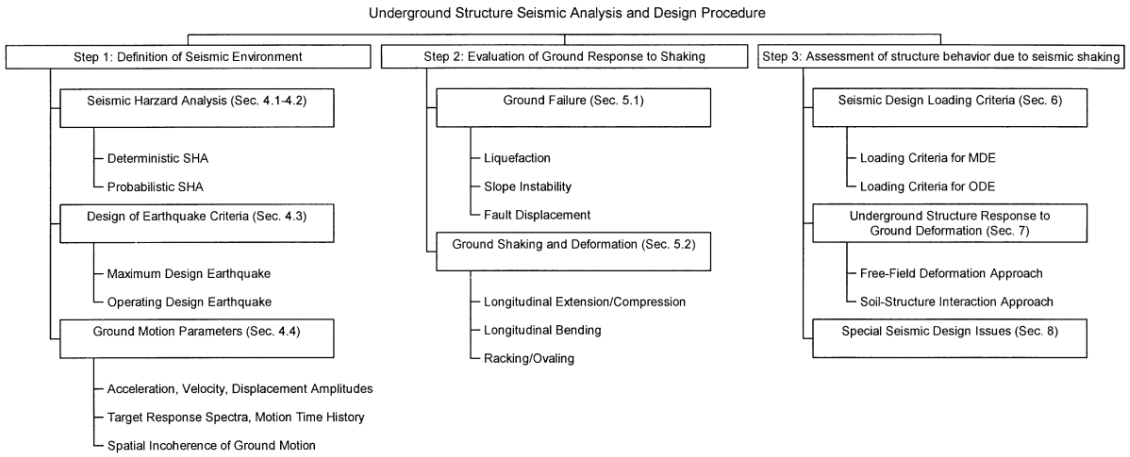

Figure 2-1 Underground Structure Seismic Analysis and Design Procedure (Hashash et al., 2001)

As explained previous chapters, this thesis focus on the seismic analysis of the circular tunnel in heterogeneous soil formation according to current national code (NTC, 2018) or EC8 by using a case study in south Italy. So, schema on above is tried to follow by considering these codes. There is some insertions or extraction on the phases. Specially seismic part is set out in all thesis.

2.1 Static and Seismic Site Characterization

Underground excavation involves the alteration of the pre-existing natural equilibria in the medium in which one is working. Precise design of the excavation requires as complete a prior knowledge as possible of the natural equilibria of the site. The investigation phase involves the acquisition, processing, and interpretation of the results of the investigations carried out in the medium. During the investigation phase it is necessary to pay attention to:

- Geological-tectonic complexity of the area;
- Length of the route;
- Extent of Overburden

First, it is necessary to carry out a geological characterization of the site by going to investigate geomorphological, hydrogeological and other aspects related to the characteristics of the soil or rock mass.

Once the geological investigation has been carried out, it is possible to move on to the geotechnical characterization of the site, so as to derive the mechanical parameters of the medium, and in particular:

- Structure of the material;
- Density (ρ);
- Strength parameters;
- Deformability parameters;
- Permeability (k);
- Shear wave propagation velocity (Vs).

Laboratory tests, in situ tests, and empirical correlations can be used to derive these parameters.

Geotechnical characterization represents a key element for the study of local seismic response and for the evaluation of the risk associated with earthquake-induced instability phenomena. It is therefore very important to be able to grasp all the aspects related to the construction of a geotechnical reference model for the study of ground response to earthquakes. This study is explicitly requested in recent national and international standards for the evaluation of the reference seismic action to be used for the design and verification of geotechnical and structural systems.

The local seismic response can be defined as the set of modifications of the seismic motion induced by the topographic and lithostratigraphic conformation of the site. In what follows,

reference will be made mainly to the phenomenon of stratigraphic amplification, linked to the mechanical properties of the soil deposits and therefore to the passage of waves through media of different stiffness.

Therefore, in order to assess the mechanical parameters of the soil, so as to have an adequate knowledge of its stiffness, it is appropriate to understand which in-situ and laboratory tests are commonly used, trying to mainly highlight potentialities and limitations, while the technical details relating to the execution and interpretation of the tests themselves will be omitted, referring these to the specially dedicated Guidelines (Foti et al., 2010).

2.1.1 Laboratory Tests

The experimental determination of decay curves is carried out in the laboratory using specific equipment for applying cyclic loads.

The most common tests are:

- the cyclic torsional shear test
- the resonant column test.

The two tests have in common how the external stress is applied and can often be performed using the same test equipment, appropriately configured.

The resonant column test is based on the application of the resonance concept to a cylindrical specimen subjected to torsional excitation. In the most common test mode, cyclic stresses of constant amplitude and variable frequency are applied at the upper base of a specimen embedded in the lower base. By monitoring the induced rotations, the resonance frequency is identified, as shown Figure 2-2, from which the shear modulus of the specimen can be traced via a mathematical inversion procedure. Furthermore, from the shape of the frequency response (half-power bandwidth method) or from the time decay of the free vibrations, the damping ratio can be traced.

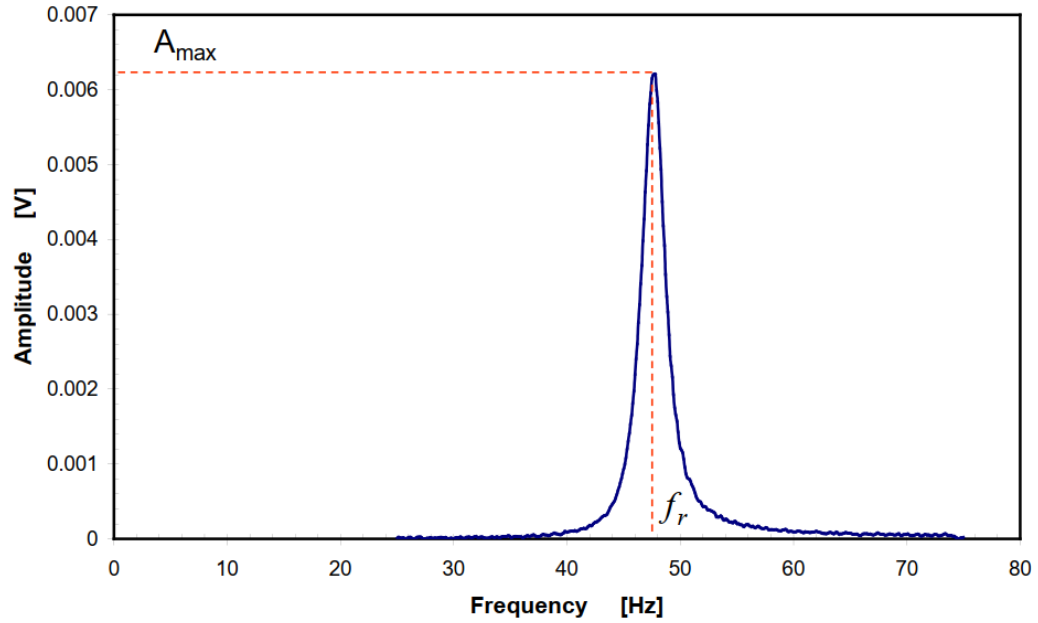

Figure 2-2 Frequency response obtained from a resonant column test (Cosentini, 2 C.E.)

In the cyclic torsional shear test, using a stress system similar to the resonant column test, the secant shear modulus and the damping ratio are determined directly from the cyclic stress-strain curve Figure 2-3. Again, by varying the maximum applied stress over the cycles, it is possible to evaluate the shear modulus and damping ratio for different deformation levels.

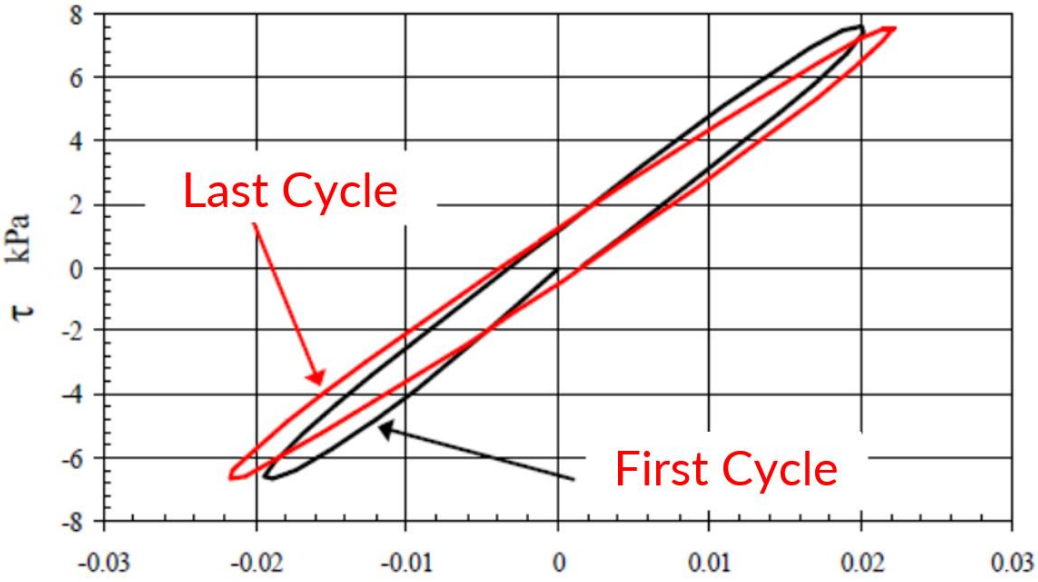

Figure 2-3 Stress-strain curve obtained from a cyclic torsional shear test (Cosentini, 2 C.E.)

The two types of tests therefore vary slightly in the way the load is applied and how the result is derived, but fundamentally the response is very similar. The main difference lies in the different speed at which the load is applied:

- the cyclic torsional shear test operates at low frequencies because it needs to describe well the deformation behavior of the material
- the resonant column test works instead on a frequency very close to the resonance of the sample.

This is a very important aspect because in earthquakes the frequency content varies between 5 and 10 Hz, thus showing an intermediate frequency range, which explains why it it is convenient to perform both tests.

2.1.2 Site Tests

On-site geophysical tests based on the propagation of seismic waves allow the estimation of elastic moduli at very small deformations (initial tangent moduli) since the sources used for the generation of the waves release modest amounts of energy, which at most can cause localized plasticization phenomena around the point of application. For this reason, the use of geophysical tests in the geotechnical-seismic characterization of construction sites is mainly aimed at determining the shear modulus G_0 and reconstructing the layering geometry of deposits(Lai et al., 2000) .

From the point of view of characterizing the mechanical properties of materials, geophysical tests aimed at determining the propagation velocity of shear waves are of particular importance, while those based on the propagation velocity of compression waves are of less relevance since, in light of the particulate and multi-phase nature of soils and the theory of seismic wave propagation in saturated porous media, it is strongly influenced by the compressibility of the interstitial fluid and therefore is not a valid indicator of the elastic properties of the solid skeleton.

The propagation velocity of shear waves V_S is related to the shear modulus at small deformations G_0 via the classical formula of wave propagation theory in a linear elastic medium.

$$G_0 = \rho * V_s^2 \quad (1)$$

being ρ the density of the material.

There are many site geophysical tests to obtain the propagation velocity of shear waves, But Down-Hole and HSRV test are explained as it is used in case study in below

2.1.2.1 DOWN HOLE

The seismic test DHT is a survey method aimed at determining the velocity profiles of shear wave (SH) and compression wave (P) seismic waves in soil deposits.

The velocity profiles obtained from DHT measurements represent average velocity values across the thickness of the layers since they are calculated along paths of inclined seismic rays. These paths have been subsequently corrected, assuming a mouth-to-source distance of 2 m, to be reported along a straight path along the vertical.

The important characteristic of this method is to study the state and behavior parameters by referring them to volumes of soil that are representative of the megastructural characteristics of deposits. This is achieved through measurements capable of providing average values, not just point values, of the geotechnical parameters of geomaterials.

The essential characteristic of the seismic method used is its capability to determine deformability parameters by referring to very low values of deformation levels (<10-5 m), below the threshold of cyclic linear deformation.

Figure 2-4 Typical configuration used in down-hole seismic testing and Site Application

For data interpretation, the method employed is called the "Interval" method, where the travel times of the seismic wave between two receivers at different depths are measured (interval velocity).

The parameters calculable with the assistance of the DHT method are:

- Dynamic Poisson's Ratio,
- Dynamic Young's Modulus (or longitudinal modulus of elasticity),
- Dynamic Shear Modulus (or modulus of rigidity),
- Bulk Modulus (incompressibility modulus), and consequently,
- Dynamic Compressibility Modulus.

The dynamic values calculated with these techniques can differ from values obtained from specific static tests (usually even by an order of magnitude), especially in materials like the ones under consideration.

Furthermore, the parameter V_{seq} can be obtained, which is calculated by the weighted average of the layer velocities up to the depth where Vs=800 m/s within 30 meters, applying the formula described. In case this depth is greater than 30 m, V_{seq} is equal to $Vs_{,30}$.

2.1.2.2 HVSR (Horizontal to Vertical Spectral Ratio)

The HVSR investigation is a non-invasive, single-station passive seismic survey technique aimed at determining certain characteristics of surface sedimentary deposits. Specifically, it focuses on studying the resonance frequencies of the ground, which is a crucial feature for assessing site effects in the presence of potential seismic events.

The HVSR test, also known as H/V (Nakamura method, 1989), involves measuring ambient microtremors in three spatial dimensions (x, y, z). Its processing allows for the analysis of frequency spectra, resulting in a graph of the amplitude ratio between horizontal components (H) and the vertical component (V).

From the extracted graph, the trend of the frequency ratio between horizontal and vertical components (H/V) at various frequencies is highlighted. It reveals the frequency at which ground motion is amplified due to resonance, known as the fundamental frequency.

The use of the HVSR test proves beneficial in the following disciplines:

- Identification of site resonance frequencies.
- Identification of resonance frequencies of a structure/building.
- Seismic micro zonation through the observation of frequency peaks.
- Estimation of equivalent shear wave velocity (VS eq) and determination of seismic category.
- Estimation of the depth of substrate discontinuities.

Particular attention should be given to non-invasive seismic geophysical tests, given their increasing use in local seismic response studies. These tests offer a favorable cost-benefit ratio, especially concerning the assessment of the average propagation velocity (VS,30), which is used in modern seismic regulations to classify deposits, as we will see in the following chapters. These seismic soil categories are then employed for a rough evaluation of site effects in cases where a specific detailed study of local seismic response is not conducted.

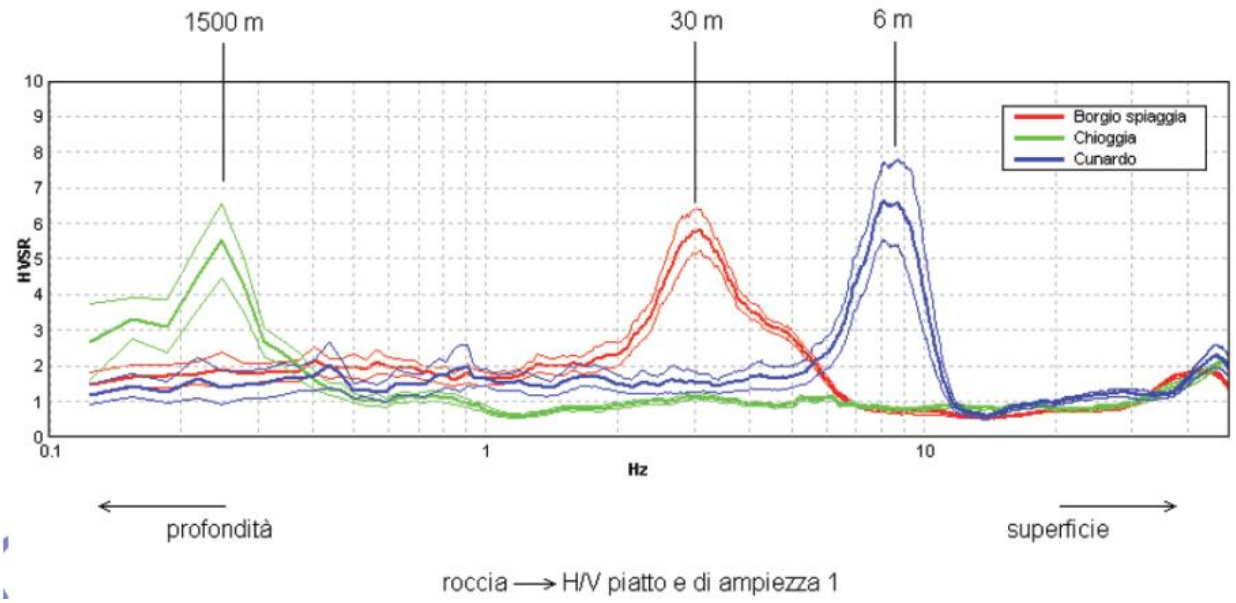

Figure 2-5 Reading H/V graphs in the amplitude-frequency and amplitude-depth domains. (from case site investigation

2.2 Definition of the Site Soil Class

For defining the seismic action for the project, the effect of local seismic response is assessed through specific analyses, to be carried out in the manner indicated in the (NTC, 2018) at paragraph 7.11.3. Alternatively, if the stratigraphic conditions and soil properties are clearly attributable to the categories defined in the in Table 3.2.II, a simplified approach based on the classification of the subsurface according to the values of shear wave propagation velocity, Vs, may be used.

The soil classification is carried out based on the stratigraphic conditions and the values of the equivalent shear wave propagation velocity, Vs,eq (in m/s), defined by the expression:

$$V_{S,eq} = \frac{H}{\sum_{i=1}^{N}\left(\frac{h_i}{V_{S,i}}\right)} \tag{2}$$

where:

- h_i thickness of the i-th layer;
- $V_{S,i}$ shear wave velocity in the i-th layer;
- N number of layers;

- H depth of substrate, defined as that formation consisting of very stiff rock or soil, characterized by V_S of not less than 800 m/s.

The subsoil categories, which allow the use of the simplified approach, are defined in Table 2-1

Soil Category	Characteristics of the topographic surface
A	Exposed rocky masses or very rigid soils characterized by shear wave velocity values exceeding 800 m/s, potentially including surface soils with poorer mechanical characteristics up to a maximum thickness of 3 m.
B	Soft rocks and deposits of densely packed coarse-grained soils or very consistent fine-grained soils, characterized by improved mechanical properties with depth and equivalent velocity values ranging from 360 m/s to 800 m/s.
C	Moderately packed deposits of medium-coarse-grained soils or moderately consistent fine-grained soils with substrate depth exceeding 30 m, characterized by improved mechanical properties with depth and equivalent velocity values ranging from 180 m/s to 360 m/s.
D	Sparsely packed deposits of poorly packed coarse-grained soils or poorly consistent fine-grained soils, with substrate depth exceeding 30 m, characterized by improved mechanical properties with depth and equivalent velocity values ranging from 100 to 180 m/s.
E	Soils with characteristics and equivalent velocity values attributable to those defined for Categories C or D, with substrate depth not exceeding 30 m.

Table 2-1 Soil Categories, TAB. 3.2.II NTC 18

2.3 Numerical Modelling of The Excavation Tunnel - Static Model

Before examining the specific characteristics that distinguish a more accurate dynamic analysis from a simplified one, it is important to highlight the main steps in the numerical modelling of a tunnel. Initially employed to ascertain the stresses and displacements resulting exclusively from the excavation impact. Later, with enhancements driven by reflections arising from dynamic load considerations, it will guide the evaluation of how such events affect the structure under investigation.

The finite element model of the subsoil and the tunnel is created in Plaxis 2D. In the static analysis, the lateral boundary conditions involved fixed displacements horizontally at the vertical sides of the model and fixed displacements in both directions at the bottom. Displacements along the upper surface are left unconstrained. (Fabozzi & Bilotta, 2016)

An interface is incorporated between the segment and the soil, with a reduction factor (R = 0.7) being applied to both the strength and stiffness of the interface material in comparison to the surrounding soil.

- *Phase 1. Generation of the initial lithostatic stress field;*

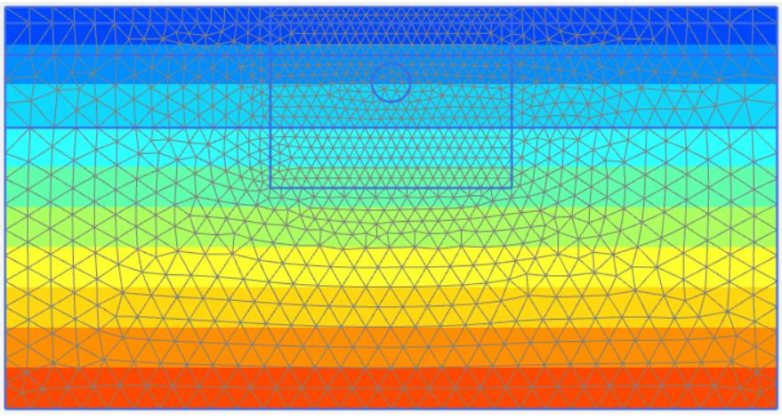

Figure 2-6 Intial Lithostatic Stress Field – Plaxis 2D Model

- *Phase 2. Excavation and Stress relaxation*

To simulate the stress state around the tunnel cavity, considering the 3D arching effect within the soil and deformations prior to lining installation, the initial lithostatic stress (σ_0) was proportionally diminished around the cavity.

$$\sigma = (1 - \lambda) * \sigma_0 \quad (3)$$

- *Phase 3. Lining installation and grouting, in drained conditions*

Numerous circular tunnels incorporate bolted or unbolted segmental linings, introducing a non-monolithic structural characteristic. Additionally, concrete linings, when subjected to bending and thrust, frequently exhibit crack formations and nonlinear behavior. Consequently, when applying the results presented here, it is imperative to initially estimate the effective (or equivalent) stiffness of the lining. Various simple and approximate methods, addressing the influence of joints on lining stiffness, are available in the existing literature.(J. Wang, 1993)

The most well-known and commonly used method is recommended by (Muir Wood, 1975) With equation below:

$$I_e = I_j + I\left(\frac{4}{n_j}\right)^2 \quad (4)$$

where:

- *Ie* effective stiffness of lining
- *n* is the number of joints,
- *Ij* effective stiffness of lining at joint,
- *I* lining stiffness of the intact, full-section

For simplicity, segments are simplified in the model to represent an equivalent continuous concrete ring, as shown in Figure 2.7,.

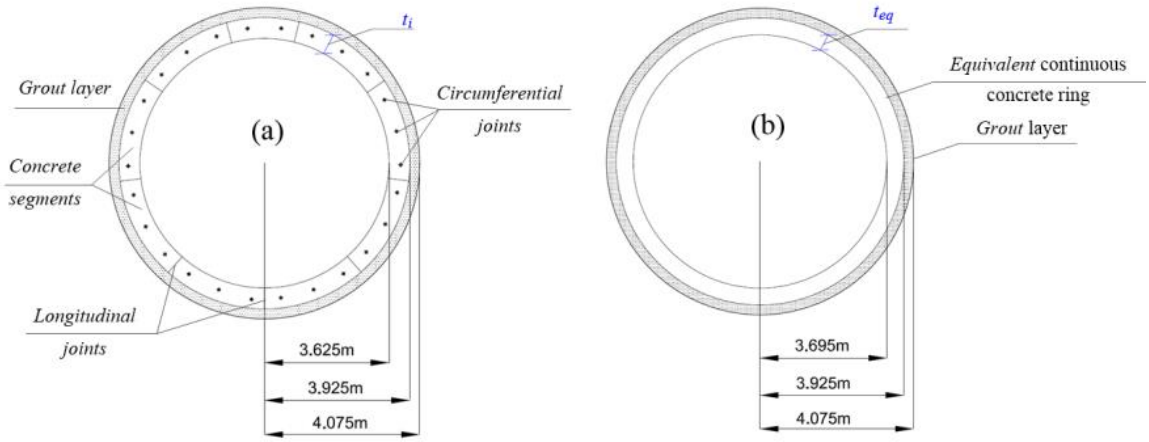

Figure 2-7 Real (a) and Simplified geometry of the segmental lining (Fabozzi & Bilotta, 2016)

2.4 Definition of the seismic environment

The seismic action on buildings is assessed starting from a 'basic seismic hazard,' under ideal conditions of a rigid reference site with a horizontal topographic surface.

The results of the hazard study are provided at points along a grid (reference grid) whose nodes are sufficiently close to each other (not more than 10 km apart) and under the conditions of a rigid horizontal reference site.

• In terms of values of maximum horizontal acceleration ag, the maximum value of the amplification factor of the spectrum in horizontal acceleration F_0, and the period at the beginning of the constant segment of the spectrum in horizontal acceleration Tc*;"

• For different exceedance probabilities in 50/75/100 years and/or different return periods TR."

Therefore, to identify, based on the available seismic hazard data, the corresponding seismic actions, it is necessary to establish.

The reference life (VR) of the structure

The exceedance probabilities over the reference life (PVR) associated with each of the considered limit states (in the case addressed in this report, only SLV)

In fact, given the reference life (VR), TR can be expressed in terms of PVR through the expression.

$$T_R = \frac{V_R}{\ln(1 - P_{V_R})} \tag{5}$$

The reference life is calculated as:

$$V_R = V_N * C_U \tag{6}$$

Where:

- V_N is the nominal life of the structure;
- C_U is the serviceability class.
- P_{VR} is the exceedance probability over the reference period

V_N, defined as the number of years in which the structure, subject to necessary maintenance, is expected to maintain specific performance levels.

The minimum values of V_N to be adopted for the different types of construction are given in Table 2.1.

TIPI DI COSTRUZIONI		Valori minimi di V_N [anni]
1	Costruzioni temporanee e provvisorie	10
2	Costruzioni con livelli di prestazioni ordinari	50
3	Costruzioni con livelli di prestazioni elevati	100

Table 2-2 Nominal design life values (NTC2018)

With reference to the consequences of operational interruption or potential collapse, constructions are classified into the following designated classes of use:

- Class I: Constructions with only occasional presence of people, such as agricultural buildings.
- Class II: Constructions intended for normal crowding, without hazardous contents for the environment, and without essential public and social functions. Industries with non-hazardous activities for the environment. Bridges, infrastructural works, road networks not falling into Class III or Class IV, railway networks whose interruption does not cause emergency situations. Dams whose collapse does not result in significant consequences.
- Class III: Constructions with significant crowding. Industries with hazardous

activities for the environment. Extra-urban road networks not falling into Class IV. Bridges and railway networks whose interruption causes emergency situations. Dams significant for the consequences of their potential collapse.

- Class IV: Constructions with important public or strategic functions, including those related to civil protection management in case of disasters. Industries with particularly hazardous activities for the environment. Road networks of type A or B, as defined by DM 5/11/2001, n. 6792, "Functional and geometric norms for the construction of roads," and of type C when part of routes connecting provincial capitals not otherwise served by type A or B roads. Bridges and railway networks critical for maintaining communication routes, especially after a seismic event. Dams connected to the operation of aqueducts and electric power generation plants

CLASSE D'USO	I	II	III	IV
COEFFICIENTE Cu	0.7	1.0	1.5	2.0

Table 2-3 Values of the serviceability coefficient Cu (NTC2018)

P_{VR} is the exceedance probabilities over the reference period associated with the considered limit state to identify the corresponding seismic actions Table 2-4."

Stato Limite		P_{VR} : Probabilità di superamento nel periodo di riferimento VR
Stati limite di esercizio	SLO	81%
	SLD	63%
Stati limite ultimo	SLV	10%
	SLC	5%

Table 2-4 Exceedance Probability (NTC2018)

Noting the expected maximum horizontal acceleration on a rigid reference site ag, the peak ground acceleration a_{max} is assessed based on local seismic response:

$$a_{max} = S_S * S_T * a_g \quad (7)$$

Where ;

- S_S is the coefficient that includes the effect of stratigraphic amplification,
- S_T is the coefficient that includes the effect of topographic amplification.
- a_g the peak acceleration on outcropping rock site

In relation to the subsoil category, the stratigraphic coefficient S_S is determined: the expression of the stratigraphic coefficient according to the subsoil category is given in the following Table 2-5 **Error! Reference source not found.**

Soil Category	S_S
A	1,00
B	$1,00 \le 1,40 - 0,40 \cdot F_o \cdot \frac{a_g}{g} \le 1,20$
C	$1,00 \le 1,70 - 0,60 \cdot F_o \cdot \frac{a_g}{g} \le 1,50$
D	$0,90 \le 2,40 - 1,50 \cdot F_o \cdot \frac{a_g}{g} \le 1,80$
E	$1,00 \le 2,00 - 1,10 \cdot F_o \cdot \frac{a_g}{g} \le 1,60$

Table 2-5 Expressions of S_S - TAB. 3.2.IV NTC 18

For complex topographic conditions, it is necessary to prepare specific local seismic response analyses. For simple surface configurations, the following classification can be adopted **Error! Reference source not found.**.

Category	Characteristics of the topographic surface
T1	Flat surface, slopes, and isolated elevations with an average inclination of ≤ 15°
T2	Slopes with an average inclination i > 15°
T3	Elevations with crest width much smaller than at the base and average inclination 15° ≤ i ≤ 30°
T4	Elevations with crest width much smaller than at the base and average inclination i > 30°

Table 2-6 TOPOGRAPHIC CATEGORIES - TAB. 3.2.III NTC 18

To consider the topographic conditions and in the absence of specific local seismic response analysis, the values of the topographic coefficient S_T given in Table 2-7 are used.

Topographic Category	Characteristics of the topographic surface	S_T
T1	-	1
T2	At the top of the slope	1,2
T3	At the crest of an elevation with an average slope less than or equal to 30°	1,2
T4	At the crest of an elevation with an average slope greater than 30°	1,3

Table 2-7 Maximum values of the topographic amplification coefficient S_T

2.4.1 Definition of the expected maximum horizontal acceleration on a rigid reference site (ag)

For the definition of the expected maximum horizontal acceleration on a rigid reference site (ag), the 'Ministry Spectra' sheet with coordinate search (Spectra-NTCver.1.0.3) is used.

Using the geographical coordinates of individual tunnel critic section, a specific point on the grid is taken as a reference point from which the response spectrum representative of the horizontal component of the seismic actions for the specific site is extracted for the Life Safety Limit State (SLV), considering a subsurface class A, topographic category T1, nominal life VN, and reference CU (Table 2-2, Table 2-3)

2.4.2 Disaggregation analysis

The disaggregation analysis is carried out using the website of the INGV (National Institute of Geophysics and Volcanology, 'esse1-gis.mi.ingv.it').
Since the data from the INGV are exclusively referred to a reference period (VR=50 years), different from that of the specific project, the disaggregation analysis is conducted considering the PVR available from the INGV source most similar to that of the site, which is equal to 5%
In the detailed report for each individual tunnel section, the main results of the seismic disaggregation data search will be presented, revealing:

- Magnitude
- Distance from the epicentre

2.4.3 Natural Accelerograms

The search for natural accelerograms compatible with a given reference spectrum is carried out using the REXEL program with reference to the European Strong Motion Data recordings.
In the program, the 'user-defined spectrum' option is used to load the regulatory spectrum obtained through the 'Ministry Spectra' sheet with coordinate search (Spectra-NTCver.1.0.3). This sheet is derived for a rigid soil type A and topographic category T1, imposing a specific nominal life (VN) and usage class (CU) for each tunnel section, appropriately scaled to obtain acceleration in m/s^2. Only the life safety limit state (SLV) is considered. The search for the accelerogram data to be used in the analyses was conducted considering magnitude and source distance, in relation to the findings of the disaggregation data analysis.
The identified natural accelerograms and their corresponding identifying data are synthesized in a single representation for ease of comparison, as well as individually.

- There is a total of 7 accelerograms on soil type A and topographic category T1.
- They are scaled with a mean scaling factor of < 5.

- They are compatible with the elastic spectrum (5%), assessed with a tolerance range of 10% to 30%.
- The spectrum compatibility has been extended up to a period of 2 seconds.

2.5 Definition of the Ground Response and Shaking

In the tunnel lining structure, stress increases occur as a result of an earthquake, depending on: relative soil-structure stiffness, interface conditions, initial stress-strain state of the subsurface, structural type of lining and, considering the linear development of the tunnel and the variability of subsurface conditions along the route (Figure 2-8). The effects of an earthquake on underground structures can be distinguished in:

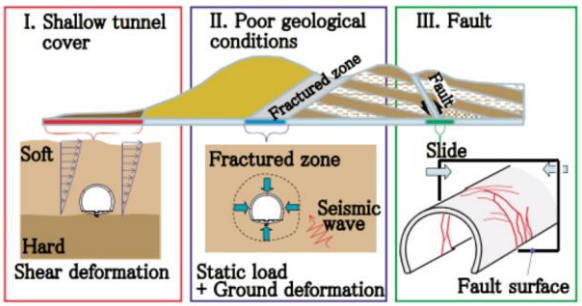

Figure 2-8 Seismic Impacts on the tunnel depends on the condition.(Do et al., 2014)

1) Ground failure (liquefaction, groundwater displacement, slope instability). These effects are usually found more in surface tunnels.

2) Ground shaking and Deformation, which refers to ground deformation produced by seismic waves propagating through the earth's crust. The main factors influencing damage due to shaking, as mentioned earlier, are the shape, size and depth of the structure; the properties of the surrounding soil or rock; the properties of the structure; and the degree of seismic shaking.

In this thesis focusing on the second type, seismic waves produce deformation of the lining in transverse directions. In the transverse direction the tunnel section is subject to ovalization (Figure 2-9)due to shear deformations of the ground and the resulting bending moments.

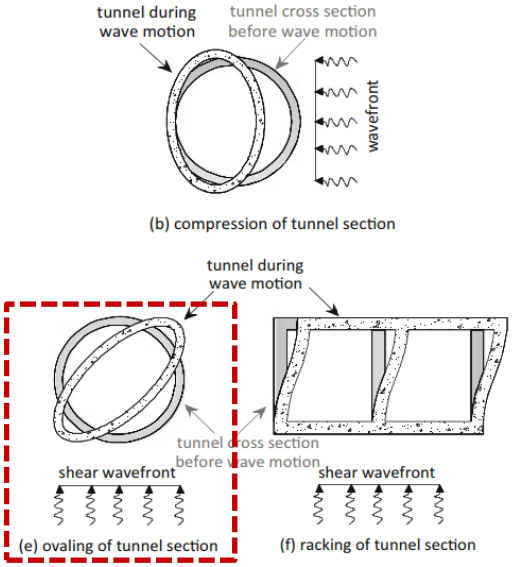

Figure 2-9 Ground Shaking and Deformation (Tsinidis et al., 2020)

2.5.1 Ovaling Effect on Circular Tunnels

The ***distortion*** of a circular tunnel lining due to ***ovalization*** is primarily a result of seismic waves traveling in planes perpendicular to the tunnel axis. Usually, the critical deformation of the lining is produced by vertically propagating shear waves.

As shown in Figure 2-8, the magnitude of the shear deformation is the main phenomenon for shallow tunnels in soil formation for distortion.

The findings reveal repetitive stress concentrations involving alternating compression and tension in the tunnel lining. These dynamic stresses overlay the pre-existing static stresses in the lining. Two critical conditions may emerge from this situation, as noted by (J. Wang, 1993).

• The dynamic compressive stresses, in conjunction with static compressive stresses, have the potential to surpass the local compressive capacity of the lining.(Owen, 1981)

• Dynamic tensile stresses, when coupled with static compressive stresses, decrease the flexural capacity of the lining, and in certain instances, the resultant stresses may exhibit tensile characteristics.(Owen, 1981)

2.5.2 Free-Field Shear Deformations

In estimating free-field shear distortion, analytical procedures through numerical methods are often necessary, especially for soil sites with varying stratigraphy. Various computer codes such as SHAKE, PLAXIS, DEEPSOIL and others, are available for this purpose.

The predominant approach involves simplifying the site geology into a horizontally layered system and applying one-dimensional wave propagation theory for analysis, as

introduced by(Schnabel et al., 1972). The resultant free-field shear distortion is expressed as a shear strain distribution or shear deformation profile with respect to depth.

2.5.2.1 Simplified Equation for Shear Deformations

2.5.2.1.1 For Deep & Shallow Tunnel

In the case of a deep tunnel situated in a relatively uniform soil or rock without detailed site response analyses, the simplified approach proposed by (Hung et al., 2009)could offer a reasonably accurate estimation. It's important to note, though, that this method tends to yield more conservative outcomes.

Here, the maximum shear strain in the free field, Υ_{max}, can once again be formulated as:

$$\gamma_{max} = \frac{V_S}{C_{Se}} \tag{8}$$

Where:

- V_S = Peak particle velocity
- C_{se} = The effective shear wave velocity of the vertically propagating shear wave,

The estimation of C_{se} values involves appropriately reducing the small-strain shear wave velocity, Cs, obtained from in-situ testing (utilizing techniques like cross-hole, down-hole, and P-S logging), considering the strain-level dependent effect.

In the case of rock, it is assumed that the ratio of Cse to Cs is equal to 1.0. For stiff to very stiff soil, the C_{se}/C_s ratio may vary from 0.6 to 0.9.(Hung et al., 2009)

Alternatively, specific site response analyses can be conducted to estimate Cse. Particularly, site-specific response analyses are necessary for determining Cse in tunnels situated in soft soils.(Hung et al., 2009)

$$V_S = k * a_{z,max} \tag{9}$$

Where;

- k ratio of the peak ground velocity (cm/s) to peak ground acceleration (g) in Table 2-8
- $a_{z,max}$ the peak acceleration at the depth of the tunnel

Moment magnitude (M_w)	Ratio of peak ground velocity (cm/s) to peak ground acceleration (g)		
	Source-to-site distance (km)		
	0–20	20–50	50–100
Rock[a]			
6.5	66	76	86
7.5	97	109	97
8.5	127	140	152
Stiff soil[a]			
6.5	94	102	109
7.5	140	127	155
8.5	180	188	193
Soft soil[a]			
6.5	140	132	142
7.5	208	165	201
8.5	269	244	251

[a]In this table, the sediment types represent the following shear wave velocity ranges: rock ≥ 750 m/s; stiff soil is 200–750 m/s; and soft soil < 200 m/s. The relationship between peak ground velocity and peak ground acceleration is less certain in soft soils.

Table 2-8 Ratios of peak ground velocity to peak ground acceleration at surface in rock and soil (Power et al., 1996)

$$a_{z,max} = C * a_{max,s} \quad (10)$$

Where:

C is the ratio of ground motion at the Tunnel Depth to Motion at ground surface in Table 2-9

$a_{max,s}$ is the peak ground acceleration (Equation (7))

Tunnel Depth (m)	Ratio Of Ground Motion At Tunnel Depth To Motion At Ground Surface
≤ 6	1.0
6 -15	0.9
15 -30	0.8
≥ 30	0.7

Table 2-9 Ground Motion Attenuation with Depth (Hung et al., 2009)

2.5.2.1.2 For Shallow Tunnels

A simplified method for calculating free-field shear deformation, γ_{max}, involves computing the ratio between the earthquake-induced maximum shear stress, τ_{max}, and the shear modulus G_m. This method is especially suitable for surface tunnels (Fabozzi & Bilotta, 2016)

In this simplified approach, the calculation of the maximum shear strain in the free-field ground is determined through the following equation:

$$\gamma_{\max(z)} = \frac{\tau_{\max(z)}}{G_m} \tag{11}$$

$$\tau_{\max(z)} = \frac{a_{max,s}}{g} \cdot \sigma_v(z) \cdot R_d(z) \tag{12}$$

There are several equations in the literature for the depth-dependent stress reduction factor. The most used ones are equation (13) suggested by (Iwasaki et al., 1978) and eqution (14) suggested by (Hung et al., 2009). The compatibility of the (Iwasaki et al., 1978) formula with SSR analysis has been proven by (Bilotta et al., n.d.), so this equation is used in this thesis.

$$R_d(z) = 1 - 0.015z \tag{13}$$

Or

- R_d = 1.0 - 0.00233z for z < 30 ft
- R_d = 1.174 - 0.00814z for 30 ft < z < 75 ft
- R_d = 0.744 - 0.00244z for 75 ft < z < 100 ft (14)
- R_d = 0.5 for z > 100 ft

Where:

- G_m = Effective strain-compatible shear modulus of ground surrounding tunnel (kPa)
- τ_{max} = Maximum earthquake-induced shear stress (kPa)
- σ_v = Total vertical soil overburden pressure at invert elevation of tunnel (kPa)
- γ_t = Total soil unit weight (kN/m^3)
- H = Soil cover thickness measured from ground surface to tunnel crown (m)
- D = Height of tunnel (or diameter of circular tunnel) (m)
- R_d = Depth dependent stress reduction factor,
- z = the depth (ft) from ground surface to the invert elevation of the tunnel and is represented by z = (H+D)
- a_{max} is defined at the equation (7)

In computations that consider dynamic ground properties, it is important to consider the distinction between small-strain values G_0, obtained from measured V_S, and shear stiffness values G, which are consistent with the strain amplitudes induced by the seismic design motion. (Eurocode8, 2022)

For shallow tunnel (overburden less than 20m), Effective strain-compatible shear modulus of ground surrounding tunnel should be obtained by multiplying G_0 with appropriate ratio

comes from Table 2-10 depends on the shear wave propagation velocity and seismicity level.

Seismicity level	**$150 \le v_s < 250$ m/s**		**$250 \le v_s < 400$ m/s**		**$400 \le v_s < 800$ m/s**		**800 m/s $\le v_s$**	
$S_{a,475}$ (m/s2)	G/G_0	ξ	G/G_0	ξ	G/G_0	ξ	G/G_0	ξ
Very low (<1,0)	0,7 (±0,08)	0,04	0,8 (±0,09)	0,03	1	0,03	1	0,02
Low (1,0-2,5)	0,5 (±0,14)	0,07	0,65 (±0,16)	0,05	0,8 (±0,10)	0,03	1	0,02
Moderate (2,5-5,0)	0,3 (±0,10)	0,1	0,5 (±0,20)	0,07	0,7 (±0,10)	0,05	1	0,02
High (>5)	0,2 (±0,10)	0,2	0,4 (±0,20)	0,12	0,6 (±0,20)	0,1	0,9 (±0,10)	0,02

Table 2-10 Damping ratios and average reduction factors (± one standard deviation) of the normalized shear modulus G/G0 within 20 m depth (Eurocode8, 2022)

***$S_{a,475}$:** Reference spectral acceleration, corresponding to the maximum value maximum constant at the 'plateau' of the elastic response spectrum (damping 5%), for a soil class A, relative to a reference return time T_{ref} = 475 years

The small strain stiffness value, G_0, should be taken from equation (15)

$$G_0 = \rho v_s^2 \tag{15}$$

Where:

- ρ is the mass density;
- Vs is the small strain shear wave propagation velocity of the ground.

2.5.2.2 Site Response Analysis for Shear Deformation

In this chapter, the local seismic response is being defined by analyzing the propagation of linear elastic waves through a stratified medium in which the properties of the soil depend on its deformation characteristics. Additionally, a nonlinear analysis is being carried out on which the soil is dependent.

2.5.2.2.1 The Adopted Soil Model

The most used models are the one-dimensional (1D) models, which are based on a series of assumptions and simplifications introduced in the geometric and mechanical characterization of the deposit and in the laws of seismic wave propagation and soil behaviour; in particular, it is assumed that:

- the bedrock is horizontal and indefinitely extended;
- the deposit is horizontally layered;

- the seismic stress consists of only horizontally polarised shear waves (SH) incident on the bedrock with vertical propagation direction.

Specifically, the parameters required for numerical modelling are:

- thickness of layers
- shear wave velocity in the individual seism strata identified
- volume weight
- dynamic parameters of the soils (damping and shear modulus as a function of deformation

In this thesis, reference is made to a one-dimensional model on which non-linear analyses are performed.
On the other hand, the hypotheses concerning seismic stress and its propagation modes within the deposit are justified as follows:

- with regard to the direction of propagation assumed to be vertical, by the fact that seismic waves undergo numerous reflection and refraction phenomena when crossing the ground and the relative stratigraphic discontinuities, according to angles linked to the speed of propagation within each of the layers crossed by Snell's law; since the velocities of the more superficial layers are on average lower, seismic waves tend to assume a vertical direction of propagation near the surface;
- with regard to the predominance of SH waves, from the fact that, from an engineering point of view, the most significant seismic stresses for safety purposes are horizontal shear stresses.

2.5.2.2.2 Non-Linear Analysis

The commonly used equivalent linear approach allows the calculation of the ground response in many practical cases, however, it represents the real behaviour of the ground in a simplified manner and the response is approximate. Alternatively, it is possible to conduct a non-linear analysis that considers the differential form of the parameters expressing the dynamic characteristics of the soil and evaluates the response, by finite difference integration, directly of the equation of motion in the time domain (Equation (16)).

$$\frac{\partial \tau}{\partial z} = \rho \frac{\partial^2 u}{\partial t^2} = \rho \frac{\partial \dot{u}}{\partial t} \tag{16}$$

Regarding the non-linear constitutive bond, there are several models that are able to describe the cyclic behaviour of the soil. These models are generally characterized by a reference curve (backbone curve), i.e. the constitutive bond, and a series of laws, the Masing rules, which govern the load and unload cycles:

- the first load curve turns out to be the backbone, denoted by F_{bb}
- when a load reversal occurs, identified with the coordinates (γ_{rev}, τ_{rev}), the discharge curve follows the trend in Equation (17), i.e. it originates at the point of reversal and is scaled by a factor of 0.5

$$\frac{\tau - \tau_{rev}}{2} = F_{bb}\left(\frac{\gamma - \gamma_{rev}}{2}\right) \tag{17}$$

- If the loading or unloading section intersects the backbone curve, then the tension-forming path continues to follow that curve to the next reversal point.
- If the loading or unloading section undergoes an inversion without intersecting the backbone curve, then the tensional deformation path evolves along the curve tensional path evolves along the curve provided by Equation (17).

The above is a description of what is summarised in Figure 2-10.

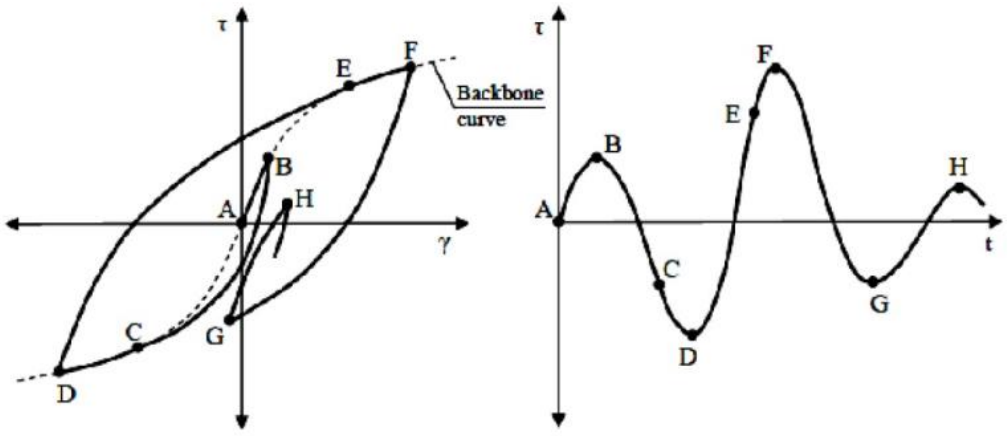

Figure 2-10 Non-linear model diagram

The load cycle begins at point A and proceeds to point B, following the reference curve as required. At point B, an initial load reversal occurs, following the curve provided by Eq.2. The unloading process subsequently intersects the backbone at point C, so the path continues along it until it reaches inversion point D. From point D the path evolves along the curve predicted by Eq.2 and the process repeats similarly for the rest of the load.

It can be seen that for the models just discussed, through the definition of the backbone curves the hysteresis cycles and consequently the damping of the material are drawn, i.e. the control of stiffness reduction with the deformation state does not allow the same control for the automatically defined damping. For this reason, this method of reconstructing material dynamic behavior curves is called MR, Modulus Reduction, because in fact the reduction factor is only applied to the G-modulus.

2.5.2.2.3 Calculation programme and model adopted

The set of 7 spectrum-compatible accelerograms by using Rexel v. 3.5 software, is used for the local seismic response analysis, exploiting the DEEPSOIL software. Which, in a completely non-linear context, performs a one-dimensional analysis with solution of Equation (16) according to a discrete mass model in the time domain.

With regard to the non-linear constitutive bond, DEEPSOIL has several models that can describe the cyclic behaviour of the soil.

The Generalized Quadratic/Hyperbolic (GQ/H) Model with Shear Strength Control was chosen as the reference curve (backbone curve) for the analyses in this report. The GQ/H Model features a calibration procedure that automatically corrects the reference curves based on the specified shear strength (parameter τ_{max} in Equation (18)). Deepsoil has a routine that calculates the calibration parameters of the curve from θ1 to θ5 (Eq.4) in order to ensure that the decay curve of the individual layer that makes up the soil column under investigation is as close as possible to the decay curve used as a reference (i.e. Seed&Idris, Vucetic&Dobry, etc.), modifying the deformation values according to the shear strength of the specified deformation.For the analyses covered by this report, the Generalized Quadratic/Hyperbolic (GQ/H) Model with Shear Strength Control was chosen as the reference curve (backbone curve). The GQ/H Model features a calibration procedure that automatically corrects the reference curves based on the specified shear strength (parameter τ_{max} in Equation (18)). Deepsoil has a routine that calculates the calibration parameters of the curve from θ1 to θ5 (Eq.4) in order to ensure that the decay curve of the individual layer that makes up the soil column under investigation is as close as possible to the decay curve used as a reference (i.e. Seed&Idris, Vucetic&Dobry, etc), by adjusting the deformation values based on the shear strength of the specified deformation.

The GQ/H model uses the values τmax, G_0, and θ_1 to θ_5 to construct the shear strength and shear deformation curve using the following functions:

$$\theta_\tau = \theta_1 + \theta_2 * \frac{\theta_4 * (\frac{\gamma}{\gamma_r})^{\theta_5}}{\theta_3{}^{\theta_5} + \theta_4 * (\frac{\gamma}{\gamma_r})^{\theta_5}} \quad (18)$$

where, γr is the reference deformation and is calculated as $\gamma_r = \tau_{max} / G_0$. Once θτ has been determined, the curve shear stress - shear deformation is constructed as follows:

$$\tau = \tau_{max} * [\frac{1}{\theta_\tau} * \left\{1 + \left(\frac{\gamma}{\gamma_r}\right) - \sqrt{\left\{1 + \frac{\gamma}{\gamma_r}\right\}^2 - 4 * \theta_\tau * \frac{\gamma}{\gamma_r}}\right\}] \quad (19)$$

2.5.2.2.4 Definition Soil Profile

The layered medium to be traversed by the selected accelerograms is defined according to the reference seismic test reference and for each layer it is necessary to define:

- Thickness [m]
- Weight per unit volume [kN/m^3].
- Shear wave velocity [m/s]
- Shear resistance [kPa]

With which one should always check that the wavelength within the individual layer is not too small in relation to the thickness of the layer itself. In particular, the Max Frequency represents, for each layer:

$$f_{max} = \frac{V_s}{4 * H} \quad (20)$$

$$\lambda_{min} = \frac{V_s}{f_{max,seismic}} \quad (21)$$

As Rule of thumbs , $f_{max,seismic}$ can be accepted equal to 25 Hz.

Thicknesses of individual layers are sought

$$H_{max} = \frac{\lambda_{min}}{4} = \frac{V_s}{4 * 25\ Hz} \quad (22)$$

At this point we must manually split the layers to avoid errors in the calculation of the shear deformation at the centre of the layer, which would be insignificant.

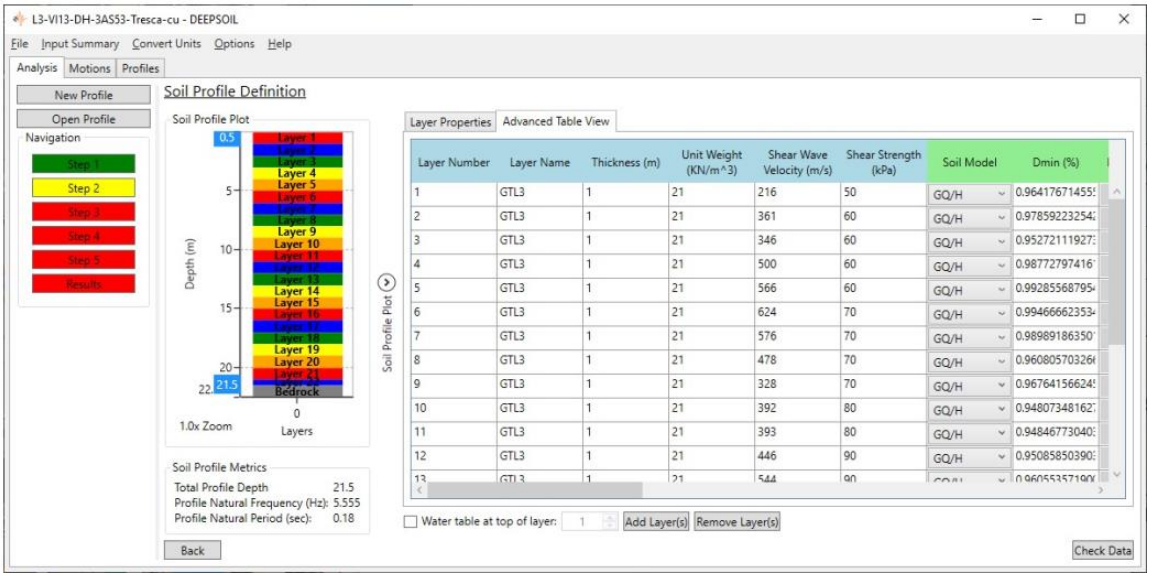

Figure 2-11 Schematic Soil Profile Definition

A reference decay curve is then selected for each layer. When absence of the decay curve for site specific soil formations, for granular soils, the Seed&Idriss (1970) decay curve can be chosen, while for cohesive soils, the Vucetic&Dobry (1991) decay curve associated with the plasticity index of the soil composing the individual layer can be chosen. And on this curve, the calibration of the layer-specific decay curve is made.

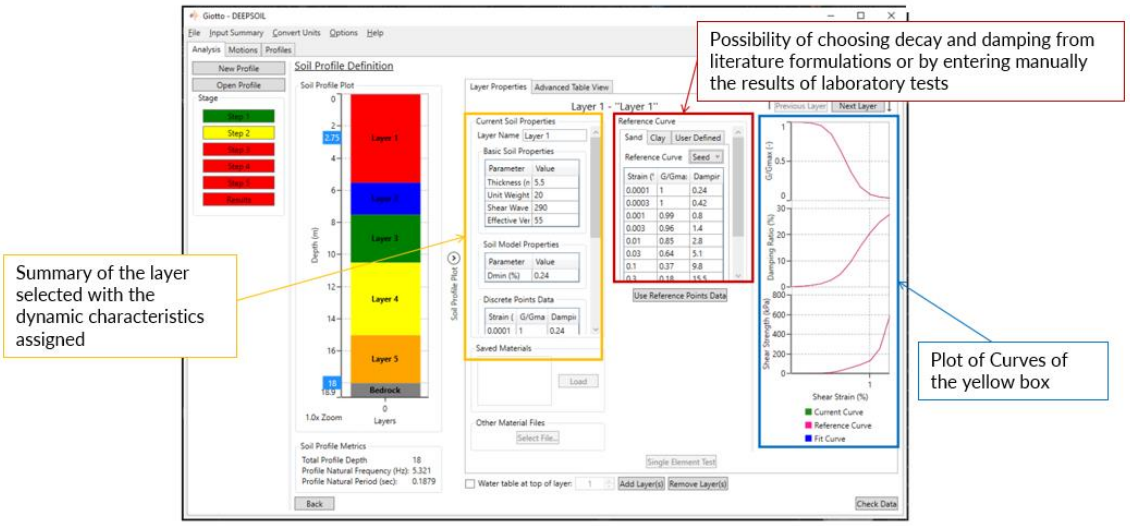

Figure 2-12 Schematic Soil Layer Definition(Cosentini, 2 C.E.)

With regard to the seismic bedrock (considered as an elastic half-space), the unambiguously defined volume weight of 24 kN/m3 must be indicated, and a Vs of 800 $m.s^{-1}$ is assumed (Figure 8); in cases where the reference seismic test does not reach this value, the position of the bedrock has been inferred by interpolating the test data.

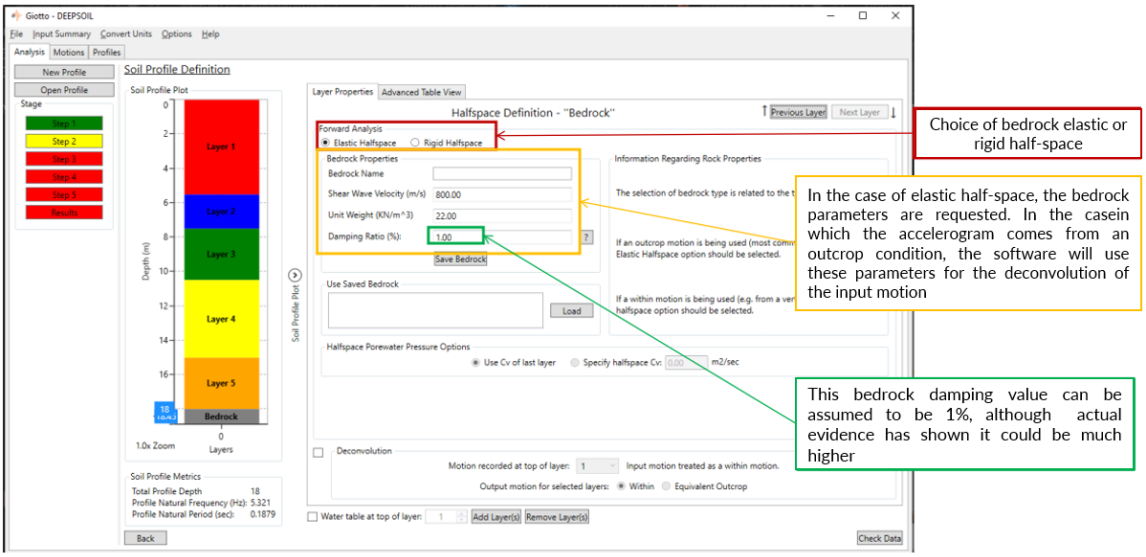

Figure 2-13 Definition of the Bedrock (Cosentini, 2 C.E.)

The seismic input, comprising the 7 spectro-compatible accelerograms (Figure 9) obtained through Rexel, is then uploaded. The calculation code structure involves the initial insertion of the accelerogram to be applied to the bedrock with the P.G.A. specified in [g]. Subsequently, the output files from Rexel (in ms-2) will be appropriately modified. Additionally, the amplitude of the accelerogram must be scaled for the maximum expected acceleration at the site (PGA) using the Rexel scaling factor.

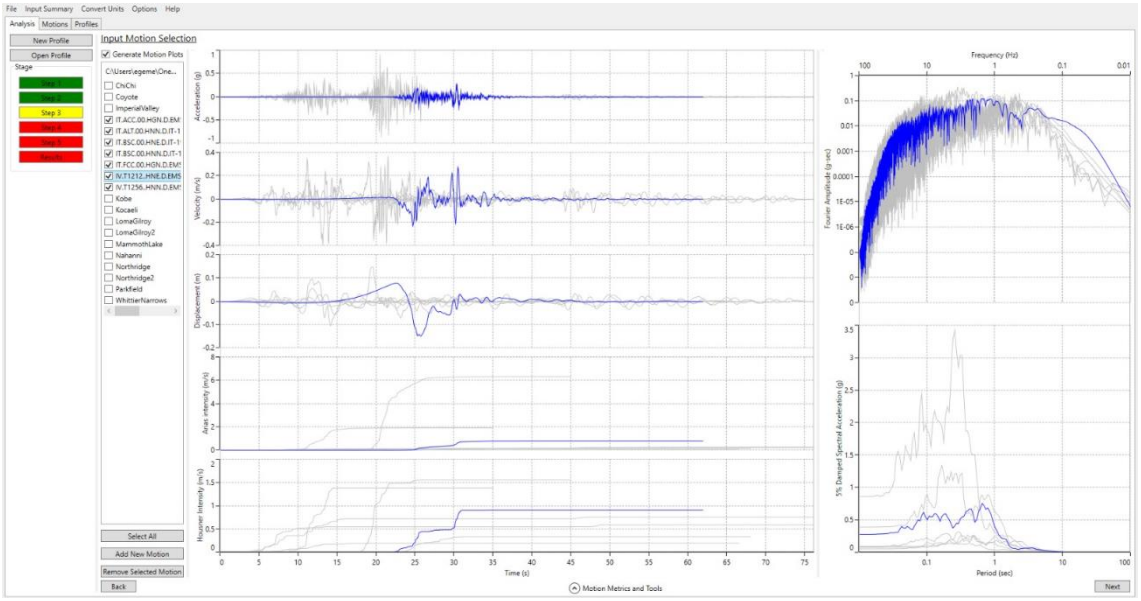

Figure 2-14 Seismic Input

From the non-linear Local Simic Response analysis, directly PGA, PGD, Max Strain(%), Max Stressr Ratio and Effective Vertical Stress (kPa) and indirectly horizontal displacement and operational shear modulus are obtained *(Figure 2-15)*

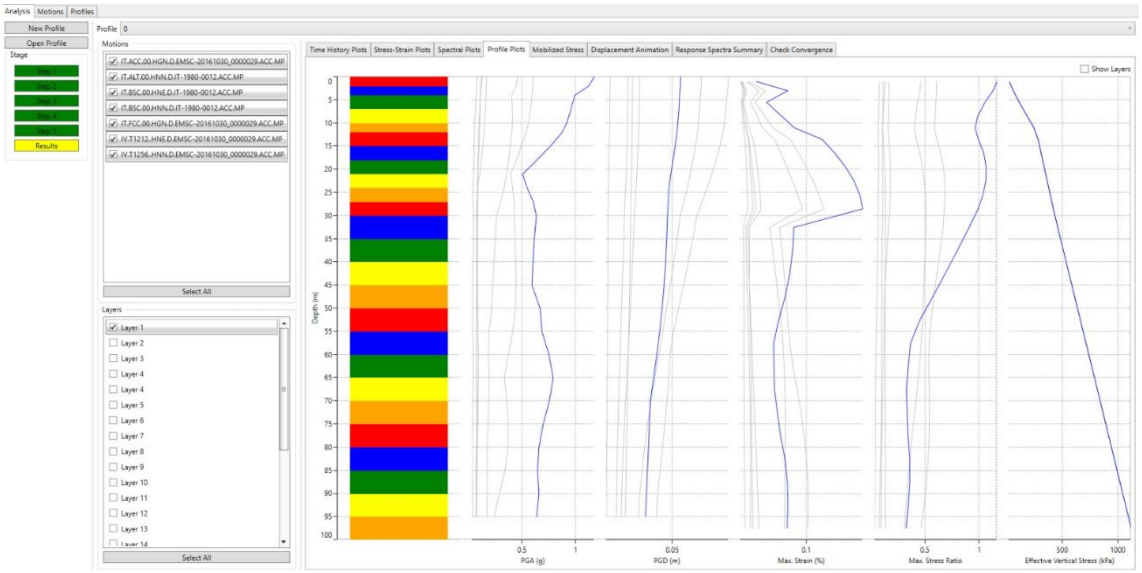

Figure 2-15 DeepSoil Output

2.5.3 Soil-Structure Interaction

Therea are 2 important phenomena which affect tunnel behaviour under seismic actions , related with soil-structure interaction. These are Lining Stiffness and Interface Conditions.

2.5.3.1 Importance of Lining Stiffness

The tunnel's stiffness in relation to the surrounding soil is determined by the compressibility ratio C and flexibility ratio F, representing axial and flexural stiffness, respectively. Both parameters play a role in the lining's ability to resist ovalization.

$$C = \frac{E_m R(1-\nu_l^2)}{E_l t(1+\nu_m)(1-2\nu_m)} \tag{23}$$

$$F = \frac{E_m R(1-\nu_l^2)}{6E_l I(1+\nu_m)} \tag{24}$$

Where:

- E_m = modulus of elasticity of the medium
- n_m = Poisson's Ratio of the medium
- E_l = the modulus of elasticity of the tunnel lining
- n_l = Poisson's Ratio of the tunnel lining
- R = radius of the tunnel lining
- t = thickness of the tunnel lining
- I = moment of inertia of the tunnel lining (Equation (4))

The flexibility parameter regulates the stiffness of the tunnel lining in relation to

that of the surrounding soil. With

- F << 1, the structure is very rigid, resisting deformation and opposing the movement of the soil, resulting in high values of bending moment.
- F = 1, the structure has stiffness equal to that of the medium, indicating free-field deformation.
- F > 1, the structure is less rigid than the medium, tends to follow the seismic-induced movements, undergoes deformation, and absorbs less stress.

Of these two parameters, the flexibility ratio is frequently deemed more crucial since it is linked to the lining's ability to resist distortion imposed by the surrounding ground. As will be discussed later in this chapter, the compressibility ratio also plays a role in influencing the lining's thrust response.

2.5.3.2 Interface Conditions

In tunnel seismic analysis, the consideration of full-slip and non-slip conditions refers to the modeling of the interface between the tunnel lining and the surrounding soil during seismic events. These conditions affect the interaction between the tunnel and the soil, influencing the response of the tunnel to seismic waves. Here's an overview of full-slip and non-slip conditions in tunnel seismic analysis:

Full-Slip Condition:

- **Definition:** In a full-slip condition, the interface between the tunnel lining and the surrounding soil is assumed to allow for complete sliding or separation during seismic motion.
- **Modeling:** The full-slip condition implies that there is no resistance to sliding along the tunnel-soil interface, and the tunnel lining is essentially decoupled from the soil motion.
- **Effects:** Full-slip conditions often result in reduced seismic forces on the tunnel lining compared to non-slip conditions. It can lead to lower bending moments and axial forces.

Non-Slip Condition:

- **Definition:** In a non-slip condition, the interface between the tunnel lining and the soil is assumed to be fully connected, with no relative sliding between the two.
- **Modeling:** Non-slip conditions imply that the tunnel lining and the soil move together as a single entity during seismic motion. The lining and soil are essentially coupled.
- **Effects:** Non-slip conditions typically result in higher seismic forces on the tunnel lining compared to full-slip conditions. The tunnel lining and soil interact more strongly, leading to increased bending moments and axial forces.

The choice between modeling full-slip or non-slip conditions depends on the specific characteristics of the tunnel and the surrounding soil, as well as the objectives of the analysis. It's common to analyze both conditions to understand the range of responses and assess the potential impact of the tunnel-soil interaction on structural performance.

Advanced numerical methods, such as finite element analysis, are often employed for tunnel seismic analysis considering full-slip and non-slip conditions. These analyses help engineers design tunnels that can withstand seismic events while ensuring the safety and stability of the structure.

In this thesis, numerical models incorporate Rinter=0.1 to represent full-slip conditions, while Rinter=1 is employed to depict non-slip conditions. The subsequent calculations are performed based on these considerations.

2.6 Seismic Design Approaches

In this thesis, the following 4 different approaches will be carried out in the same analysis cross-section and a relationship between them will be tried to be established. Two of these approaches are the analytical method and the simplified numerical method, where the tunnel section is considered as a homogeneous formation and shear deformation which is derived by using simplified method, is applied. This method is frequently used by project companies, especially in the preliminary design phase.

The other approaches that are uncoupled and coupled, require specialized and more time-consuming calculations. Thanks to these approaches, multi-layered formations can be used in calculations without simplification. In this way, it is possible to obtain more precise results.

The way these approaches are followed is explained and in the following sections it is demonstrated in a practical way on a case study.

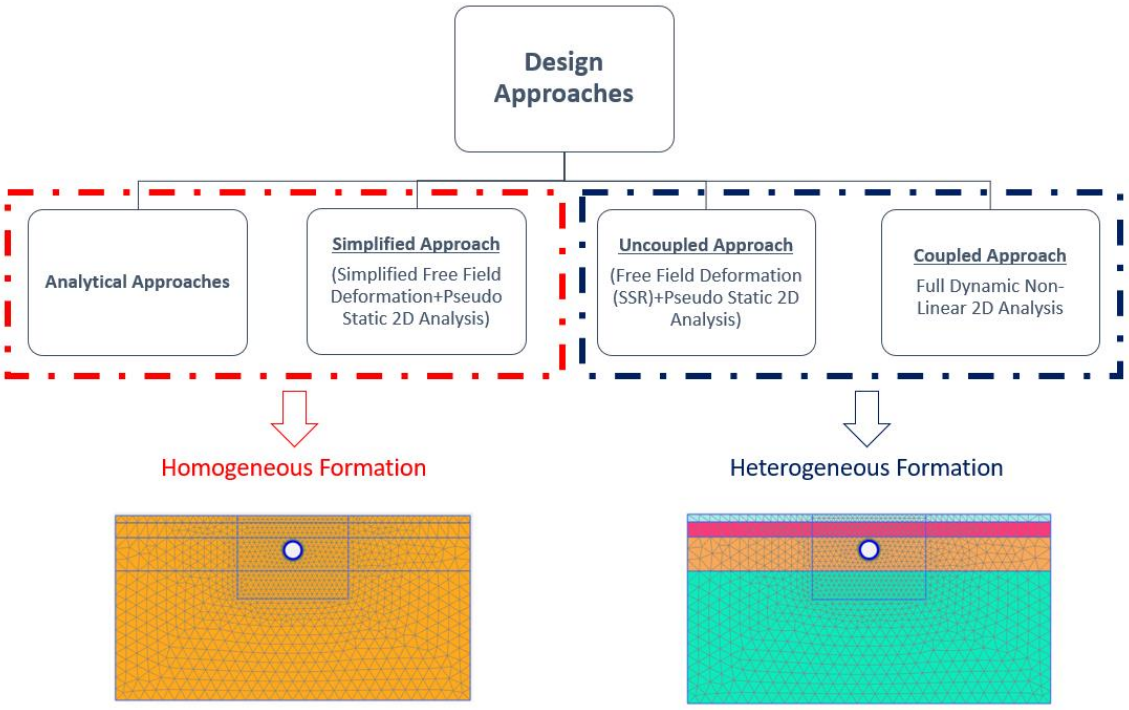

Figure 2-16 Design Approaches

2.6.1 Analytical Methods

The transverse seismic analysis of underground structures has been addressed through the utilization of the deformation model applied to the free field, considering the propagation of shear waves. Closed-form solutions for this analysis were presented by (Newmark, 1968), (J. Wang, 1993), (Power et al., 1998), and (Penzien & Wu, 1998). In these solutions, the transverse ovalling/racking is employed to calculate the strains and forces acting on

the lining of the underground structures.(J. H. Wang et al., n.d.)

The equations associated with the assessment of the free field ground and the internal forces within the linings are outlined following chapter, employing two most known methods: (Penzien, 2000) and (J. Wang, 1993) .

2.6.1.1 Wang (1993)

2.6.1.2 No Slip Condition

- Diametric Strain (25)

$$\frac{\Delta d_{lining}}{\Delta d_{free-field}} = \frac{2}{3} K_1 F \tag{25}$$

- Normal Force (26)

$$N_{max} = \pm K_2 \frac{E_m}{2(1+\nu_m)} R\gamma_{max} \tag{26}$$

- Bending Moment (27)

$$M_{max} = \pm \frac{1}{6} K_1 \frac{E_m}{(1+\nu_m)} R^2 \gamma_{max} \tag{27}$$

Where K_2 (28)

$$K_2 = 1 + \frac{F[(1-2\nu_m)-(1-2\nu_m)C]-\frac{1}{2}(1-2\nu_m)^2+2}{F[(3-2\nu_m)+(1-2\nu_m)C]+C\left[\frac{5}{2}-8\nu_m+6\nu_m^2\right]+6-8\nu_m} \tag{28}$$

Where;

- F = flexibility ratio as defined in Equation (23)
- C = Compressibility ratio as defined in Equation (24)
- E_m, n_m = modulus of elasticity and Poisson's Ratio of medium
- R = radius of the tunnel lining
- γ_max = maximum free-field shear strain

2.6.1.3 Full Slip Condition

- Diametric Strain (29)

$$\frac{\Delta d_{lining}}{\Delta d_{free-field}} = \frac{2}{3} K_1 F \tag{29}$$

- Normal Force (30)

$$N_{max} = \pm\frac{1}{6}K_1\frac{E_m}{(1+\nu_m)}R\gamma_{max} \quad (30)$$

- Bending Moment (31)

$$M_{max} = \pm\frac{1}{6}K_1\frac{E_m}{(1+\nu_m)}R^2\gamma_{max} \quad (31)$$

with K_1 (32)

$$K_1 = \frac{12(1-\nu_m)}{2F+5-6\nu_m} \quad (32)$$

Where;

- E_m, n_m = modulus of elasticity and Poisson's Ratio of medium
- R = radius of the tunnel lining
- γ_max = maximum free-field shear strain
- F = flexibility ratio

2.6.1.4 Penzien (2000)

2.6.1.5 No Slip Condition

Da non usare per la stima dello sforzo normale in quanto sottostimato.

- Diametric Strain (33)

$$\Delta d_{lining} = R^n\Delta d_{free-field} = \frac{R^n d}{2}\gamma_{max} \quad (33)$$

- Normal Force (34)

$$N_\theta = -\frac{24E_lI\Delta d_{lining}}{D^3(1-\nu_l^2)}cos2\left(\theta+\frac{\pi}{4}\right) \quad (34)$$

- Shear Force (35)

$$V_\theta = -\frac{24E_lI\Delta d_{lining}}{D^3(1-\nu_l^2)}sin2\left(\theta+\frac{\pi}{4}\right) \quad (35)$$

- Bending Moment (36)

$$M_\theta = -\frac{6E_lI\Delta d_{lining}}{D^2(1-\nu_l^2)}cos2\left(\theta+\frac{\pi}{4}\right) \quad (36)$$

With α^n (37):

$$\alpha^n = \frac{24E_lI(3-4\nu_m)}{D^3G_m(1-\nu_l^2)} \quad (37)$$

2.6.1.6 Full Slip Condition

- Diametric Strain (38)

$$\Delta d_{lining} = R^n \Delta d_{free-field} = \frac{R^n d}{2} \gamma_{max} \quad (38)$$

(1)

- Normal Force (39)

$$N_\theta = -\frac{12 E_l I \Delta d_{lining}}{D^3 (1 - \nu_l^2)} cos2\left(\theta + \frac{\pi}{4}\right) \quad (39)$$

- Shear Force (40)

$$V_\theta = -\frac{24 E_l I \Delta d_{lining}}{D^3 (1 - \nu_l^2)} sin2\left(\theta + \frac{\pi}{4}\right) \quad (40)$$

- Bending Moment (41)

$$M_\theta = -\frac{6 E_l I \Delta d_{lining}}{D^2 (1 - \nu_l^2)} cos2\left(\theta + \frac{\pi}{4}\right) \quad (41)$$

(Witj $R\hat{}n$, which is the shaking coefficient between the cladding and the surrounding medium ('Racking ratio'), and $\alpha\hat{}n$ respectively defined by formulae (42) and (43):

$$R^n = \pm \frac{4(1-\nu_m)}{(\alpha^n + 1)} \quad (42)$$

$$\alpha^n = \frac{12 E_l I (5 - 6\nu_m)}{D^3 G_m (1 - \nu_l^2)} \quad (43)$$

2.6.2 Simplified Numerical Approach

In this approach, seismic analysis is carried out by considering tunnel excavation formation and shear deformation is derived from simplified equation which is explained at the chapter 2.5.2.1

Horizontal displacements are applied to the sides and top of the numerical model such that a displacement Δx_{max} triangular linearly and uniform respectively. It is calculated using equation (44), is induced to induce a pure shear deformation in the ground, as shown in Figure 2-17

$$\Delta x_{max} = \gamma_{max} \cdot h_{mod} \quad (44)$$

Where:

- γ_{max} shear strain which is derived simplified method at the chapter 2.5.2.1.2

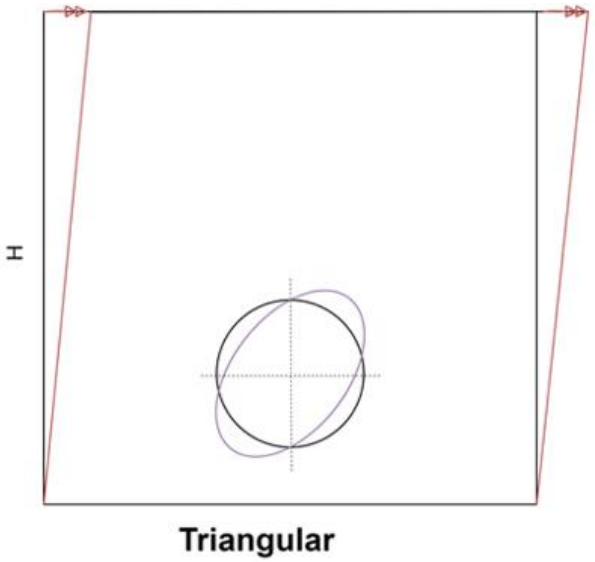

Figure 2-17 Simplified Numerical Model

Model Parameters:

- Soil Model: Linear Elastic
- Effective strain-compatible shear modulus (G) (Table 2-10) has to be defined as material properties.
- Unit Wight is equal 0 kN/m^3;
- R_{inter} is defined as 0.1 for full-slip condition, 1 for non-Slip condition;

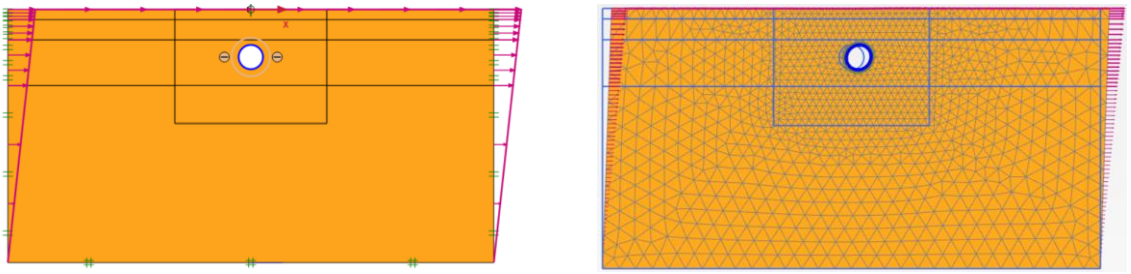

Figure 2-18 *Simplified Plaxis Model and Output*

2.6.3 Uncoupled Approach

Firstly free field deformation profile is determined from SSR analysis which is explained at the chapter 2.5.2.2. After that these deformations are applied linear elastic numerical model as explained at the simplified numerical approach. As different from simplified numerical approach, operational shear modules $G_{(\Upsilon)}$ is obtained from SSR analysis, not

from Table 2-10.

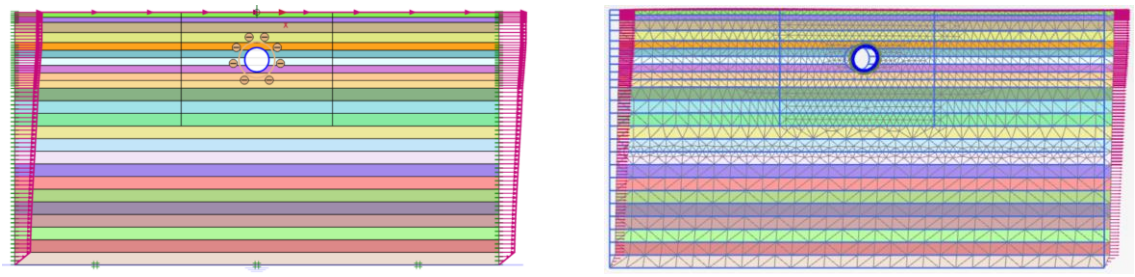

Figure 2-19 *Uncoupled Approach Plaxis Model and Output*

Model Parameters:

- Soil Model: Linear Elastic
- Effective strain-compatible shear modulus (Operational shear Modulus) $G_{(\Upsilon)}$ is obtained from SSR analysis and defined for each layer.
- Unit Wight is equal 0 kN/m^3;
- R_{inter} is defined as 0.1 for full-slip condition, 1 for non-Slip condition.

2.6.4 Coupled Approach (Fully Dynamic Analysis)

Conducting a full dynamic analysis represents the highest level of detail and comprehensiveness in seismic analysis. It involves solving the motion equations within the entire analysis domain, encompassing soil-structure interaction. This comprehensive approach enables the exploration of nonlinear behaviors exhibited by both the soil and the structure, considering the significant influence of key parameters. (Fabozzi & Bilotta, 2016)

The soil parameters, such as the shear modulus (G) and damping (D), undergo a multi-step adjustment process at each stage of the analysis. This adjustment is based on the shear deformation of the soil (γ) estimated in the preceding time step for various depths within the soil profile. The evolution of the shear soil modulus, G(γ), and the rise in damping ratio, D(γ), in response to the soil deformation levels are characterized by the chosen G(γ)-D(γ) curve.(Abate et al., 2023b)

Full dynamic analyses utilizing an integrated method for soil-structure interaction, offer a satisfactory interpretation of nonlinear boundary problems during seismic events.

They offer a dependable tool for the seismic design of tunnels, encompassing soil-structure interaction and irreversible soil behavior. (Bilotta et al., 2014)

The time history of accelerations is defined as input. Unit of the acceleration has to be

m/s^2.

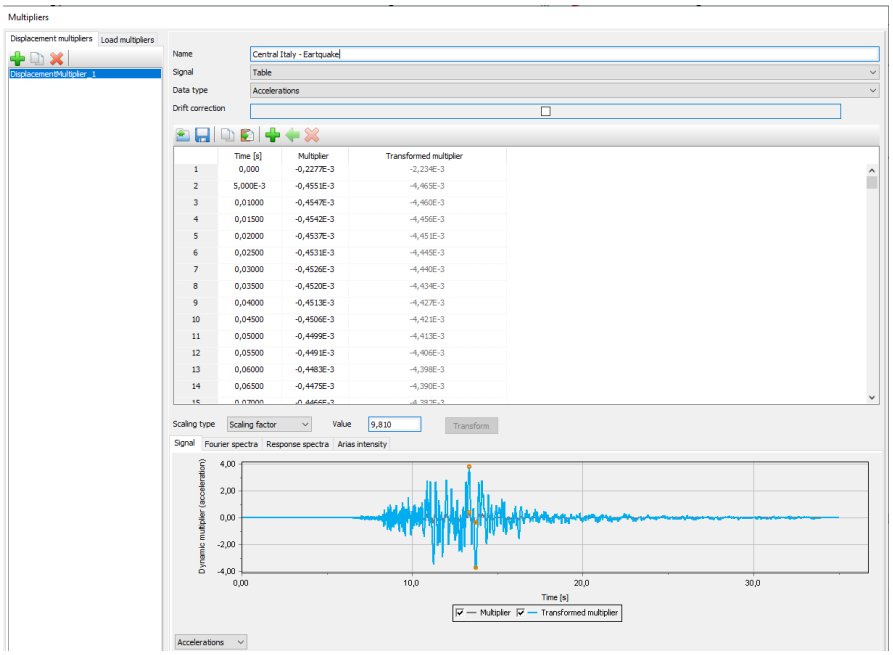

Figure 2-20 Time history acceleration

The time history of acceleration representing the reference input motion of the 7 earthquakes are imposed at the complaint base of the model. In this context, a "complaint base " signifies a fixed-end boundary, indicating that any downward-traveling waves within the soil will be entirely reflected toward the ground surface by the rigid layer. Interface has to be defined at the bottom and side boundaries inactively.

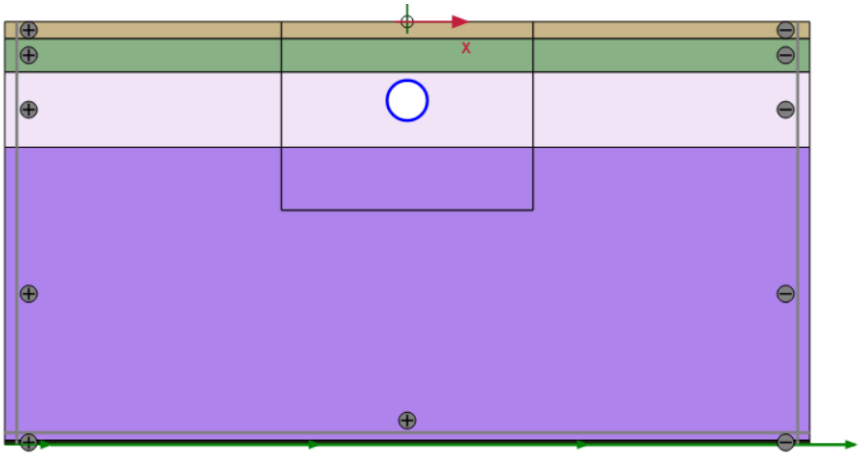

Figure 2-21 Plaxis 2D Numerical Model

Rayleigh damping formulation

Dynamic boundary condition of the sides is define viscous. Viscous damping is of Rayleigh type due to its simplicity in implementation within numerical procedures. It can be expressed as follows:

$$[C] = \alpha * [M] + \beta * [K] \tag{45}$$

Where:

- α mass-proportional proportional coefficients
- β stiffness-proportional coefficients.

The coefficients can be obtained based on the following equations:

$$\begin{Bmatrix}\alpha\\ \beta\end{Bmatrix} = \frac{2\xi_{tar}}{\omega_1+\omega_2}\begin{bmatrix}\omega_1\omega_2\\ 1\end{bmatrix} \quad (46)$$

$$\xi = 1/2\ (a/w + \beta * w) \quad (47)$$

$$w_i = 2\pi f = \frac{V_{s,av}}{4H} *2\mathrm{H} \quad (48)$$

$$w_j = n * w_i \quad (49)$$

$$\xi_{min} = \sqrt{a * \beta} \quad (50)$$

$$f_{min} = \frac{\sqrt{\frac{a}{\beta}}}{2\pi} \quad (51)$$

Where:

- $\omega_1 = \omega_I$ and $\omega_2 = \omega_j$ are the two parameters which ensure the frequency range,
- ξtar is the target damping ratio,
- f_{min} represents the central position of the approximate frequency-independent range,
- ξmin is the corresponding critical damping ratio.
- n is coefficient 3-6 (it is accepted 5 in thesis)

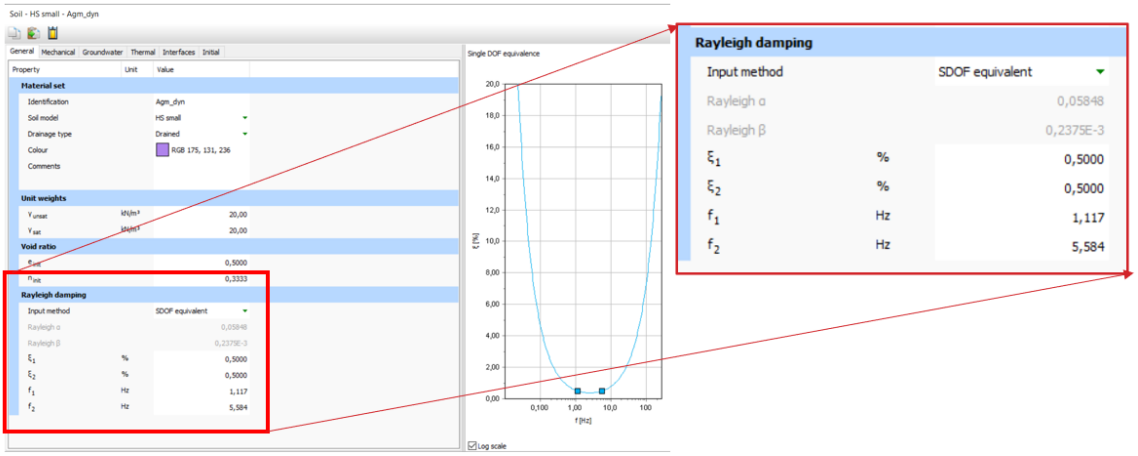

Figure 2-22 Plaxis 2D Input

Chapter 3

3 Case Study: Metropolitana di Catania Lotto 1

3.1 Project Definition

The executive project of the Stesicoro-Aeroporto - Lot 1 underground section, which is part of the railway line upgrading and transformation program launched by Ferrovia Circumcenter in order to progressively transform the current narrow-gauge line into an ordinary-gauge and electrified line, is selected as case study.

The lot consists of a section of single-track twin-track tunnel, which runs for a length of approximately 2176.92 m from the Stesicoro station (near Piazza Stesicoro) in the center of Catania, to the Via Palermo area in the south-east of the city.

Figure 3-1 Spatial localization of the Stesicoro-Aeroporto route (section in light blue)

The alignment relating to this structural lot concerns the section between the Stesicoro Station and the Palestro Station, which runs largely within the urban fabric of the city of Catania.

For the construction of the main tunnels of the section, the use of a tunnel boring machine characterized by an excavation diameter of 10.60 m is foreseen.

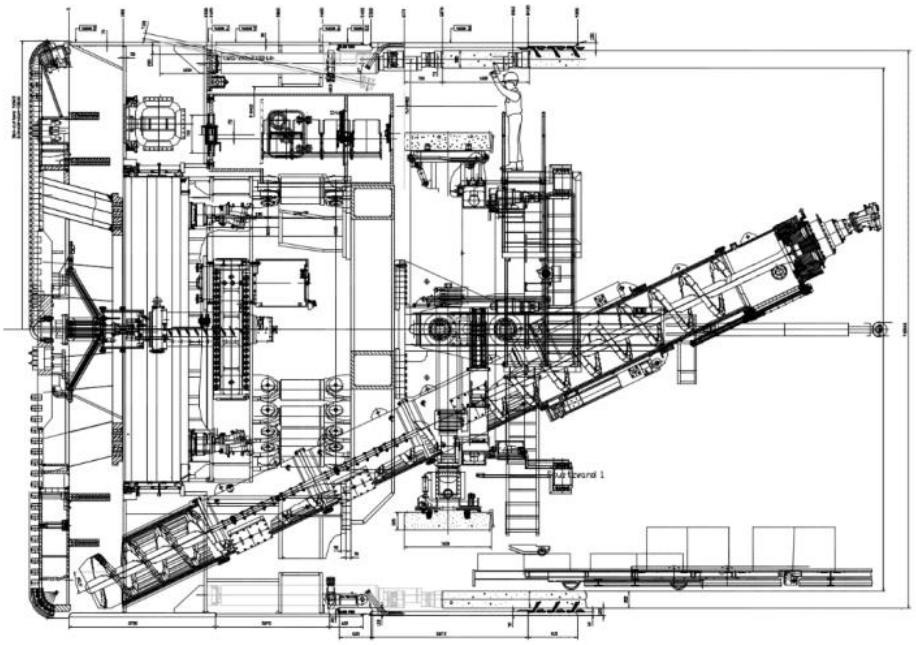

Figure 3-2 Schematic diagram of the shield tunnelling machine

The tunnel will have an internal diameter of 9.60 m and lining thickness of 0.32 m

For the construction of the line tunnel (double track), the use of an integral mechanized excavation shield machine (EPB TBM) is planned, with pressure support of the face. The lining consists of a ring of prefabricated, reinforced concrete elements assembled inside the shield of the machine.

Segments Characteristic and Material Properties

The final lining consists of prefabricated reinforced concrete rings 150cm long and 32cm thick. The characteristics of the tunnel lining ring excavated in mechanized excavation with the following:

- Internal Diameter: 9.60m
- Thickness of the Segmental Lining: 0.32m
- Type of the Ring: 6+1 conci

Material Properties

Concrete for Precast Segments with Traditional Reinforcement

- Class: C45/55
- Characteristic cubic calculation strength: Rck ≥ 55 MPa
- Characteristic cylindrical strength at 28 days: fck = 45 MPa
- Modulus of elasticity: Ec = 36283 MPa
- Concrete calculation resistance: fcd = Rck x 0.83/γc
- Poisson's Coefficient: ν = 0.2

Reinforcement bar steel

- Weldable, improved adhesion bars, type B450C with the following mechanical properties
- Characteristic ultimate tensile stress ftk ≥ 540 MPa
- Characteristic yield stress fyk ≥ 450 MPa
- Net concrete cover c'=4cm

3.2 Site Characterization and Critic Section

The definition of the soil categories present in the area crossed by the planned route was made possible through the interpretation of the data emerging from the geophysical investigation campaign carried out for the executive design, and in particular the HVSR passive seismic measurements (obtained in the same position as the boreholes) and the Down Hole tests. Below is a summary table of the investigations performed with the definition of the soil category.

Tromografic Boreholes	TSi1	TSi2	TSi3	TSi4	TSi5	TSi6	TSi7	TSi8	TSi11	TSi12	TSi15	TSi16	TSi17	TSi17b	TSi17c	TSi19	TSi20	TSi21	TSi22
$V_{s,30}$ (m/sec)	441	377	335	310	382	321	278	398	397	427	353	441	327	391	377	287	512	338	303
Soil Type (NTC2018)	B	B	C	C	C	B	C	C	B	B	C	B	C	B	B	C	B	C	C

Table 3-1 Summary table of subsurface categories for each survey in Seismic Tomographs

Down Hole BoreHoles	$V_{s,30}$ (m/sec)	Soil Type (NTC2018)
DHSi9	533	B
DHSi13	486	B
DHSi18	352	C

Table 3-2 Summary table of subsurface categories for each survey in Down-Hole Test

Site specific response analysis is mandatory for soil classes D or E according to the codes. Recommended for soil class C. In addition, the reliability of Down-Hole test results is higher than HSRV tests. Therefore, section pk 3+700 where DHSi18 and TSi17 were carried out, is selected critical section.

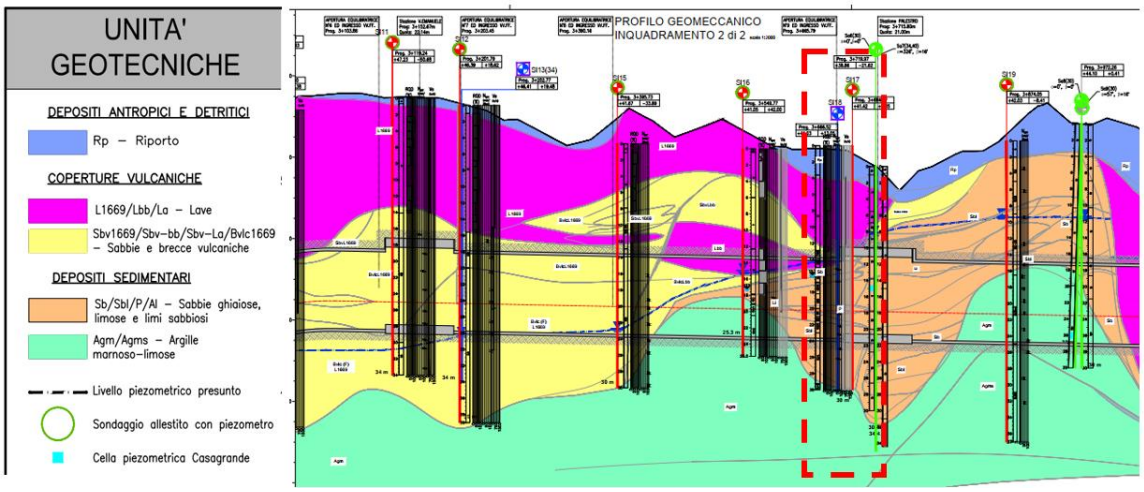

Table 3-3 Geologic Profile and Critic Section

Section Properties

- Overburden: 14m
- Water Depth: 14m from Surface Level
- Formation;

1) Rp – Riporto
2) L1669 - Lave
3) Sbl – Sabbie ghiaiose, limose e limi sobbiosi
4) Agm : Argille mornoso - limose
5) Bed Rock

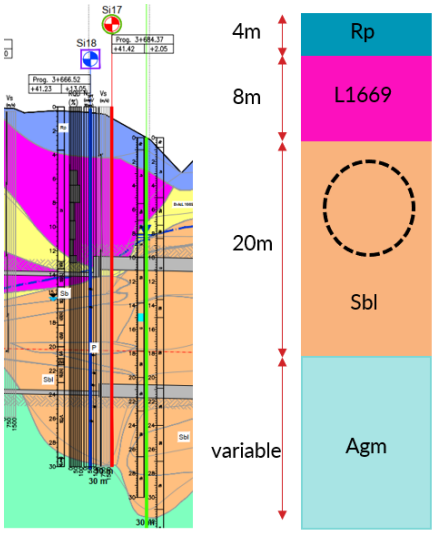

Figure 3-3: Schematic Soil Profile

3.2.1 Formations

Along the development of the tunnel, the set of on-site and laboratory investigations allowed the identification of the following geotechnical units that will affect the excavation:

3.2.1.1 Rp – Topsoil (Terreno Riporto)

These are areas of accumulation of landfill and building waste material, archaeological remains or from the collapse of historic buildings (area of the historic centre within the perimeter of the 16th-century fortifications). These are very heterogeneous deposits, predominantly sandy, sandy-loam and silty, not very thick and not very consistent with limestone and basaltic stone inclusions ranging from centimetric to decimetre in size. The thickness varies up to a maximum of 9 m, found within drill hole SI20, but also confirmed by soundings carried out during the Final Project (S0, S8 and S10)

3.2.1.2 L1699-Lava

This formation contains a series of geological elements with the period of casting as the discriminating factor. From a geotechnical-geomechanical point of view, in general the elements vary in appearance from compact to porous. Occasionally material is present in fractured condition, but in general the observation of the borehole boxes shows material of good quality.

3.2.1.3 Sbl- Yellowish silty sands and sandy loams

From a geotechnical point of view, the properties gradually change from an unconsistent to consistent behaviour, but nevertheless the sandy component is retained, which provides significant attritional values.

3.2.1.4 Agm - Marly-loamy clays

The unit appears to exhibit some variability in behaviour. Evidence from excavations within the formation showed it to be very competent, while laboratory tests indicated the material to have average characteristics within clays. This difference in behaviour, as will be reported below for other formations, is probably linked to the scale of observation, as the laboratory provides results at an extremely small scale, while at the macroscale the presence of marly elements allows, on the one hand, an increase in strength but also (and perhaps above all) prevents the clay component from decaying its mechanical properties (in general, the volumetric deformability modulus of clays is a function of the average stress and the shear modulus of the deformation level)

3.2.2 Site and Laboratory Test Results

At the critical section area, 2 boreholes have been carried out, one for sampling another one for Down-Hole test. The depth of the borehole is 30m.

3.2.2.1 Borehole Sampling – Si17

Sondaggio Si17 - Cassetta 1 – Prof. 0.00-5.00 m

Sondaggio Si17 - Cassetta 2 – Prof. 5.00-10.00 m

Sondaggio Si17 - Cassetta 3 – Prof. 10.00-15.00 m

Sondaggio Si17 - Cassetta 4 – Prof. 15.00-20.00 m

Sondaggio Si17 - Cassetta 5 – Prof. 20.00-25.00 m

Sondaggio Si17 - Cassetta 6 – Prof. 25.00-30.00 m

Figure 3-4 Borehole Si17 - Sampling

3.2.2.2 Geophysical Test Results

DOWN-HOLE SI18

DH 18	Peso per unità di volume γ	Vp	Vs	Coefficiente di Poisson σ	Modulo di taglio G_{din}	Modulo di Young E_{din}	Modulo di Bulk K_{din}
Profondità (m)	(Kg/mc)	(m/s)	(m/s)		(kg/cmq)	(kg/cmq)	(kg/cmq)
2	2700	343	171	0.34	787	2103	2134
4	2700	1571	259	0.49	1818	5403	64182
6	2700	2074	689	0.44	12811	36843	99013
8	2700	1942	582	0.45	9137	26510	89681
10	2700	2092	661	0.44	11788	34058	102447
12	2700	1949	657	0.44	11653	33465	87013
14	2700	823	405	0.34	4430	11877	12399
16	1900	870	359	0.40	2454	6858	11120
18	1900	849	319	0.42	1929	5470	11116
20	1900	780	338	0.38	2165	5995	8668
22	1900	745	311	0.39	1837	5124	8101
24	1900	754	318	0.39	1927	5362	8225
26	1900	777	344	0.38	2252	6205	8475
28	1900	711	330	0.36	2064	5627	6856
30	1900	763	340	0.38	2200	6054	8117

Vs_{30}= 352 m/s

Figure 3-5 Down-Hole Test Result

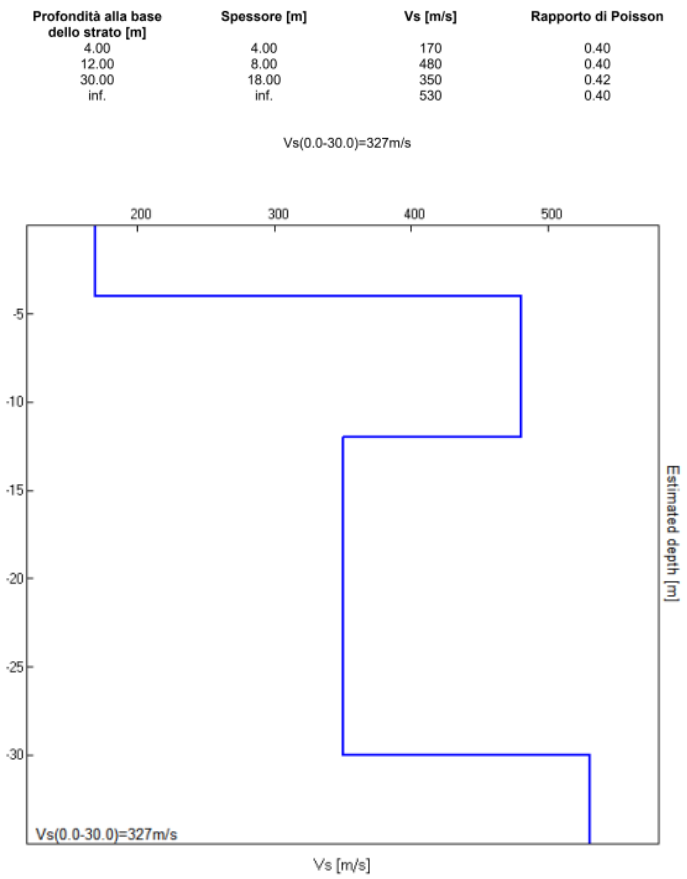

Figure 3-6 HSRV Test Results

3.2.3 Bedrock Depth and Vs Profile

Unfortunately, the survey investigation was limited to a depth of approximately 30 meters. The shear wave velocity recorded at this depth was 352 m/s (Figure 3-5), significantly deviating from the minimum required Vs value of 800 m/s for bedrocks according to both Italian and European technical regulations Depth of the bedrock is important parameters for SSR analysis. Literature research has been carried out.

In order to obtain this seismic input reference to create scenario earthquake that occurred in eastern Sicily in 1693 has been carried some research in Catania (Grasso et al., 2005) and (Priolo, 1999). They used a source mechanism modelling, assuming the source to be under the sea along the Hyblean–Maltese fault (Figure 3-7). Six transects have been selected for investigation; transect t01 crosses the area investigated in our project area. Seven points (P1–P7) have been chosen along each transect. Point P1 exactly represent our case study area.

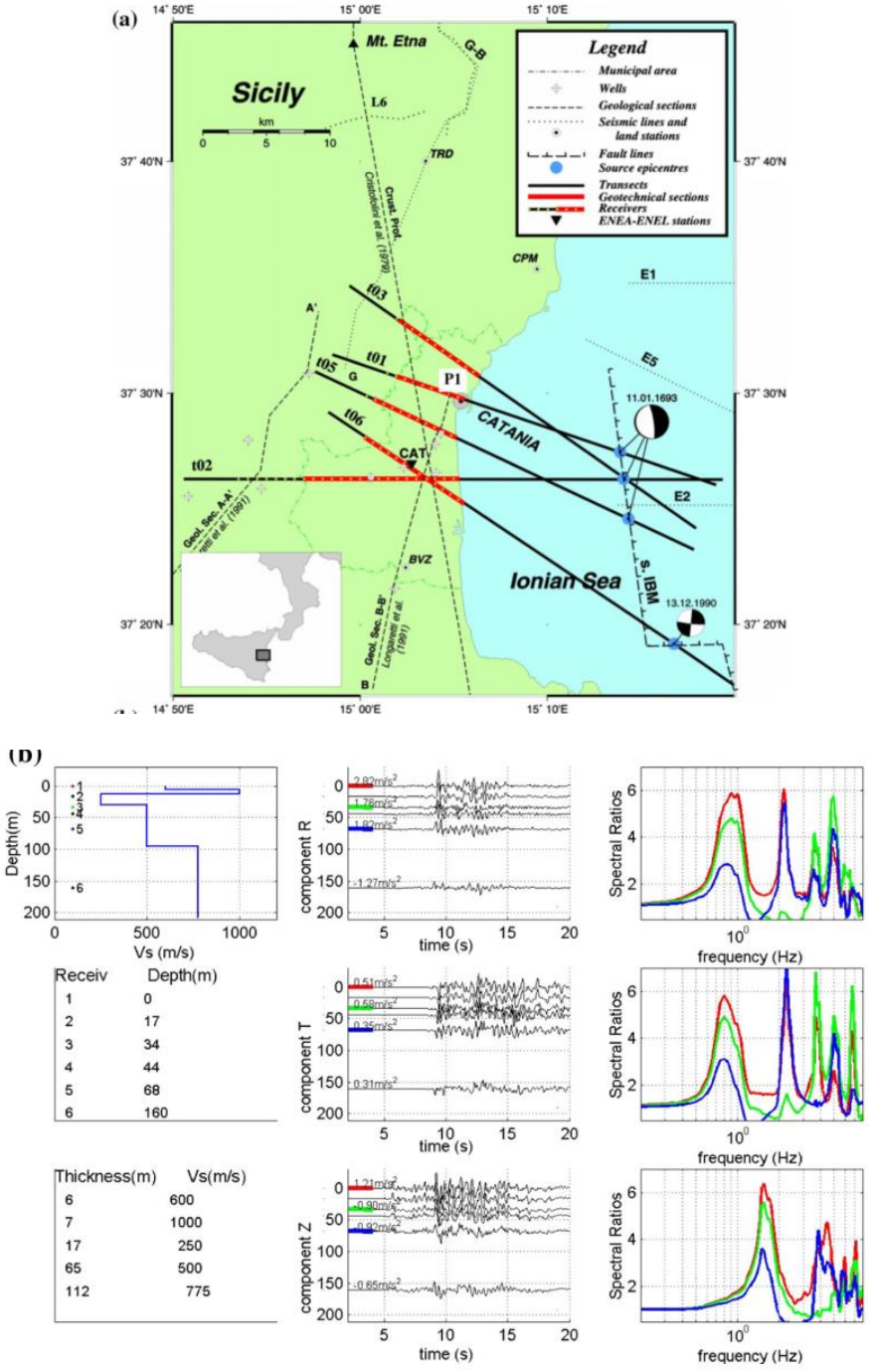

Figure 3-7 Seismic input for the scenario earthquake in Catania: a transects; b graphs related to the first point(P1) of transect t01: Vs profile, position of the receivers, accelerograms (in the radial, transverse and vertical components), spectral ratios ((Abate & Massimino, 2017)

Vs profile has been derived from results till 200m depth (Figure 3-7b). It arrived to 800m/s at 100 m depth. It is accepted bedrock depth. Figure 3-8 is presented V_s values which comes from Down-Hole Test, HSRV and Literature.

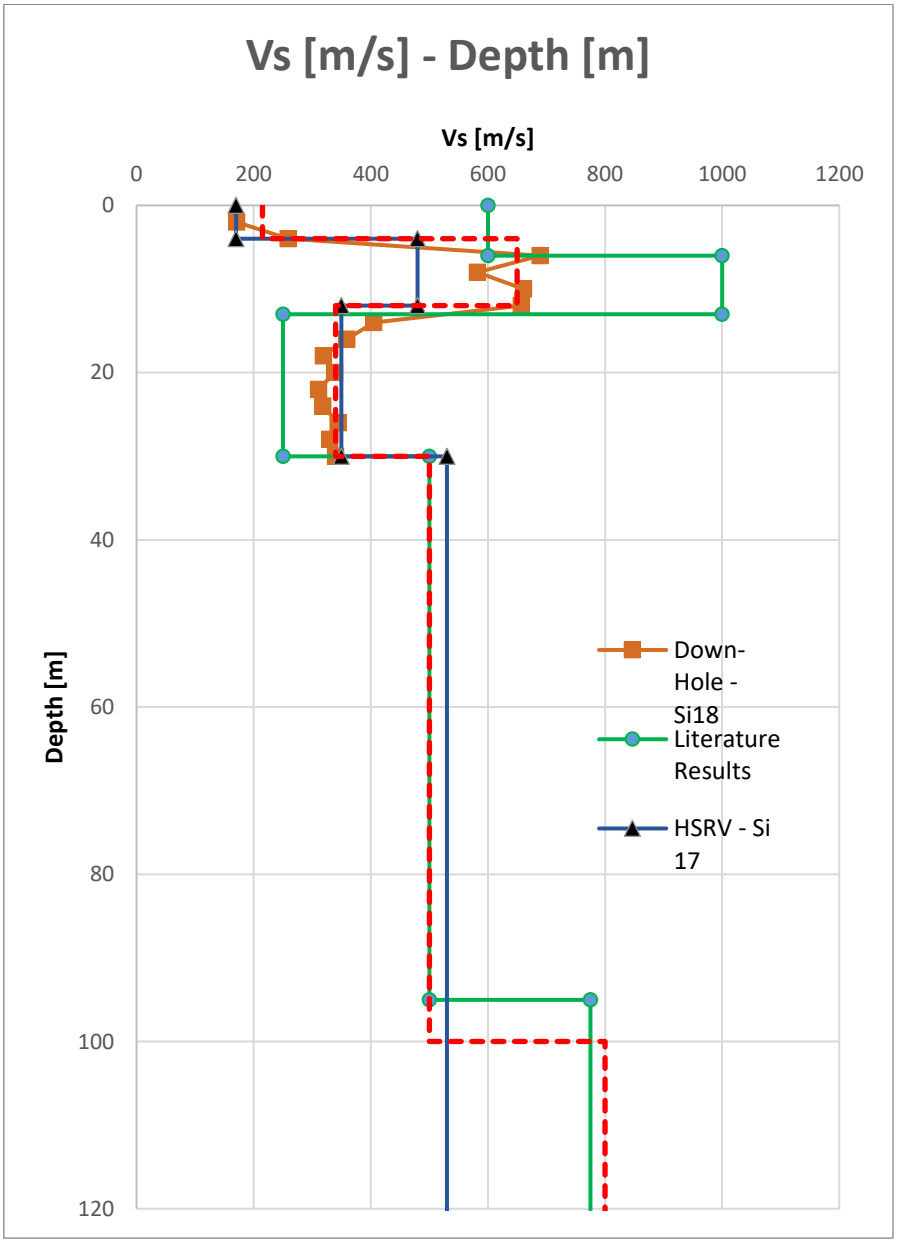

Figure 3-8 Vs-Depth Graph

The down hole test results are taken as $V_{s,design}$ values as it is more accurate result. Lower than 30m, Literature result has been considered to determined $V_{s,design}$ values.

Geological Unit	Thickness	Depth		Vs,design
-	[m]	Start[m]	End [m]	[m/s]
Riporto - Rp	4	0	4	215
Lave - L1669	8	4	12	650
Silty Sand - Sbl	18	12	30	340
Marly-Silty Clays - Agm	70	30	100	500
Bedrock	Inf.	100	Inf.	800

Table 3-4-Formation, Thickness and $V_{s,design}$ values

3.2.4 Decay Curve of Modulus and Damping

As explained in Chapter 2.1.1, laboratory experiments are required to obtain the decay curve and dumping values. However, the experiments mentioned in chapter 2.1.1 have not been carried out. therefore, these curves have been decided by literature studies.

Cavallaro et al., n.d. have been studied about site characterization at the Catania city.to assess slope stability, liquefaction potential, and foundation stability, as well as to in estigate soil-structure interaction, a total of 12 testing locations have been identified for the detection of ground properties.

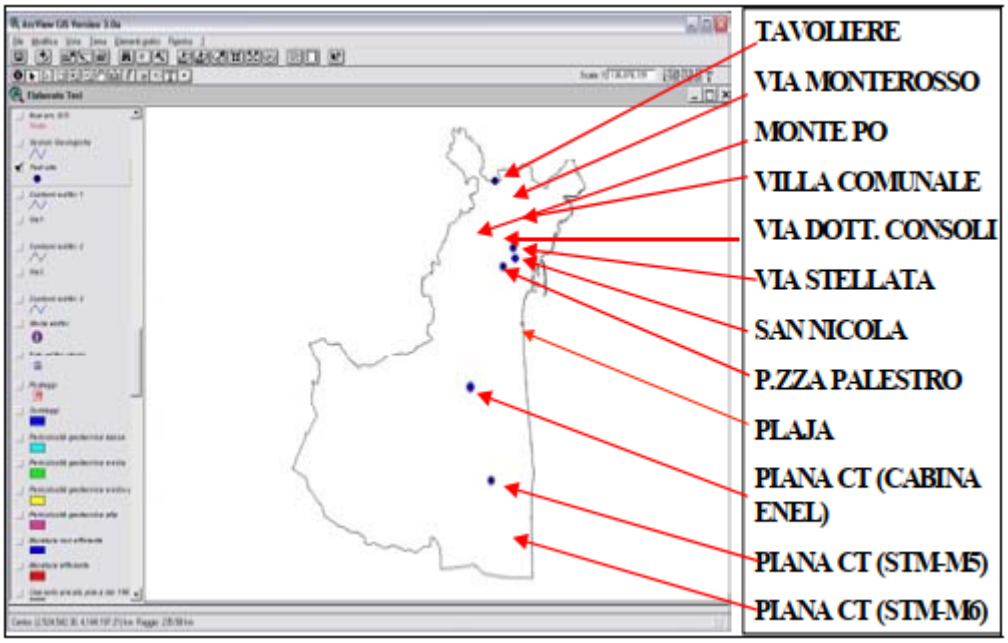

Table 3-5 Test site location (Cavallaro et al., n.d.)

Each location represents a soil formation type as mentioned in Table 3-6

Formation	Test Site
Clayey soil in the Catania plain.	No. 1 Piana di Catania (STM-M5)
	No. 2 Piana di Catania (ENEL box);
	No.12 Piana di Catania (STMM6)
Silica sandy liquefiable soil	No. 3 Playa beach
Stiff soil (scoriaceous lava) over soft soil	No. 4 Tavoliere
Clayey soil in the central area	No. 5 Via Stellata
	No. 11 Villa Comunale
Volcanic sand	No. 6 Piazza Palestro
Scoriaceous lava	No. 7 San Nicola alla Rena Church
	No. 9 Via Monterosso
Clayey soil in the central area	No. 8 Via Dottor Consoli
Terreforti clays	No. 10 Monte Po

Table 3-6 Test Site – Sample Formation

Boreholes at the designated test sites were subjected to in-situ tests and laboratory

examinations conducted on undisturbed samples extracted from these boreholes. The location No. 6 Piazza Palestro is related to volcanic sand. The locations No. 5 Via Stellata and No. 11 Villa Comunale are related to clayey soil in the central area. In Figure 3-9, It is shown that location of the test sites and tunnel critic section. Test point location has accapeble distance to consider for our analysis.

Figure 3-9 Critical Section and Test Point 5 and 6

Resonant Column Tests and Cyclic Loading Torsional Shear Tests have been performed No. 5 Via Stellata (Cavallaro et al., 1999) (Cavallaro et al., 1999) No. 6 Piazza Palestro (Cavallaro & Maugeri, 2005); These have been applied also other points.

The analysis of the findings relies on the equation introduced by (Yokota et al., 1981)

$$\frac{G_{(\Upsilon)}}{G_o} = \frac{1}{1+a*\Upsilon*(\%)^{\beta}} \quad (52)$$

Where:

- $G_{(\Upsilon)}$ = strain dependent shear modulus
- Υ= shear strain (in percent)
- α,β = soil constants

$$\xi(\Upsilon)(\%) = \eta * \exp(-\lambda * \frac{G_{(\Upsilon)}}{G_o} \quad (53)$$

Where:

- $\xi_{(\Upsilon)}$ = strain dependent damping ratio
- Υ= shear strain (in percent)
- η,λ = soil constants

(Cavallaro et al., n.d.) has been determined soil constants depends on the soil formatiom.

Site	α	β	η	λ
1. Piana di Catania (STM–M5) 2. Piana di Catania (ENEL box) 12. Piana di Catania (STM-M6)	7.15	1.223	19.87	2.16
3. Plaja beach	9	0.815	80	4
4. Tavoliere	-	-	-	-
5. Via Stellata 11. Villa Comunale	11	1.119	31	1.92
6. Piazza Palestro	6.9	1	23	2.21
7. San Nicola alla Rena Church 9. Via Monterosso	7.5	0.897	90	4.5
8. Via Dottor Consoli	16	1.2	33	2.4
10. Monte Po	-	-	-	-

Table 3-7 Soil constant values for evaluation ofG(γ) and ξ(γ): sites No. 1, 2 and 12clayey soil in the Catania plain; site No.3 silica sandy soil; sites No. 5 and 11clayey soil in the central area; site No. 6volcanic sand; sites No. 7 and No. 9scoriaceous lava; site No. 8 clayey soilin the central area.

Unfortunately, There is no any test or litterateur research for Lava (L1699) in Catania, Decay curve for rock which is presented by (Schnabel et al., 1972) is accepted for L1669 formation.

Finally , decay curves of modulus and damping factor is determined as in Figure 3-10.

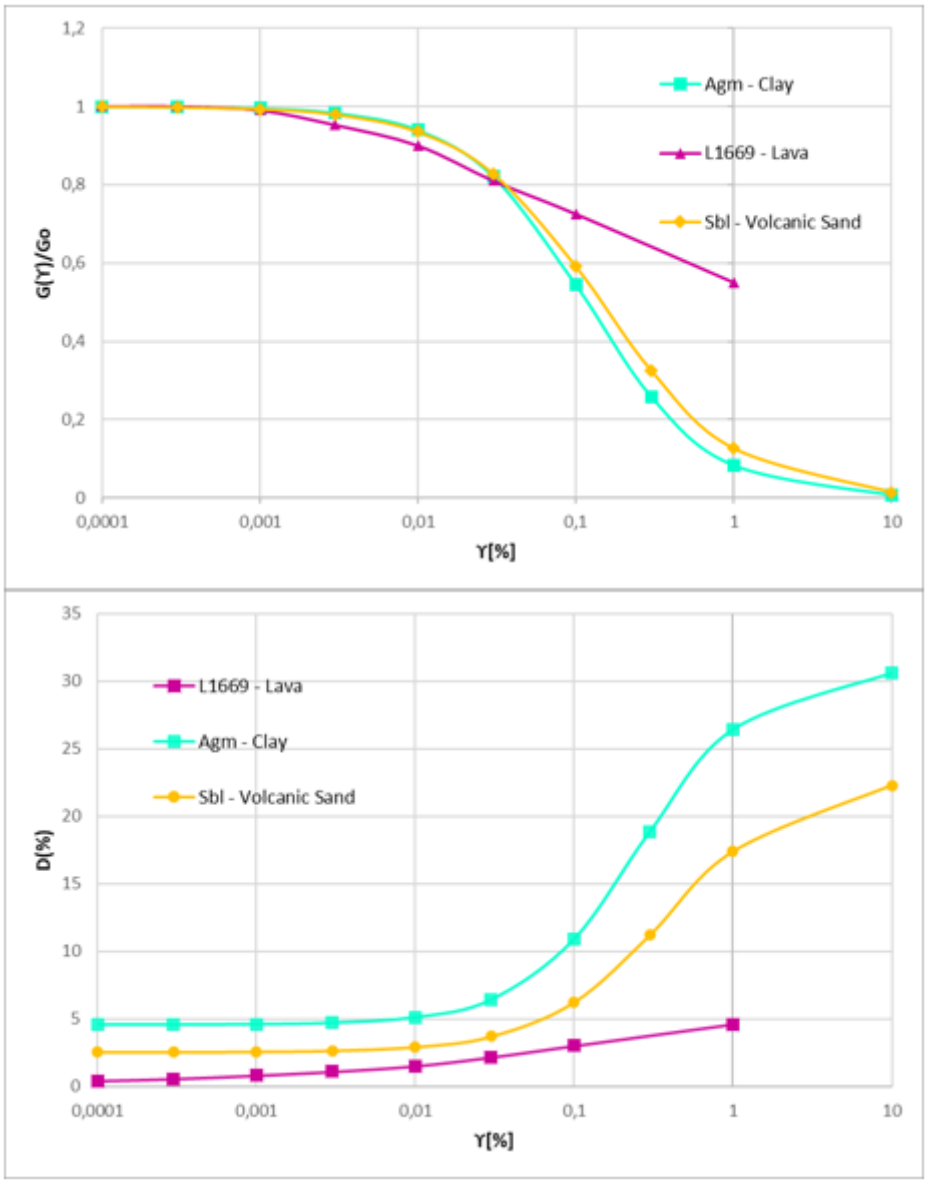

Figure 3-10 Decay curves of modulus and damping factor

3.2.5 Geotechnical Properties

In the case study project, geotechnical parameters of the formations were determined by using field tests, laboratory test results and literature, these values are summarized in the table below for the critical section.

Geological Unit	Thickness	Depth		Vs,design	ϒ	c'	Φ'	E'	Go	Poisson
-	[m]	Start[m]	End [m]	[m/s]	[kN/m^3]	[kPa]	[°]	[Mpa]	[Mpa]	[]
Riporto - Rp	4	0	4	215	18	5	30	20	85	0,3
Lave - L1669	8	4	12	650	24	300	45	5000	1033	0,3
Silty Sand - Sbl	18	12	30	340	19	1	35	100	224	0,3
Marly-Silty Clays - Agm	70	30	100	500	20	30	22	200	510	0,3

Table 3-8 Geotechnical Parameters at the pk 3+700

Chapter 4

4 Seismic Hazard Assessment and Site Response Analysis

4.1 Seismic Hazard Assessment

The Italian seismic code, grounded in Probabilistic Seismic Hazard Analysis (PSHA), determines the "design earthquakes" by calculating the average return period of ground motions that surpass a specified intensity measure (IM) threshold at the designated site. This involves considering parameters such as magnitude, location, faulting style, and other relevant factors.(Bilotta et al., 2014)

- 1. Identification all earthquake sources capable of producing damaging ground motions;
- 2. Characterization of the earthquake magnitudes distribution (the rates at which earthquakes of various magnitudes are expected to occur);
- 3. Characterization of the source-to-site distances distribution associated with potential earthquakes;
- 4. Prediction of the resulting distribution of ground motion intensity as a function of earthquake magnitude, distance, etc., by adopting ground-motion prediction equations;
- 5. Combination of uncertainties in earthquake size, location and ground motion intensity, using a calculation known as the total probability theorem;(Hashash et al., 2001)

4.1.1 Geological Framing

The area under study is in the central region of the Mediterranean (Figure 4-1) and owes its geological-structural setting to the convergence process between the European plate and the African plate that, during the Tertiary, leads to the formation of the Apennine-Maghrebid chain. In particular, the urban area of Catania is located in the eastern portion of Sicily, near the collisional front of the Apennine-Maghrebid chain, which developed, as mentioned earlier, as a consequence of the Africa-Europe convergence of the Neogene-Quaternary.

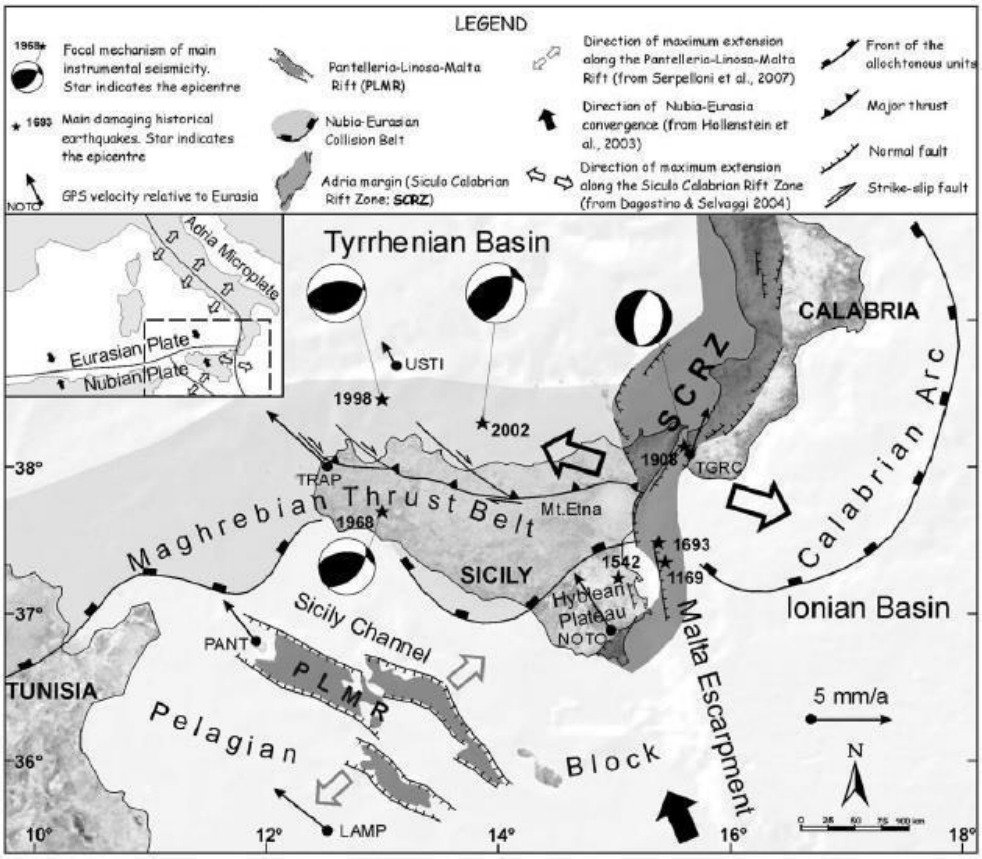

Figure 4-1 Schematic Map of Central Mediterranean Tectonics (Catalan et al., 2008)

In broad outlines, the geological framework of the area sector under consideration can be considered the result of the combined action of three main processes related to coastal dynamics controlled, during the Quaternary period, by numerous changes in the eustatic level, tectonic and volcanic activity, and finally to recent anthropogenic processes.

The area under study, located at the southern edge of the built-up area of Catania, is characterized by very bland morphological forms, with low-acclivity slopes sloping toward the the sea shaped by numerous alluvial and marine terraces.

In this study, reference will be made to the nomenclature of formations proposed in the Geological Map of Italy (CARG), which is the official reference for geological studies.

The substratum consists of sedimentary successions formed by silty clays, dated Lower-Middle Pleistocene (Formation of "Gray-Blue Clays" - FAG - of the CARG Geological Map, of deltaic environment, corresponding to the PD's Agm), which transition upward to coastal sands and fluvio-delta conglomerates of Middle Pleistocene age (Formation of "Sands and Gravels of the Village of St. George" - GII, corresponding to the PD's "Terraforti").

Also present are patches of ancient alluvial terraces formed in ancient times when the watercourse flowed at higher elevations than the present valley floor.

Above and partly also intermixed with this sedimentary succession are lava flows basalt that invaded the area in prehistoric and historic times and consist of different units: the Ancient Alkaline Centers

unit (180-100 ka), the Trifoil unit (80 - 60 ka) and the Mongibello (< 40 ka).
In the southernmost sector of the route, in the area of the S. Maria Goretti and Airport, there are alluvial deposits (fluvio-lacustrine and marshy) of recent times that fill in the Catania plain behind the old (but relatively recent - Holocene) dune coastal.

4.1.2 Geomorphological Framing

The Palestro Station and last part of the project, the original morphology of the sedimentary substrate, characterized by deep paleo-valleys and marine terraces, has been, in part, obliterated by Holocene lava flows originating from eruptive fissures located in the southern slope of Mount Etna. In the latter area, the historic city and residential neighbourhoods have developed, and therefore the original morphology is obliterated by urbanization.

4.1.3 Historical Seismicity and Seismic Classification

4.1.3.1 Seismic Hazard

The main seismic characteristics of the area under consideration are described below.

Seismic hazard was assessed by consulting the "Database of Individual Seismogenic Sources" - DISS (DOI:10.13127/diss3.3.0, 2021). The extracted information is used to obtain the magnitude-distance pairs representative of the seismicity of the area under consideration. The main cataloging element of the DISS consists of seismogenic sources represented in the three dimensions, obtained by parameterizing the geometry (how the fault is positioned) and kinematics (how the fault can move) of large active faults believed to be capable of generating earthquakes of magnitude (Mw) greater than 5.5.
The sources of the strong earthquakes that struck Sicily have not yet been unequivocally identified, however, the catalog of seismogenic sources in Italy "Database of Individual Seimogenic Sources, DISS" (https://diss.ingv.it/diss330/dissmap.html), based on geological, seismological, and geophysical evidence, has identified numerous structures capable of producing earthquakes of magnitude greater than 5.5
The Figure 4-2 shows the results for Sicily, distinguishing between Individual Sources, which do not necessarily represent all potentially existing sources (because the earthquakes for which they were derived are a subset of all earthquakes) and Composite Sources, which represent a homogeneous set of possible seismogenic sources.

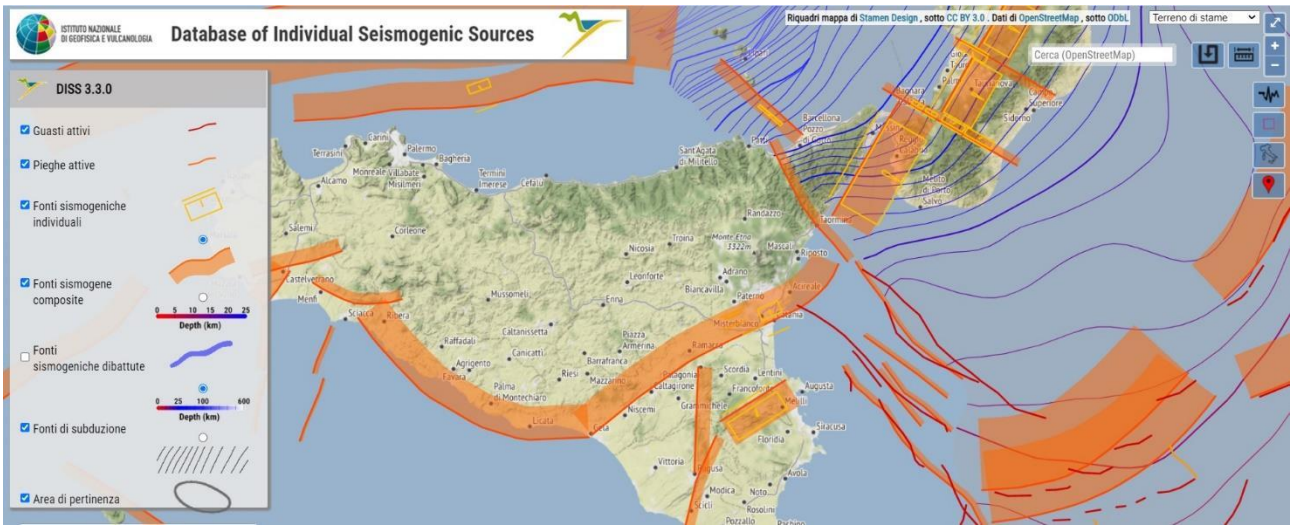

Figure 4-2 : Database "Individual Seismogenic Sources" (FONTE INGV - DISS 3.3.0)

In addition, the area in which the route falls was analysed from a tectonic point of view; it can be seen that this eastern portion of Sicily has a number of direct, active faults that do not fall within the area covered by the metropolitan section of the project. Referring to the Database provided by ISPRA (ITHACA - Catalogue of Capable Faults), it can be observed that the faults are typically arranged in a north-south direction, but the tectonic structure close to the project area is in an E-W direction. In the following Figure 4-4, the faults are shown in red, and the project area is identified in red circle

Figure 4-3Figure 4-4 : Excerpt of capable faults of the western portion of eastern sicily- ithaca working group (a database of active capable faults of the Italian territory. version december 2019)

First fault is named as San Calogero, its' kinematic is Normal fault, second is named Scaspata di Malta:01, its' kinematic is Normal fault.

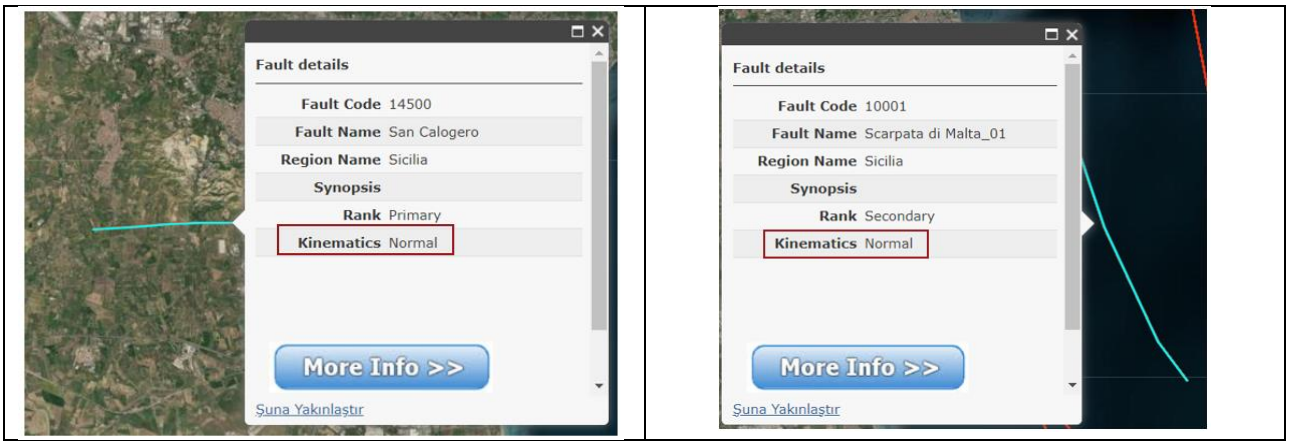

Figure 4-5 Faults Kinematics a) San Caogero and b) Scapata di Malta_01

4.1.3.2 Historical seismicity and seismic classification

The seismic history of a site, which is the chronological list of the effects caused by earthquakes near and far from the site itself, evaluated in macro seismic intensity, is the essential basis for establishing the earthquake's impact on the area over time and can also be used to assess hazard directly from intensity data at the site using a recently developed method (Magri et al., 1994).

In Catania, the greatest effects are related to the activity of regional faults, which develop along the Ionian coast of Sicily; minor damage is caused by earthquakes located in the Strait of Messina and in the inland area of the Hyblean Plateau.

Figure 4-6 Epicentres of major earthquakes in the period 1125-1990 that caused damage or were felt in Catania (from Carbone et alii, 2010)

In order to have suitable elements to evaluate the level of seismicity that characterises the territory within which the project area is integrated, a reconstruction of the historical series of events was carried out, aimed at ascertaining the macro seismic effects recorded in the past in the area of interest.

In particular, the seismicity of the area is widely documented in many archives, which the National Institute of Geophysics and Volcanology (INGV), has accounted for through the DBMI11 Macro seismic Database (M. Locati, R. Camassi and M. Stucchi (eds.), 2011. DBMI11, the 2011 version of the Italian Macro seismic Database and Locati et al., 2016. Milan, Bologna, http://emidius.mi.ingv.it/DBMI11. DOI: 10.6092/INGV.IT-DBMI11), used for the compilation of CPTI11 (Parametric Catalogue of Italian Earthquakes).

The Italian Macro Seismic Database DBMI15 (Locati et al., 2016) was initially consulted to define the historical seismicity of the area targeted by the project interventions. Figure 4-7 shows, for the municipality of Catania in which the project interventions fall and for each seismic event resented: date (year, month, year), epicentral area, epicentral intensity I0 (MCS scale values), MW moment magnitude (estimated from empirical or measured correlations) and intensity at the IS site (MCS).

Examination of the seismic history, in the catalogue, shows that the maximum resentment in the area under study (if the 1693 earthquake is excluded), with Mw=7.32, was reached during the 1908 Strait of Messina earthquakes, with Mw=7.10, Southern Calabria in 1783, with Mw=7.10, Central Calabria in 1905, with Mw=6.95, and Marsica in 1915, with MW magnitude of Mw=7.08.

A catalogue of historical seismic events that have characterized the area of the project.

Catania

PlaceID	IT_67809
Coordinate (lat, lon)	37.502, 15.087
Comune (ISTAT 2015)	Catania
Provincia	Catania
Regione	Sicilia
Numero di eventi riportati	159

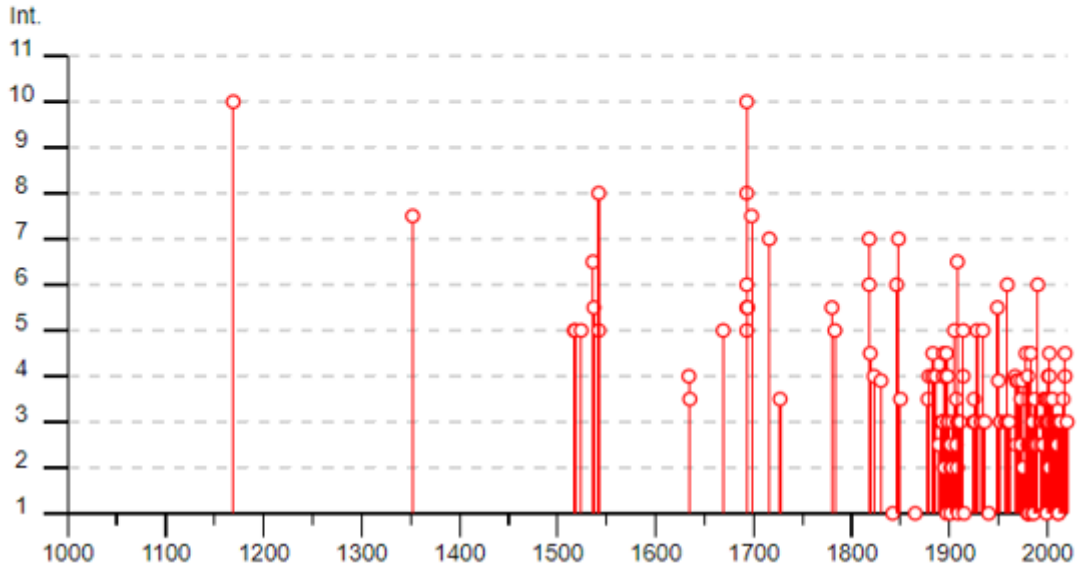

Figure 4-7 Fonte Database Macrosismico Italiano DBMI15 (https://emidius.mi.ingv.it))

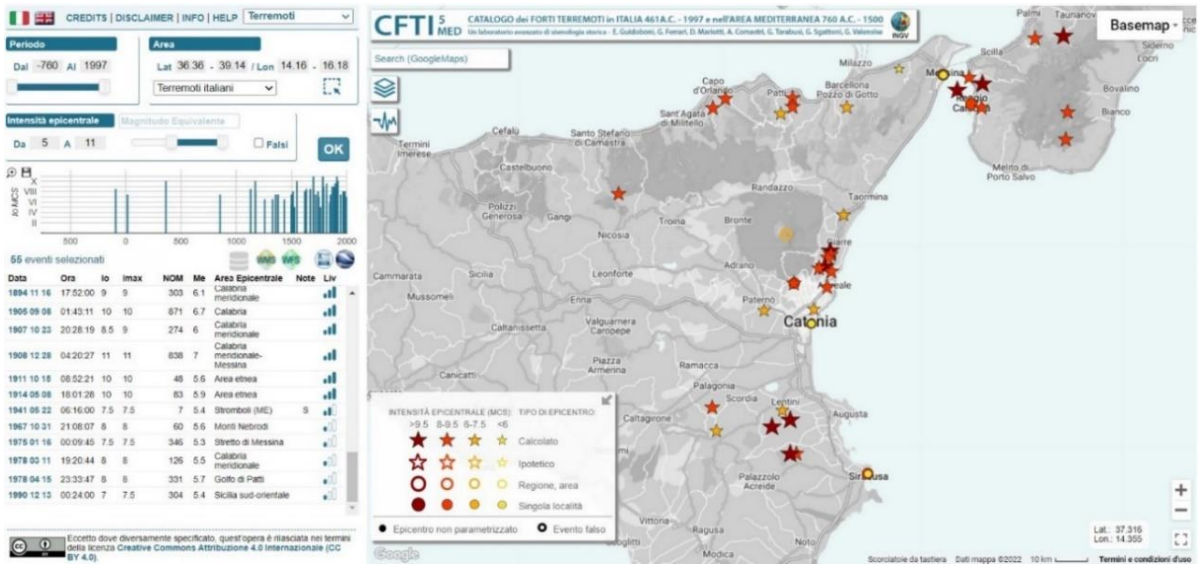

Figure 4-8 Catalog of strong earthquakes in Italy from 461 BC to 1997 - Source CFTI med from INGV

4.1.3.3 Disaggregation

The peak acceleration a_{max} from probabilistic approach (and thus relative to a certain TR) is the result not of a single magnitude value but of the contribution of the different magnitudes that contribute to the hazard of a site. The disaggregation method of a(g) referring to the site of interest was used to

determine the representative magnitude for the area under consideration.

This method allows defining the contribution to the hazard of a site of different seism genic sources at distance (D) capable of generating earthquakes of magnitude (M). In other words, the disaggregation process in (M-D) provides the earthquake that dominates the hazard scenario (scenario earthquake) understood as the magnitude (M) event at a distance (D) from the site under study that contributes most to the seismic hazard of that site.

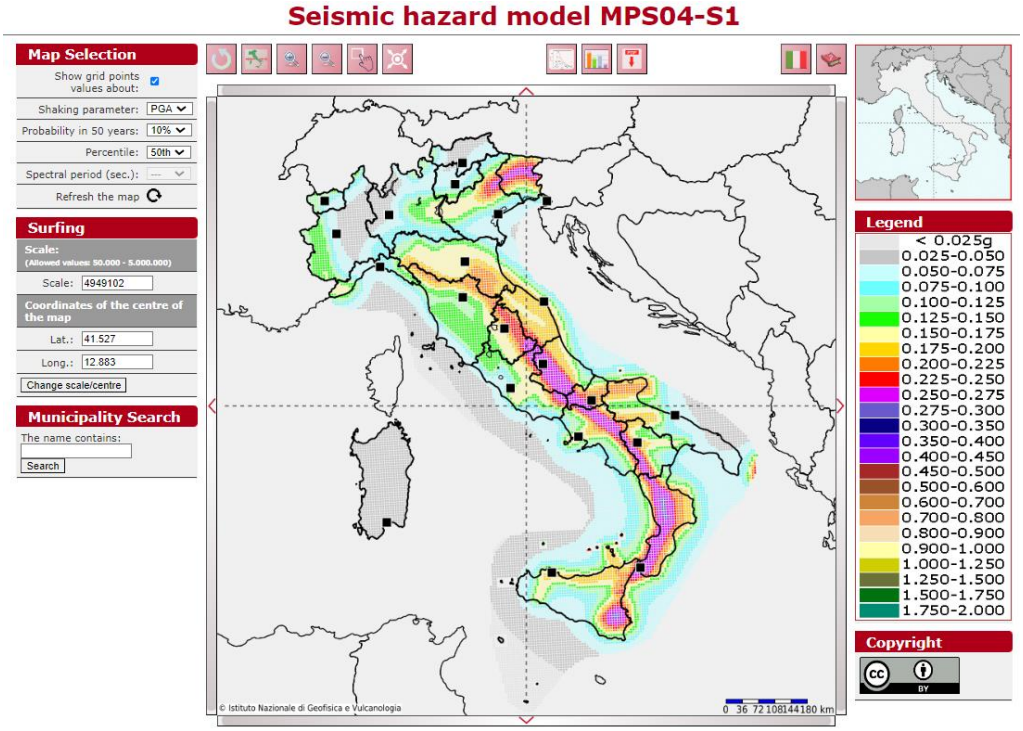

Figure 4-9Seismic Hazard Model INGV

Disaggregation is performed by calculating the magnitude and epicenter distance values relative to the area under study. The Figure 4-14 shows the results obtained. As is evident, the largest contributions to magnitude are concentrated at epicenter distance of 0-10 km and in the Mw ranges between 5.5 and 6.5. The average value of Mw is found to be 5.94, average epicenter distance of 9.1 km.

Hazard Curve

The term 'hazard curve' refers to the set of shaking values (here we refer to the PGA) for several

annual frequency of exceedance (the inverse of the return period).

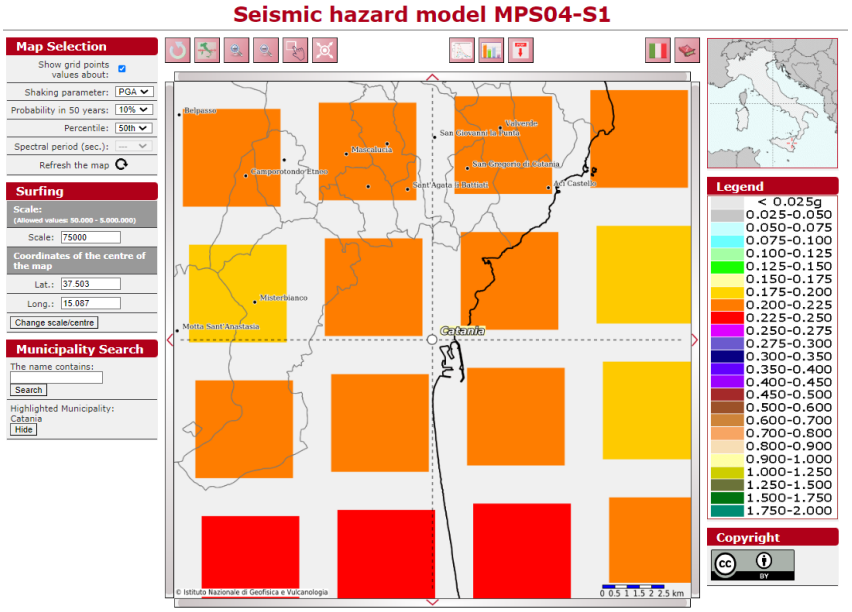

Figure 4-10 Seismicity map for the city of Catania - Seismic hazard model MPS04-S1 (Source Web Application Developed by F. Martinelli & C. Meletti, INGV)

The following table lists the values shown in the graph. The values are the median (50th percentile) and the uncertainty, expressed as the 16th and 84th percentile.

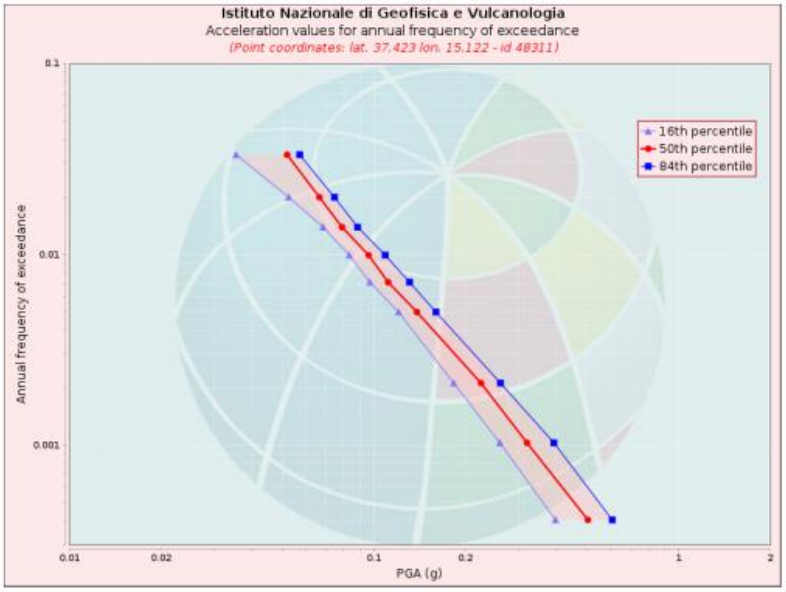

Figure 4-11 Acceleration values for annual frequency of exceedance - Graphic Elaboration form UNGV

Acceleration values for annual frequency of exceedance			
Annual frequency of exc.	PGA (g)		
	16th percentile	50th percentile	84th percentile
0.0004	0.395	0.505	0.607
0.0010	0.260	0.319	0.390
0.0021	0.183	0.225	0.261
0.0050	0.121	0.139	0.160
0.0071	0.097	0.112	0.131
0.0099	0.083	0.096	0.109
0.0139	0.068	0.079	0.089
0.0199	0.053	0.066	0.074
0.0332	0.035	0.052	0.057

Table 4-1 Acceleration values for annual frequency of exceedance

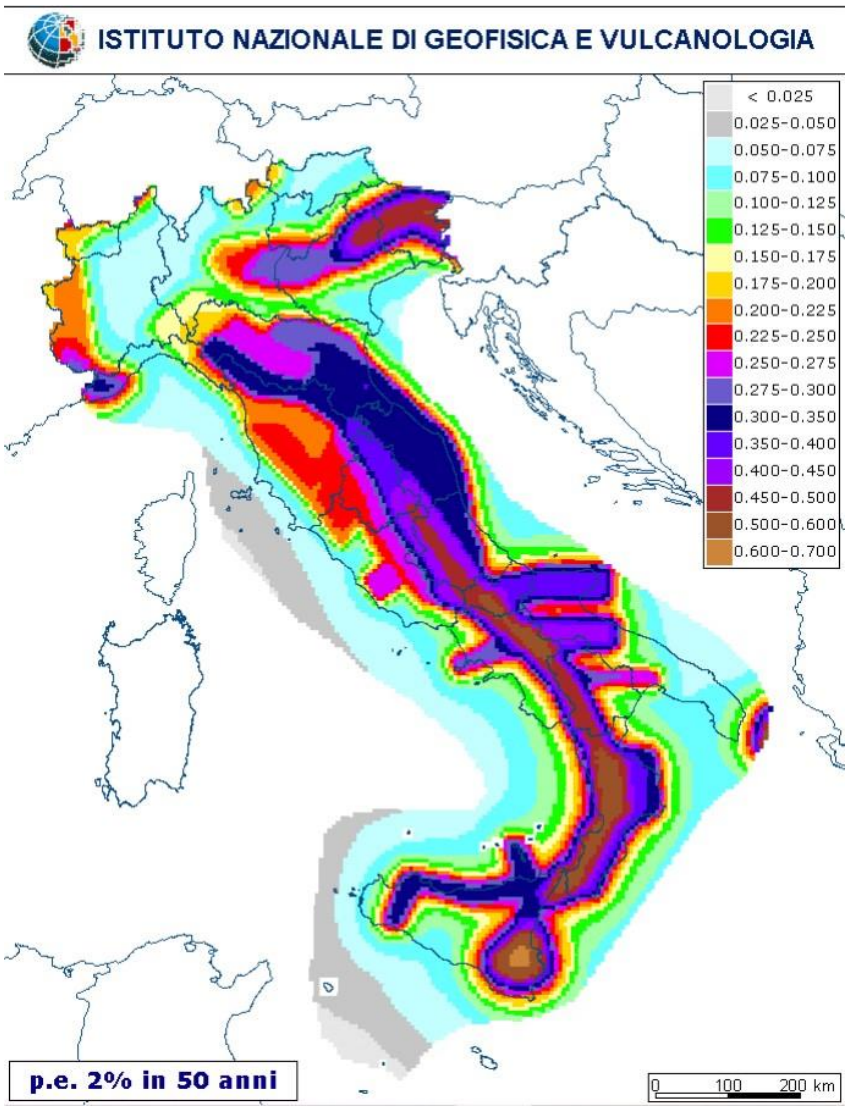

Figure 4-12 4-13 Seismic hazard estimation for a 2% exceedance probability in 50 years: ag values. DPC-INGV Project S1, Deliverable D2, http://esse1.mi.ingv.it/d2.html (Meletti C., Montaldo V., 2007)

For the purposes of the verifications reported in the following chapters, a design magnitude MW = 6.5, or equal to the maximum magnitude falling in the intervals that contribute most to the site hazard, is considered along the entire route.

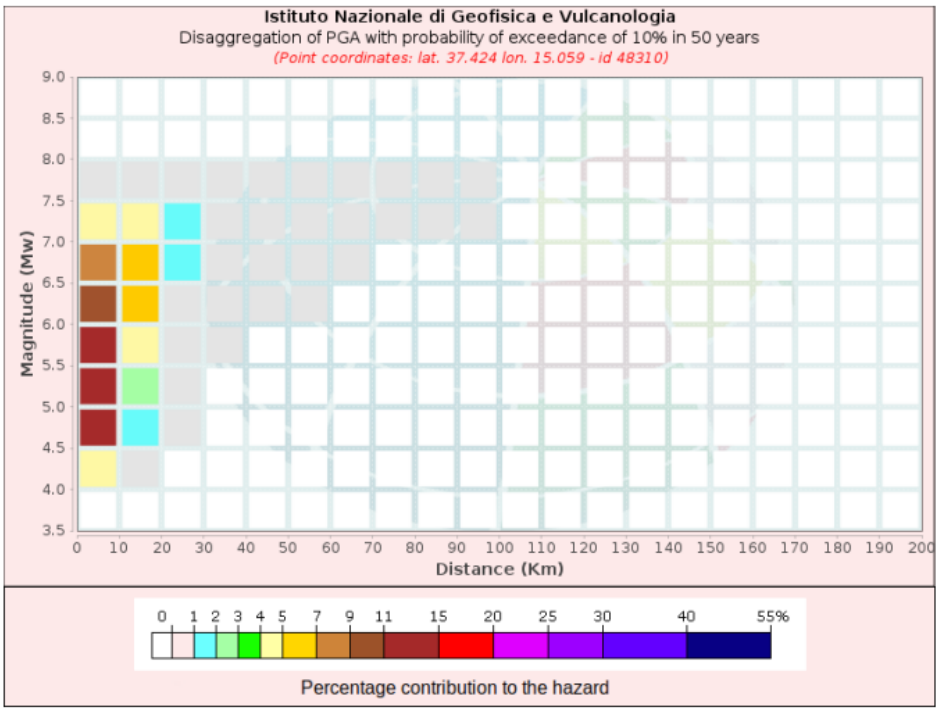

Disaggregation of PGA with probability of exceedance of 10% in 50 years

Distance	Magnitude									
in Km	3.5-4.0	4.0-4.5	4.5-5.0	5.0-5.5	5.5-6.0	6.0-6.5	6.5-7.0	7.0-7.5	7.5-8.0	8.0-8.5	8.5-9.0
0-10	0.0000	4.1300	12.6000	14.2000	13.4000	10.8000	7.4700	4.5900	0.6460	0.0000	0.0000
10-20	0.0000	0.1010	1.0200	2.6000	4.2600	5.4900	5.6900	4.8500	0.8110	0.0000	0.0000
20-30	0.0000	0.0000	0.0009	0.0711	0.3620	0.8390	1.3200	1.6000	0.3240	0.0000	0.0000
30-40	0.0000	0.0000	0.0000	0.0000	0.0210	0.1990	0.4770	0.7600	0.1780	0.0000	0.0000
40-50	0.0000	0.0000	0.0000	0.0000	0.0000	0.0292	0.1790	0.3810	0.1010	0.0000	0.0000
50-60	0.0000	0.0000	0.0000	0.0000	0.0000	0.0006	0.0641	0.2200	0.0655	0.0000	0.0000
60-70	0.0000	0.0000	0.0000	0.0000	0.0000	0.0000	0.0063	0.0549	0.0189	0.0000	0.0000
70-80	0.0000	0.0000	0.0000	0.0000	0.0000	0.0000	0.0000	0.0098	0.0050	0.0000	0.0000
80-90	0.0000	0.0000	0.0000	0.0000	0.0000	0.0000	0.0000	0.0030	0.0028	0.0000	0.0000
90-100	0.0000	0.0000	0.0000	0.0000	0.0000	0.0000	0.0000	0.0004	0.0011	0.0000	0.0000
100-110	0.0000	0.0000	0.0000	0.0000	0.0000	0.0000	0.0000	0.0000	0.0001	0.0000	0.0000
110-120	0.0000	0.0000	0.0000	0.0000	0.0000	0.0000	0.0000	0.0000	0.0000	0.0000	0.0000
120-130	0.0000	0.0000	0.0000	0.0000	0.0000	0.0000	0.0000	0.0000	0.0000	0.0000	0.0000
130-140	0.0000	0.0000	0.0000	0.0000	0.0000	0.0000	0.0000	0.0000	0.0000	0.0000	0.0000
140-150	0.0000	0.0000	0.0000	0.0000	0.0000	0.0000	0.0000	0.0000	0.0000	0.0000	0.0000
150-160	0.0000	0.0000	0.0000	0.0000	0.0000	0.0000	0.0000	0.0000	0.0000	0.0000	0.0000
160-170	0.0000	0.0000	0.0000	0.0000	0.0000	0.0000	0.0000	0.0000	0.0000	0.0000	0.0000
170-180	0.0000	0.0000	0.0000	0.0000	0.0000	0.0000	0.0000	0.0000	0.0000	0.0000	0.0000
180-190	0.0000	0.0000	0.0000	0.0000	0.0000	0.0000	0.0000	0.0000	0.0000	0.0000	0.0000
190-200	0.0000	0.0000	0.0000	0.0000	0.0000	0.0000	0.0000	0.0000	0.0000	0.0000	0.0000

Mean Values: magnitude = 5.94 ; distance = 9.1 ; epsilon = 0.598

Figure 4-14 Disaggregation of PGA with probability of exceedance of 10% in 50 years

Mean magnitude 5.94 Mw and mean distance 9.1 km are derived from result of the disaggregation study.

4.1.4 Selection of the strong motion time histories

For the identification of the design seismic action, reference was made to Ministerial Decree 17/01/2018. The following characteristics are considered for the project work:

- Design Life V_N=100 years;
- Use class IV, to which corresponds a use coefficient C_U=2.
- P_{VR}

Seismic actions are evaluated in relation to the reference period VR, which is derived from the product of the nominal design life VN and the use coefficient CU:

$$V_R = C_U \cdot V_N$$

Hence, the VR reference life results in:

$$V_R = C_U \cdot V_N = 2 \cdot 100 = 200\ anni$$

The ultimate limit states SLV are considered, to which the P_{VR} exceedance probability and return period thus determined correspond:

$$T_R = -\frac{V_R}{\ln(1 - P_{VR})} = 1898\ anni$$

4.1.4.1 Expected maximum horizontal acceleration on a rigid reference site (ag)

The SPETTRI-NTC Excel document provides the response spectra representative of the components (horizontal and vertical) of the design seismic actions for the generic site of the national territory. The definition of the response spectra for a Limit State is divided into 3 phases, each of which requires the user to choose the values of certain parameters:

- PHASE 1. Identification of the site hazard (based on the results of the S1 - INGV project);
- PHASE 2. Choice of design strategy.
- PHASE 3. Determination of the design action.

FASE 1: Individuazione della pericolosità del sito	
Regione:	Sicilia
Provincia:	Catania
Comune:	Catania

Valori dei parametri a_g, F_0, T_C*

T_R [anni]	a_g [g]	F_0 [-]	T_C* [s]
30	0,062	2,553	0,245
50	0,077	2,547	0,263
72	0,089	2,520	0,277
101	0,103	2,514	0,285
140	0,119	2,467	0,295
201	0,140	2,463	0,313
475	0,206	2,459	0,358
975	0,283	2,426	0,442
2475	0,440	2,381	0,530

Figure 4-15 Identification of the site hazard (based on the results of the S1 - INGV project);

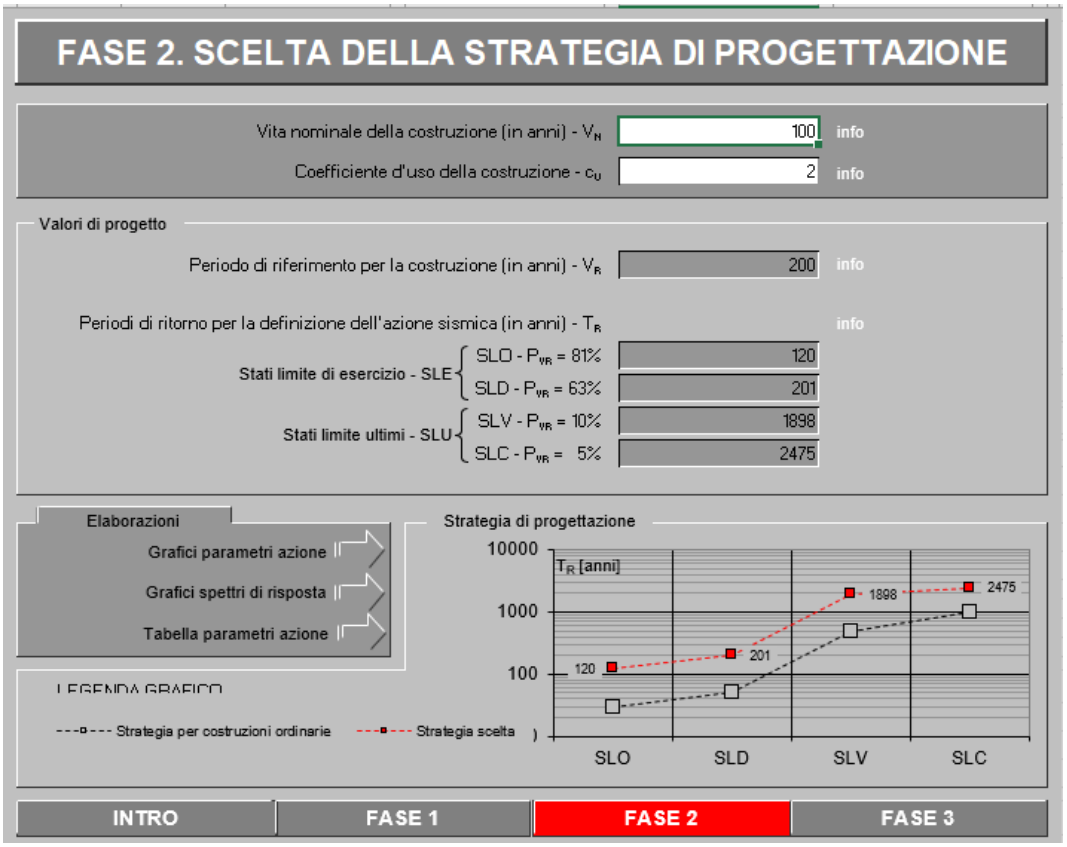

FASE 2: Scelta della strategia di progettazionre	
Vita nominale della costruzione (in anni) - V_N:	100
Coefficiente d'uso della costruzione - c_U:	2,0

Valori di progetto:			
Periodo di riferimento per la costruzione - V_R:		200	
Periodo di ritorno per la definizione dell'azione sismica:			
SLE	SLO - PVR = 81%	120	[anni]
	SLD - PVR = 63%	201	[anni]
SLU	SLV - PVR = 10%	1898	[anni]
	SLC - PVR = 5%	2475	[anni]

Valori dei parametri per i periodi di ritorno associati a ciascuno SL:

STATO LIMITE	T_R [anni]	a_g [g]	F_0 [-]	T_C* [s]
SLO	120	0,111	2,489	0,290
SLD	201	0,140	2,463	0,313
SLV	1898	0,388	2,394	0,503
SLC	2475	0,440	2,381	0,530

Figure 4-16 Choice of design strategy,

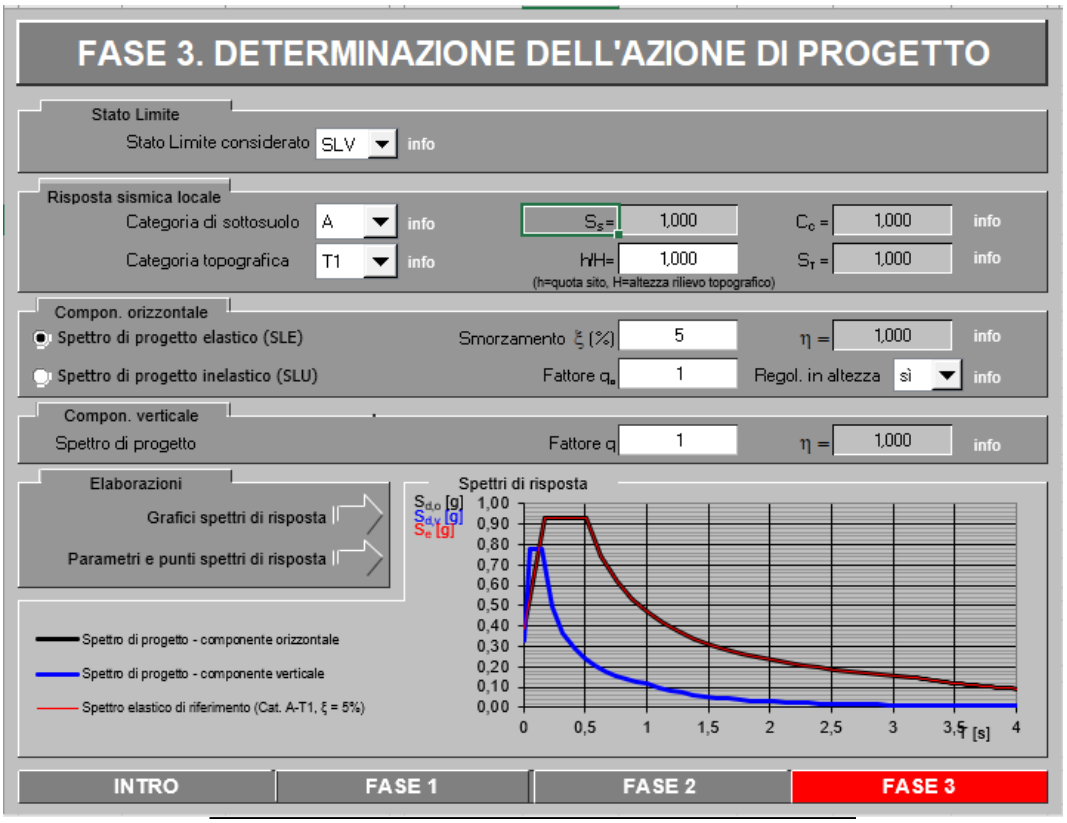

FASE 3: Determinazione dell'azione di progetto			
Risposta sismica locale:			
Categoria di sottosuolo:	A		
Categoria Topografica:	T1		
Componente orizzontale			
Smorzamento ξ (%)	5	η =	1,0
Regolare in altezza	no		
Fattore di struttura q_o	1		
Componente verticale			
Fattore di struttura q	1	η =	1,0

Parametri indipendenti:

STATO LIMITE	SLV	
a_g	0,388	[g]
F_0	2,394	[-]
T_C*	0,503	[s]
S_S	1,1424328	[-]
C_C	1,32	[-]
S_T	1	[-]
q	1	[-]

Parametri indipendenti:

S	1,14	[-]
η	1,00	[-]
T_B	0,22	[s]
T_C	0,66	[s]
T_D	3,15	[s]

Figure 4-17 Determination of the design action

The peak ground acceleration a_{max} is computed 0.443 g as below.

$$a_{max} = S_S * S_T * a_g = 1{,}14 * 1 * 0{,}388\ g = 0.443\ g$$

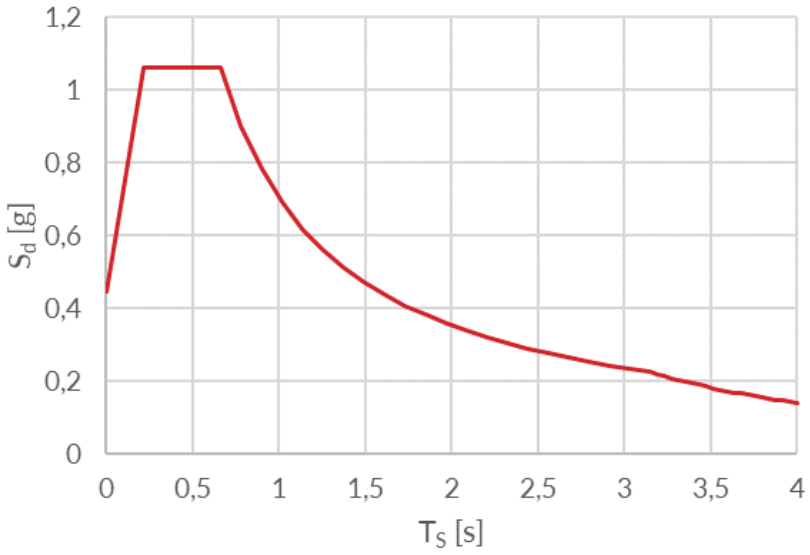

Figure 4-18 Design Target Spectrum

4.1.4.2 Earthquake Selection

As explained in Chapter 2.4.3, 7, Accelerograms are chosen by using REXEL. You can see step by step the using this tool below.

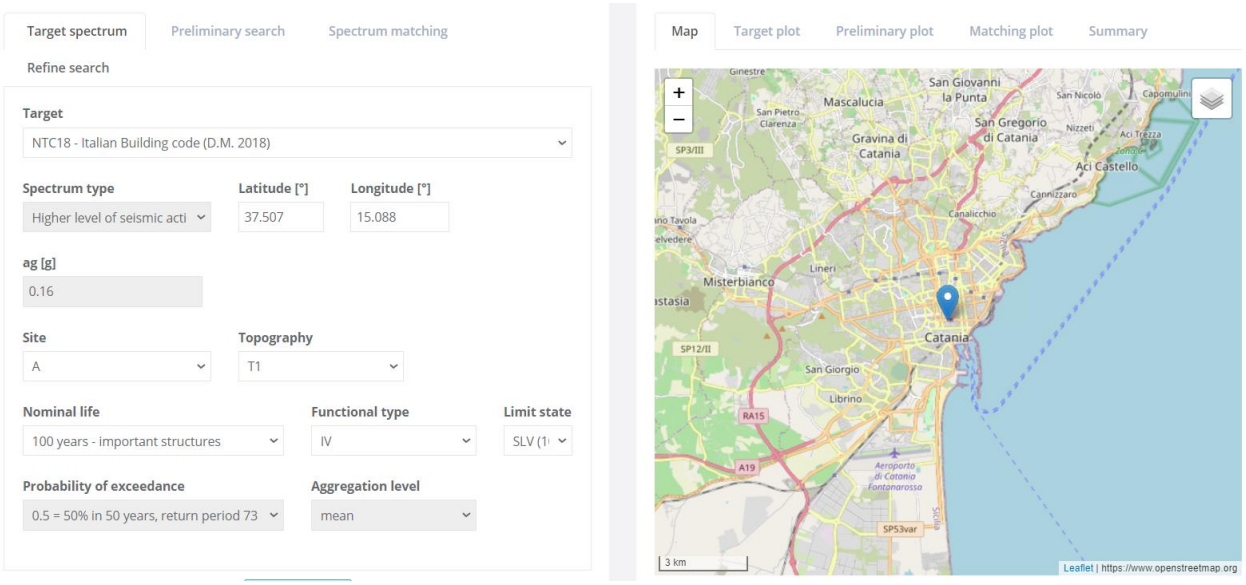

Figure 4-19 Step1: Refine Search Screen

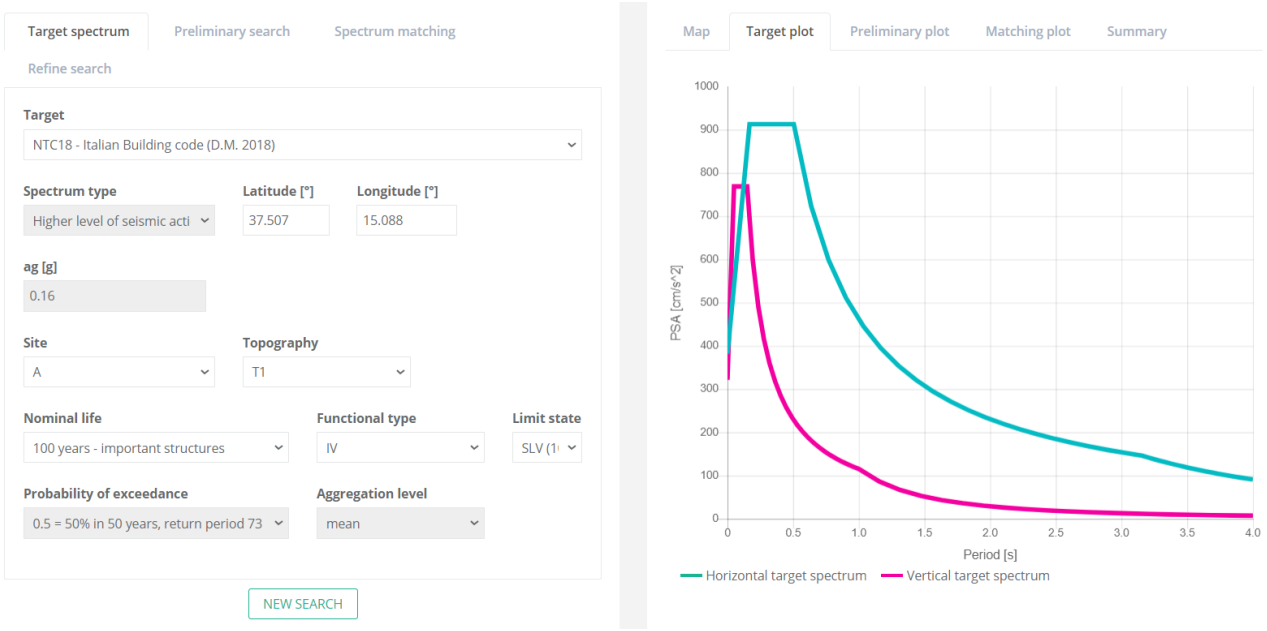

Figure 4-20 Step2: Design Target Spectrum Definition

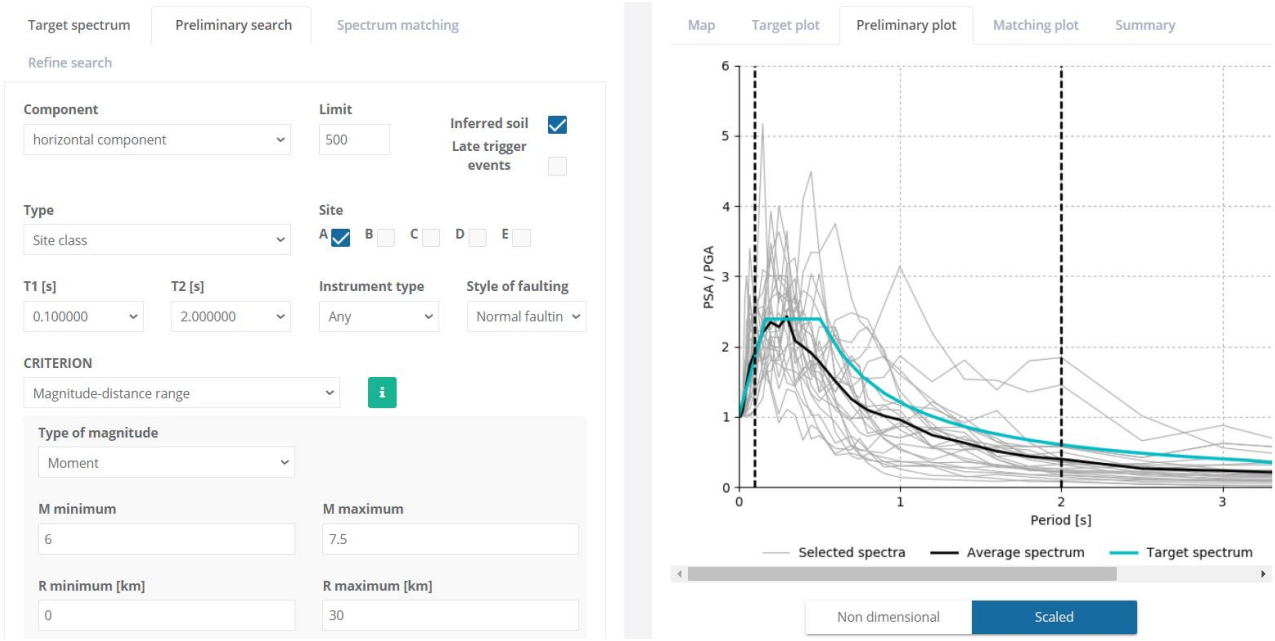

Figure 4-21 Step3: Preliminary Search

Selected 7 accelerograms are presented in Table 4-2. While Earthquake No.3, No.4, No.5 have suitable scale factor, Earthquake No.1, No.2 and No.7 have high scale factor .

No.	Earthquake Name	Station Code	Date	Mw	Fault Mechanism	Epicentral Distance (km)	Eurocode 8 Site Class	Scale
1	Irpinia (Italy)	BSC (E)	23/11/1980	6.9	Normal	28.3	A	4,89
2	Umbria Marche (Italy)	CSC	14/10/1997	5.6	Normal	24.3	B	6.15
3	Central (Italy)	ACC	30/10/2016	5.6	Normal	18,5	A	0,99
4	Central (Italy)	T1212	31/10/2016	6.6	Normal	11,6	A	1,39
5	Fruli (Italy)	TLM1	01/02/1976	6.4	Thrust	27.7	B	1.23
6	Central Italy	FCC	02/11/2016	6.6	Normal	10,9	A	0,45
7	Irpinia (Italy)	BSC (N)	23/11/1980	6.9	Normal	28,3	A	4,08

Table 4-2 Selected Natural 7 Accelerograms

In Figure 4-22, Design spectrum and selected accelerograms are presented. While, Irpinia earthquakes (No.1 and No.2) represent unfavored matching. Another's can be said that representative favored matching.

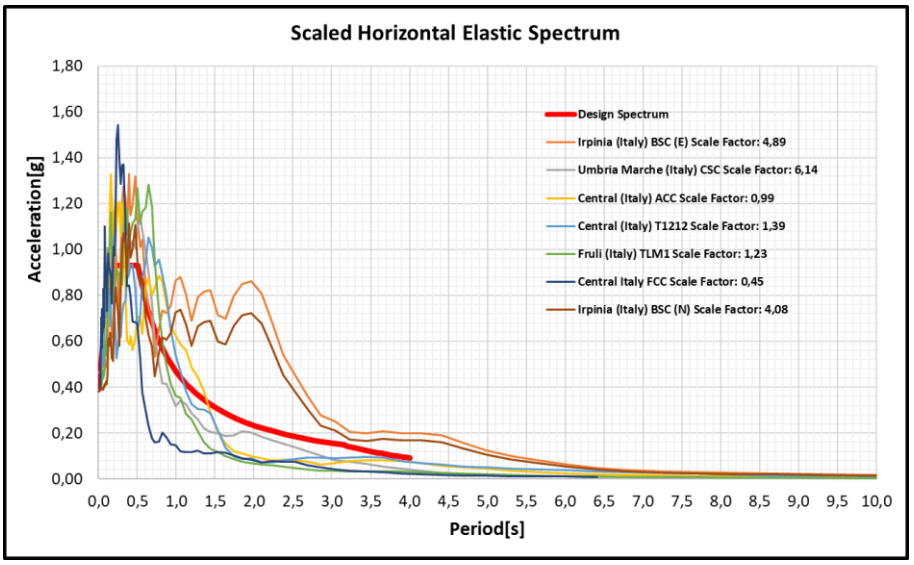

Figure 4-22 7 Accelerograms and Design Target Spectrum

Average of accelerograms is shown good matching with design target spectrum. So, these scalograms can be used for analysis.

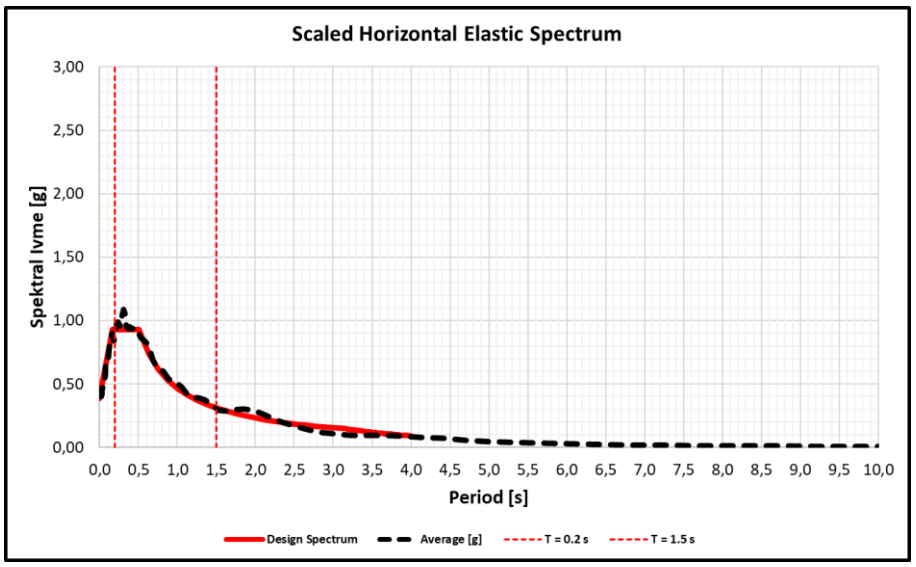

Figure 4-23 Average of 7 accelerograms and Design Target Spectrum

4.2 Free Field Shear Deformation at the Critical Section

This chapter present shear deformation and distortion by using different approaches that simplified method shear deformation methos are classified deep&shallow tunnel and shallow tunnel, and site response analysis.

4.3 Simplified Method at the Analysis Section

There are 2 approach of the simplified method. While one of them can be applied for deep and shallow tunnel, Another just for shallow tunnel. Analysis section can be considered as a shallow tunnel, so both approaches is suitable for this section. Following chapters these methods are applied.

4.3.1 Simplified Shear Deformation -Deep & Shallow Tunnel Approach

Simplified Shear Deformation - Deep Tunnel

Input	Intermediate	Output

Tunnel geometry

R [m]	4,8	*Radius*	
D [m]	9,6	*Diameter*	
H (m)	14,00	*Soil cover thickness up to tunnel crown*	
z [m]	23,60	*Depth of the Tunnel Axis*	

Seismic parameters

g [m/s^2]	9,81	*Gravity acceleration*	
a_{gR} [g]	0,388	*Reference PGA*	
Ss [-]	1,14	*Soil factor*	
S_T [-]	1,00	*Topograpghic Factor*	
$a_{max,s}$ [g]	0,443	*Site-specific PGA*	*Eq. 7*

Maximum Free-Field Shear Strain calculation

Z [m]	33,55	*Depth of axis tunnel*	
C [-]	0,8	*(see Table 2.9 on the right)*	
$a_{z,max}$ [g]	0,35	*PGA at tunnel depth*	*Eq. 10*
k [cm/(s·g)]	94	*(see Table 2-8 below)*	
V_s (PGV) [m/s]	0,33	*Peak particle Velocity (S-Waves)*	*Eq. 9*
C_s [m/s]	340	*The small-strain shear wave velocity from Site situ test*	
C_{se}/C_s	0,9		
C_{se} [km/s]	306	*Small Strain Sheaar Velocity*	
$\gamma_{max,ff}$ [-]	0,0010	*Maximum Free-Field Shear Strain*	*Eq. 8*
α [°]	0,056	*Distortion*	

4.3.2 Simplified Method - Shallow Tunnel Approach

Simplified Shear Deformation - Shallow Tunnel

Input | Intermediate | Output

Tunnel geometry

R [m]	4,8	*Radius*
D [m]	9,6	*Diameter*

Ground properties

γ_m [kN/m^3]	19,00	*Medium unit weight*
H (m)	14,00	*Soil cover thickness up to tunnel crown*
z [m]	23,60	*Depth*

Seismic parameters

$S_{a,475}$[m/s^2]	2,021	*Reference spectral acceleration,relative to a reference return time Tref = 475 years*	
Seismicity Level	Low		*Table 2-10*
a_{gR} [g]	0,388	*Reference PGA*	
Ss [-]	1,142	*Soil factor*	
S_T [-]	1,000	*Topograpghic Factor*	
$a_{max,s}$ [g]	0,443		*Eq. 7*

Geotechnical Parameters

V_s [m/s]	340	*Shear Waves Propogation Velocity*	
G_0 [MPa]	224	*Small Shear Strain Modulus*	*Eq. 15*
G/G_0	0,65	*Reduction factors of the normalized shear modulus*	

Seismicity level	$150 \le v_s < 250$ m/s		$250 \le v_s < 400$ m/s		$400 \le v_s < 800$ m/s		800 m/s $\le v_s$	
$S_{a,475}$ (m/s^2)	G/G_0	ξ	G/G_0	ξ	G/G_0	ξ	G/G_0	ξ
Very low (<1,0)	0,7 (±0,08)	0,04	0,8 (±0,09)	0,03	1	0,03	1	0,02
Low (1,0-2,5)	0,5 (±0,14)	0,07	0,65 (±0,16)	0,05	0,8 (±0,10)	0,03	1	0,02
Moderate (2,5-5,0)	0,3 (±0,10)	0,1	0,5 (±0,20)	0,07	0,7 (±0,10)	0,05	1	0,02
High (>5)	0,2 (±0,10)	0,2	0,4 (±0,20)	0,12	0,6 (±0,20)	0,1	0,9 (±0,10)	0,02

***Damping ratios and average reduction factors (± one standard deviation) of the normalized shear modulus G/G0 within 20 m depth (Eurocode8, 2022)*

Calculation

G_m [MPa]	146	*Effective strain-compatible shear modulus of ground surrounding tunnel*	*Table 2-10*
σ_v [kPa]	448	*Total vertical stress*	
R_d [-]	0,65	*Reduction Coefficient*	*Eq. 14*
τ_{max} [kPa]	128,35	*Maximum Shear Stress*	*Eq. 12*
γ_{max} [-]	0,0009	*Maximum Shear Strain*	*Eq. 11*
α [°]	0,051	*Distortion*	

Almost same result is computed from both methods. To be safe side, maximum free field shear strain is accepted equal to 0.0010 and distortion is 0.0056°

4.4 Seismic Site Response Analysis (SSR)

DEEPSOIL software is used for the seismic site response analysis. All progress is explained Step by step below.

4.4.1 Step 1. Analysis Settings

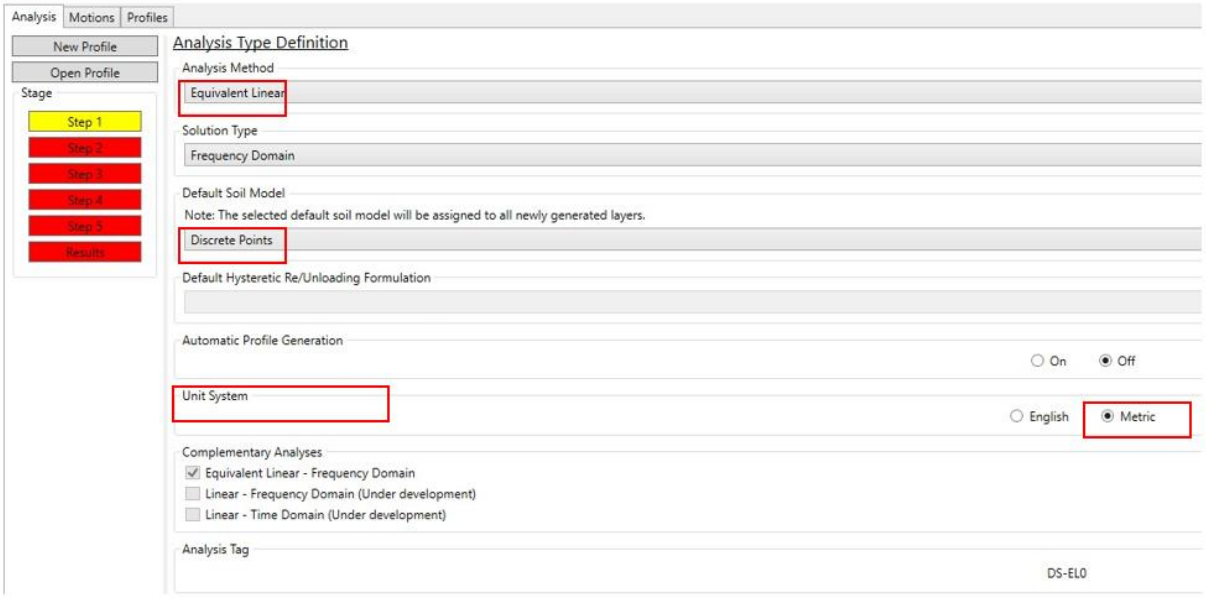

Figure 4-24 Analysis Settings

- Analysis Method: equuilvant Linear
- Solution Type: Time Domain
- Default Soil Model: Discrete Points
- Unit System: Metric
- Complementary Analyses: Equivalent Linear – Frequency Domain

4.4.2 Step 2. Layer Definition and Parameters

4.4.2.1 Layer Thickness

H_{layer} is calculated by using Equations (20), (21) and (22) as explained in Chapter 2.5.2.2.4. Totally 25 layers are defined in Deepsoil for analyses.

Geological Unit	Thickness	Depth		Vs,design	f_{max}	λmin	Hmax	$H_{deepsoil}$
-	[m]	Start[m]	End [m]	[m/s]	[Hz]	[m]	[m]	[m]
Riporto - Rp	4	0	4	215	25	8,6	2,15	2
Lave - L1669	8	4	12	650	25	26	6,5	4
Silty Sand - Sbl	18	12	30	340	25	13,6	3,4	3
Marly-Silty Clays - Agm	70	30	100	500	25	20	5	5
Bedrock	Inf.	100	Inf.	800	25	32	8	

Table 4-3 Layer Thickness in Deepsoil

4.4.2.2 Definition Geological Units

Thickness, unit weight, shear wave velocity are defined in Table 3-8 and Decay curves is defined as Figure 3-10 for each layer.

Rp – Topsoil (Riporto)

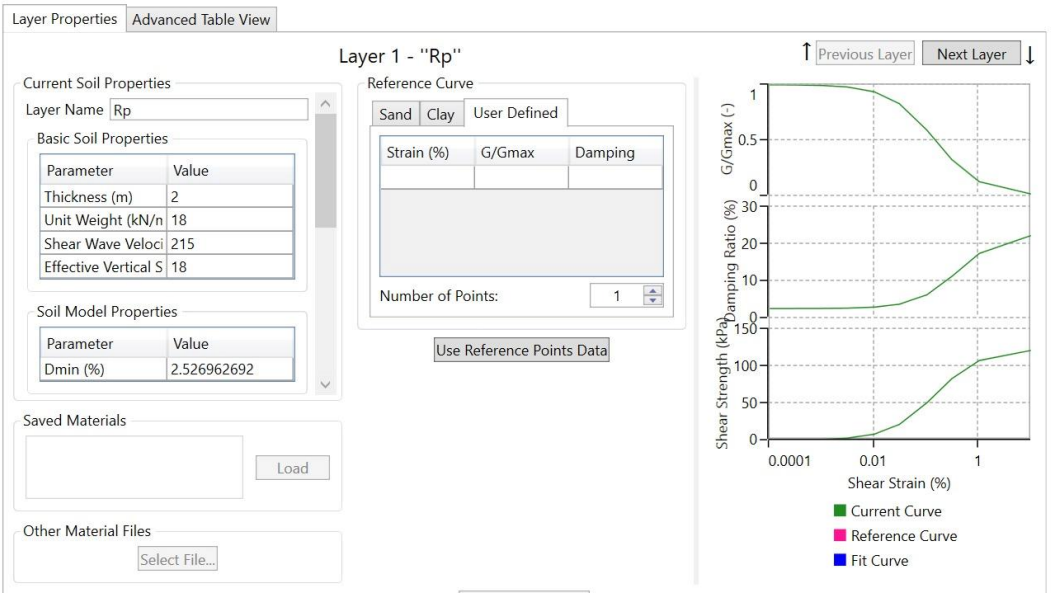

Figure 4-25 Rp – Topsoil (Riporto)

L1669 – Lave

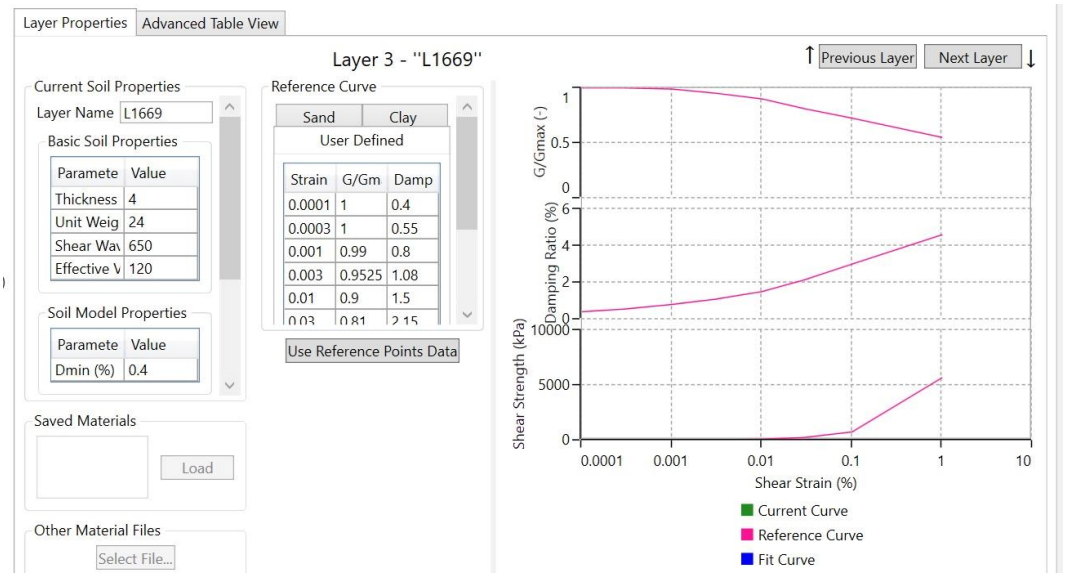

Figure 4-26 L1669 – Lave

Sbl – Silty Sand

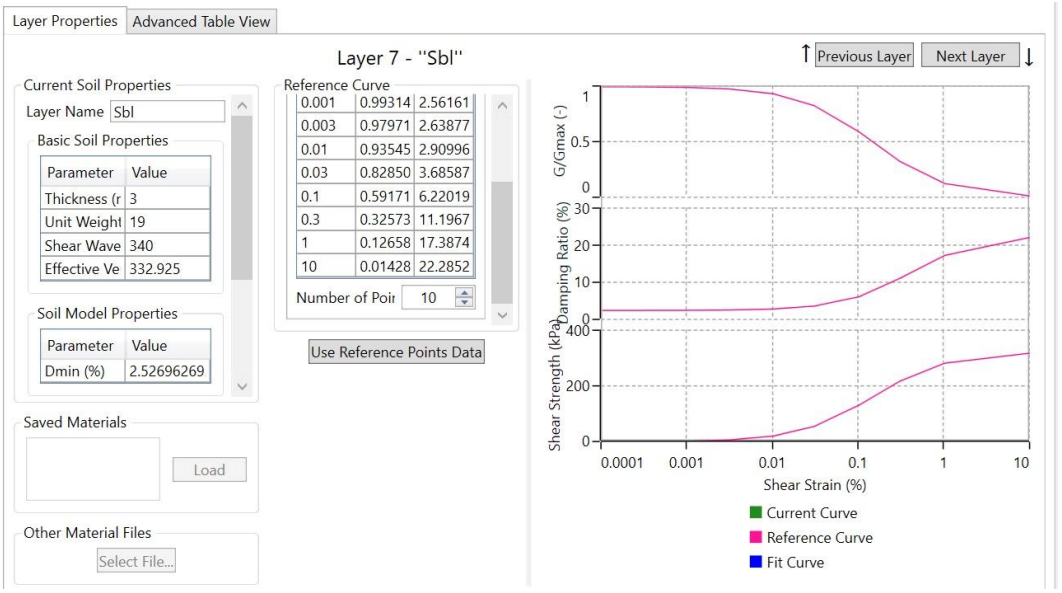

Figure 4-27 Sbl – Silty Sand

Agm- Clays

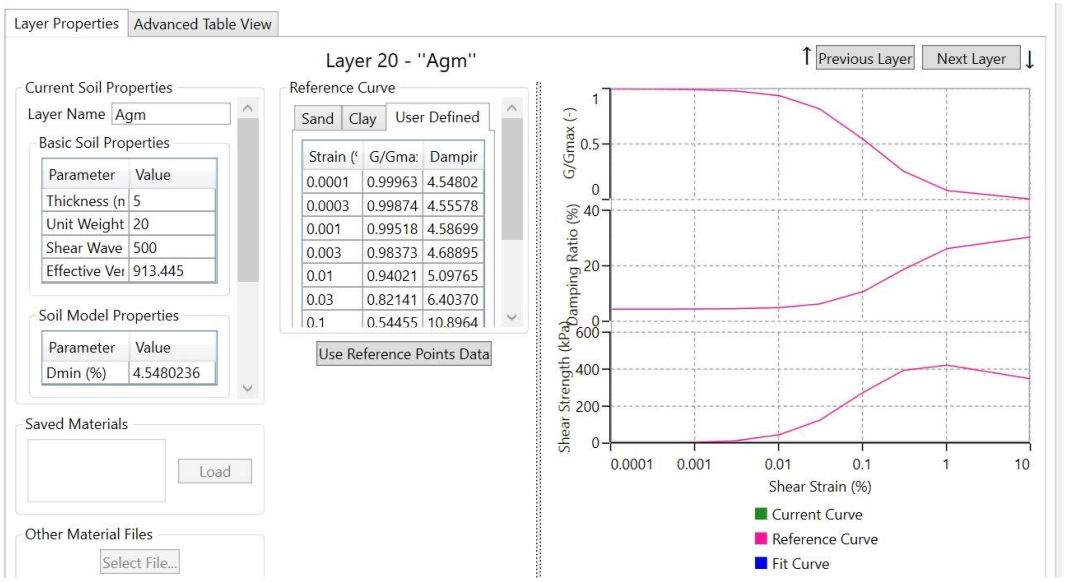

Figure 4-28: Agm- Clays

Bedrock

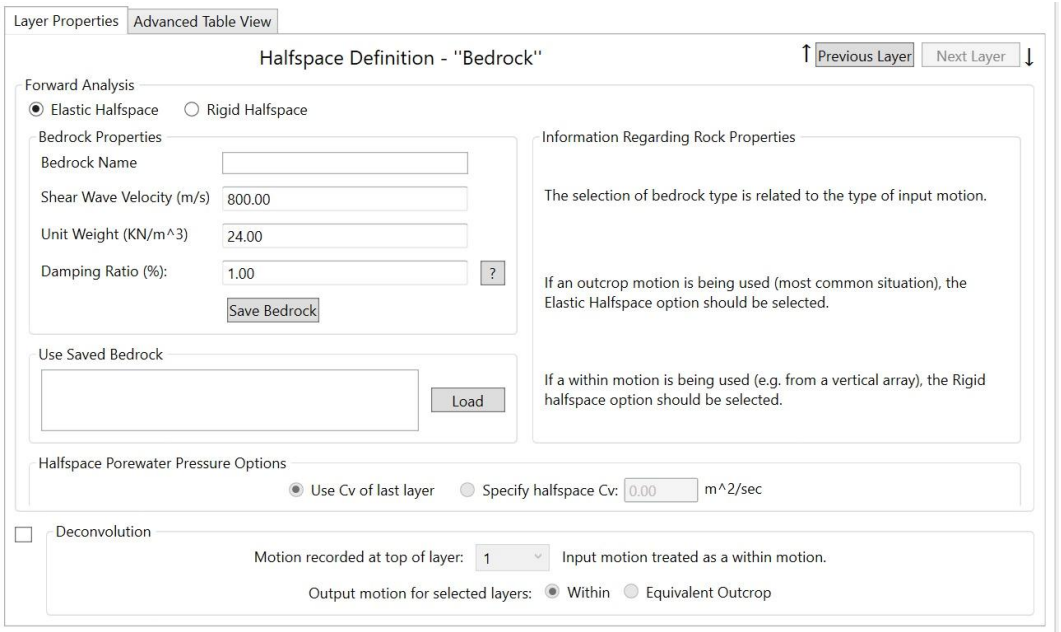

Figure 4-29 Bedrock Parameters

4.4.3 Step 3. Ground Motion Definition

7 ground motions which is showed in Table 4-2, is defined software. Accelogram data, which is taken from Rexel, is raw data. After importing the accelerograms, it must be scaled with scale factor in software. Scale factors are shown in Table 4-2.

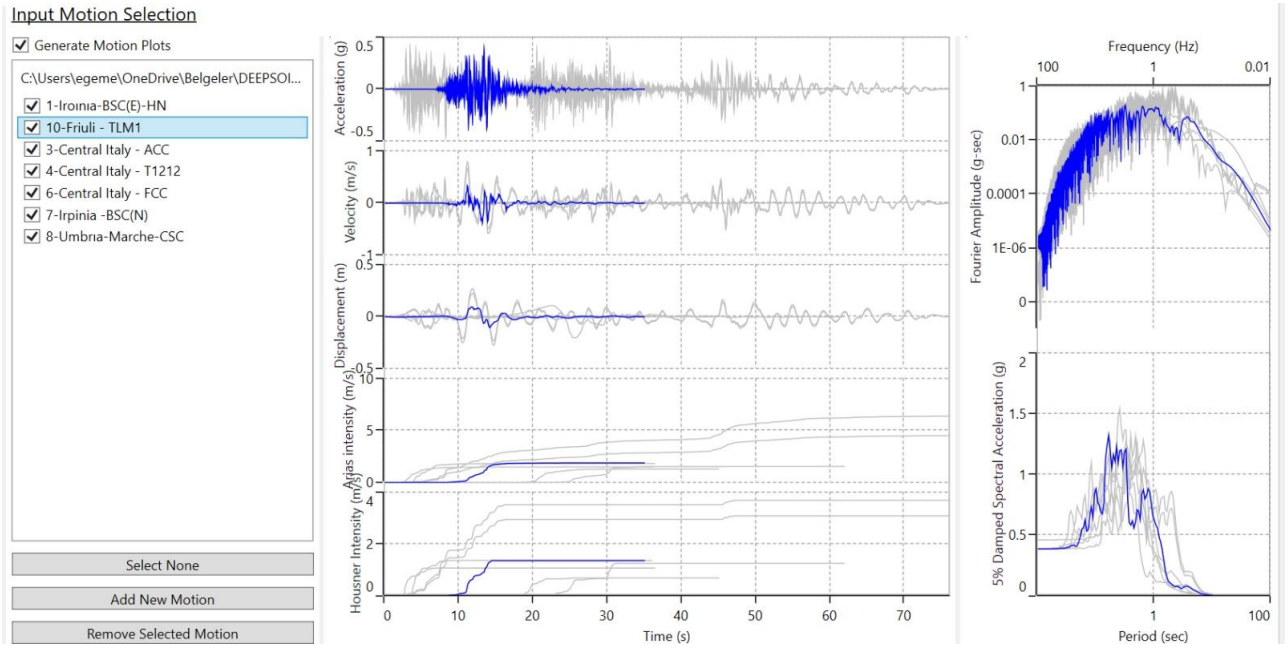

Figure 4-30 Ground Motion Definition

4.4.4 Step 4. Analysis Control Definition

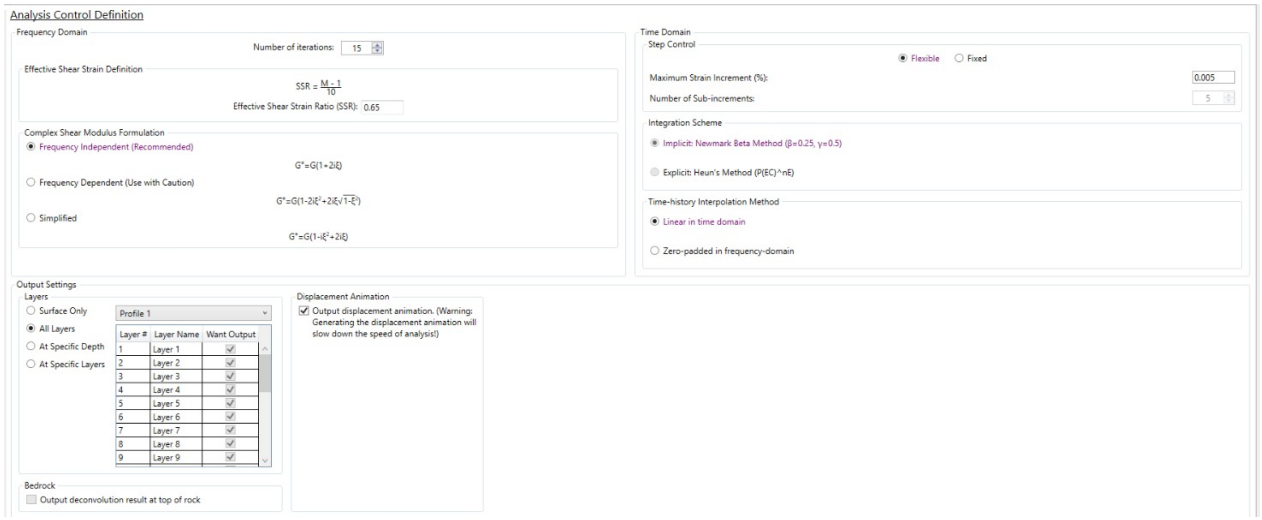

Figure 4-31 Analysis Control Definition

4.4.5 Step 5. Outputs

Deepsoil present outputs as PGA (g), PGD (m), Max Strain (%), Max Stress Ration and Effective Vertical Stress (kPa) on the screen. (Figure 4-32)

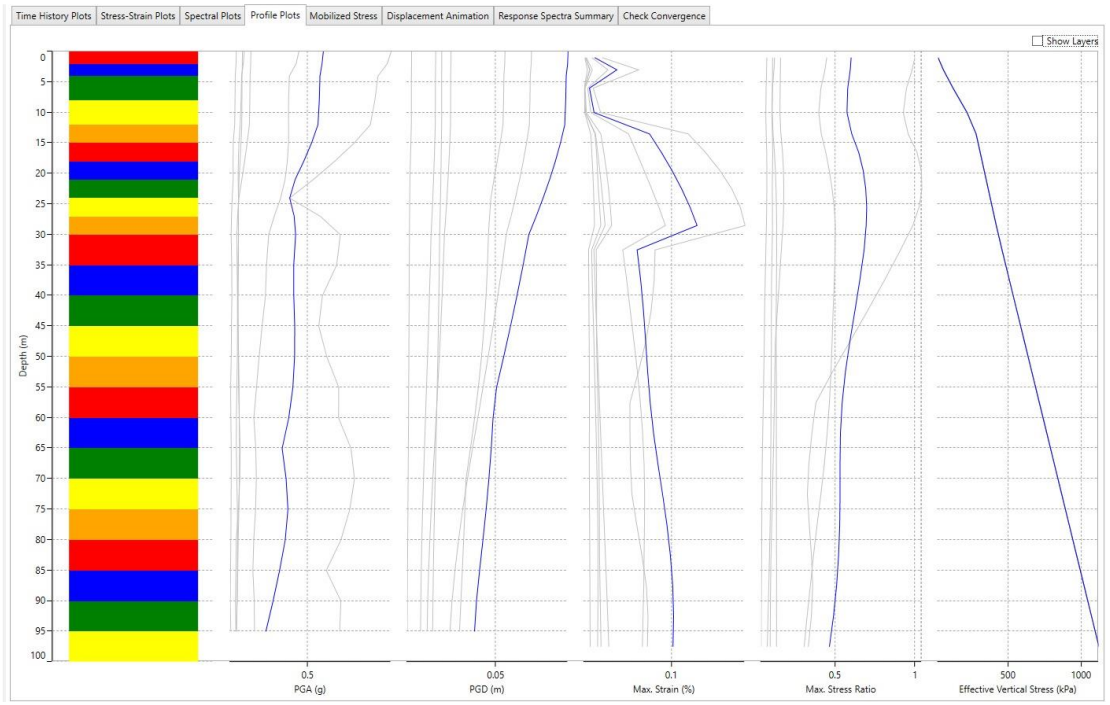

Figure 4-32 Output from Deepsoil

In addition, results are summarized below, and average of the results are shown to consider for analysis. I

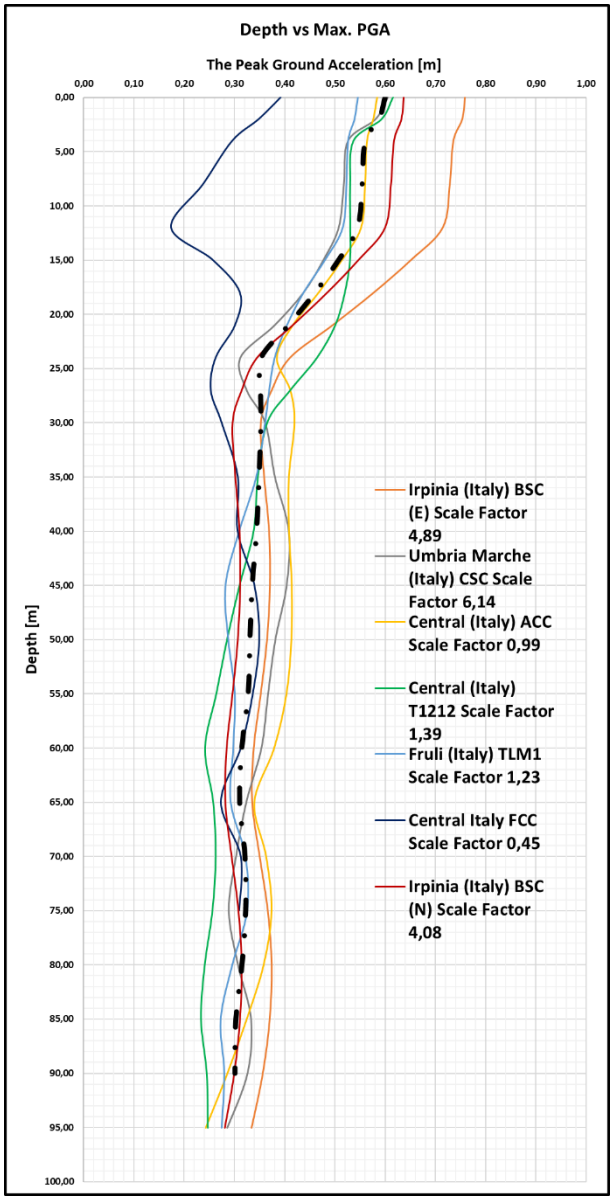

Figure 4-33 Depth vs PGA

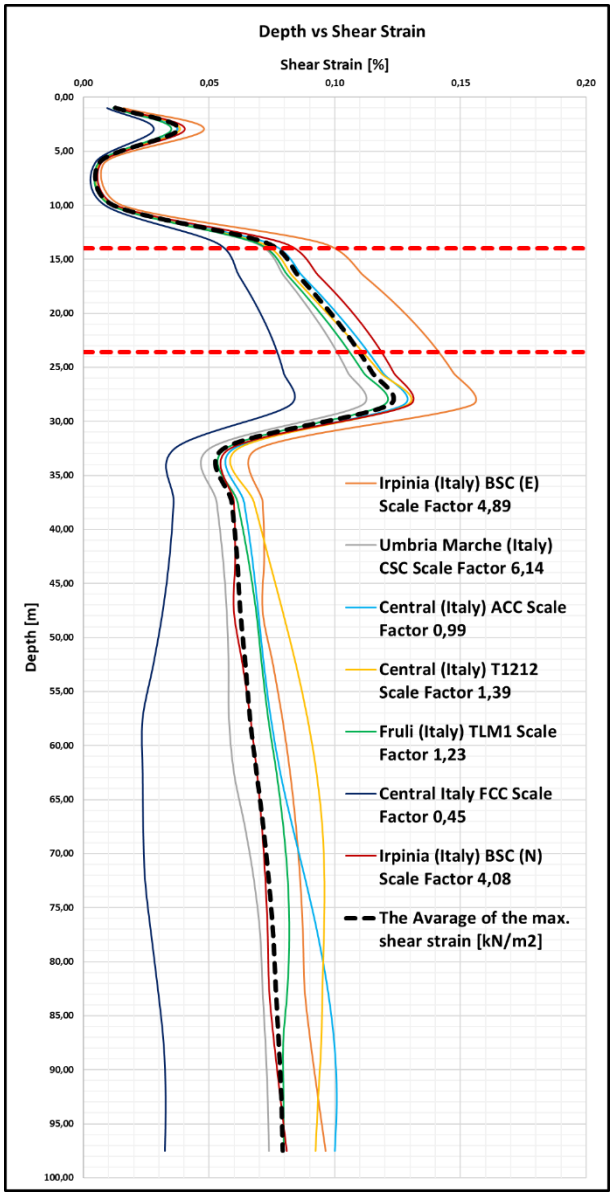

Figure 4-34 Depth vs Shear Strain

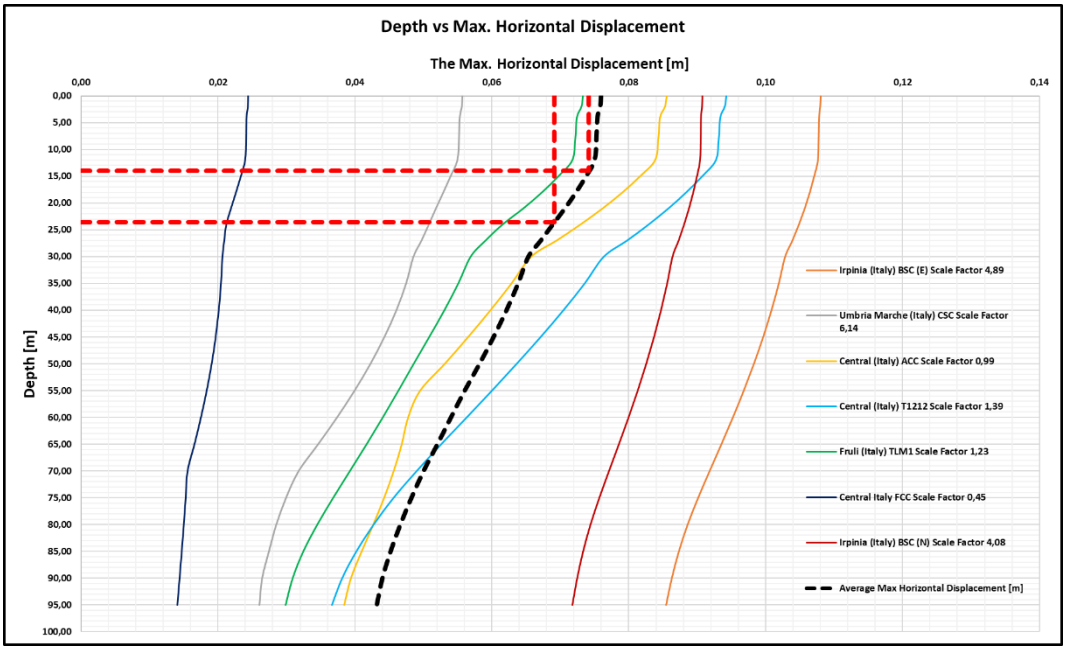

Figure 4-35 Horizontal Displacement vs Depth

Average horizontal displacement is considered design free field shear deformation from bedrock to surface. $G_{(\Upsilon)}/G_o$ ratio are derived from the corresponded average horizontal shear deformation for each layer.

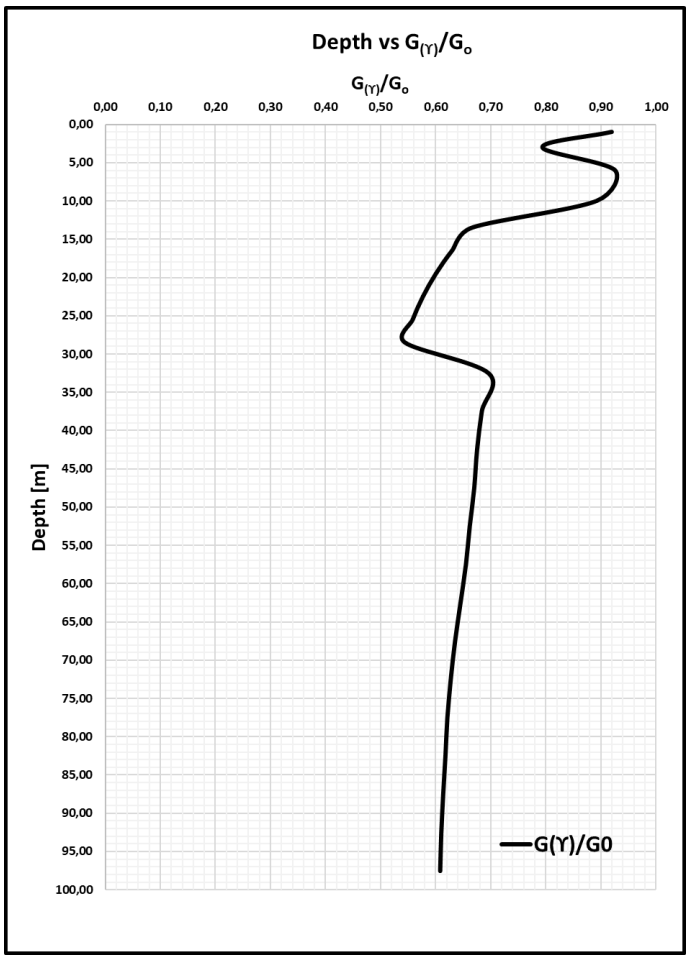

Figure 4-36 $G_{(\Upsilon)}/G_o$ vs Depth

4.4.6 Impact of the L1668-Lave geological Unit

L1699 is high quality rock formation, it is placed in above Sbl sand and Agm clay soil formation due to tectonic movement, then that it is covered with topsoil due to environmental impact in real case. Along the alignment of the project, in some section it can't be observed, and some section this formation can be placed in between Sbl and Agm formation under tunnel. These cases are evaluated to understand the impact of the L1669 layer on the free field shear deformation and impact on tunnel behavior. 2 other cases (Case 2 and Case 3) except real case are analysed by using Deepsoil. It is followed same steps are mentioned previous chapters.

While There is no L1669-Lave formation in Case2 which is consist of 4 m Rp, 26 m Sbl and 70m Agm respectively from top to bedrock at the section, L1669-Lave formation is placed under tunnel section in Case 3. From top to bedrock, 4m Rp, 20m Sbl, 8 m L1669 and 69m Agm respectively at the section in Case 3. (Figure 4-37)

Obtained horizontal shear displacement and ratio operational shear modulus and initial shaer modulus

from each analysis are compared in Figure 4-38

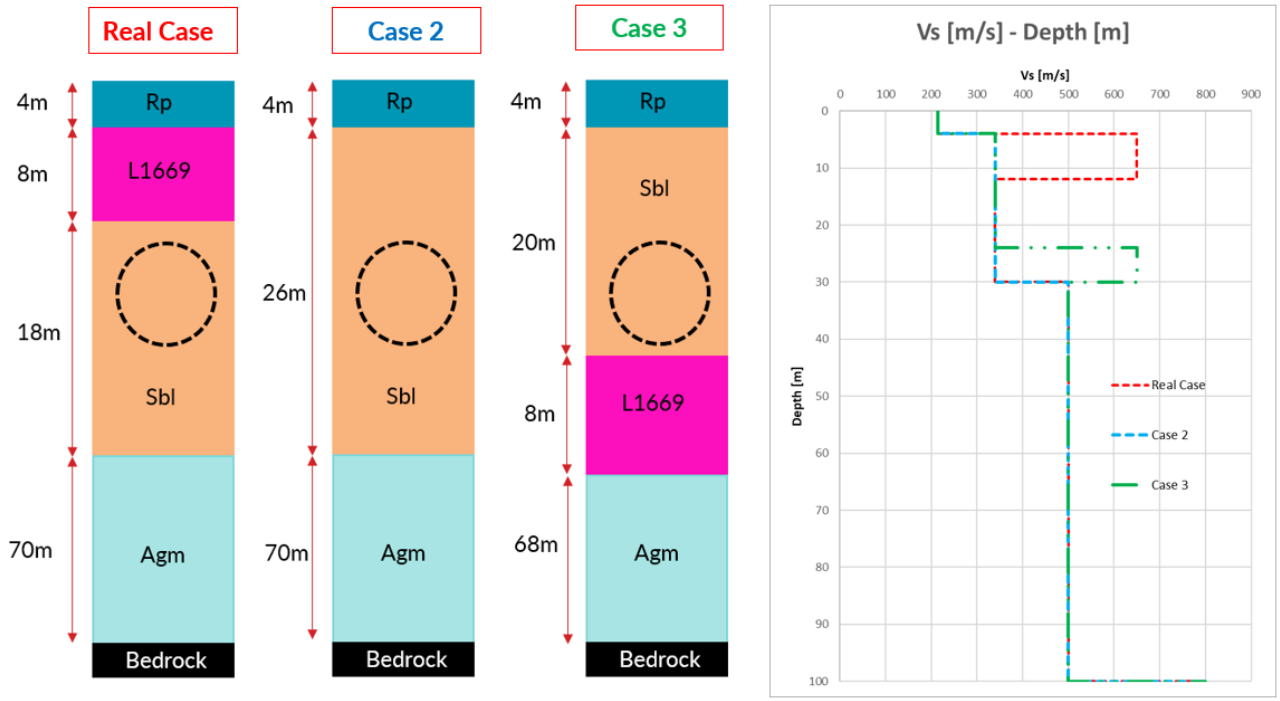

Figure 4-37 Schematic Representation of the Cases and Their Vs Profiles

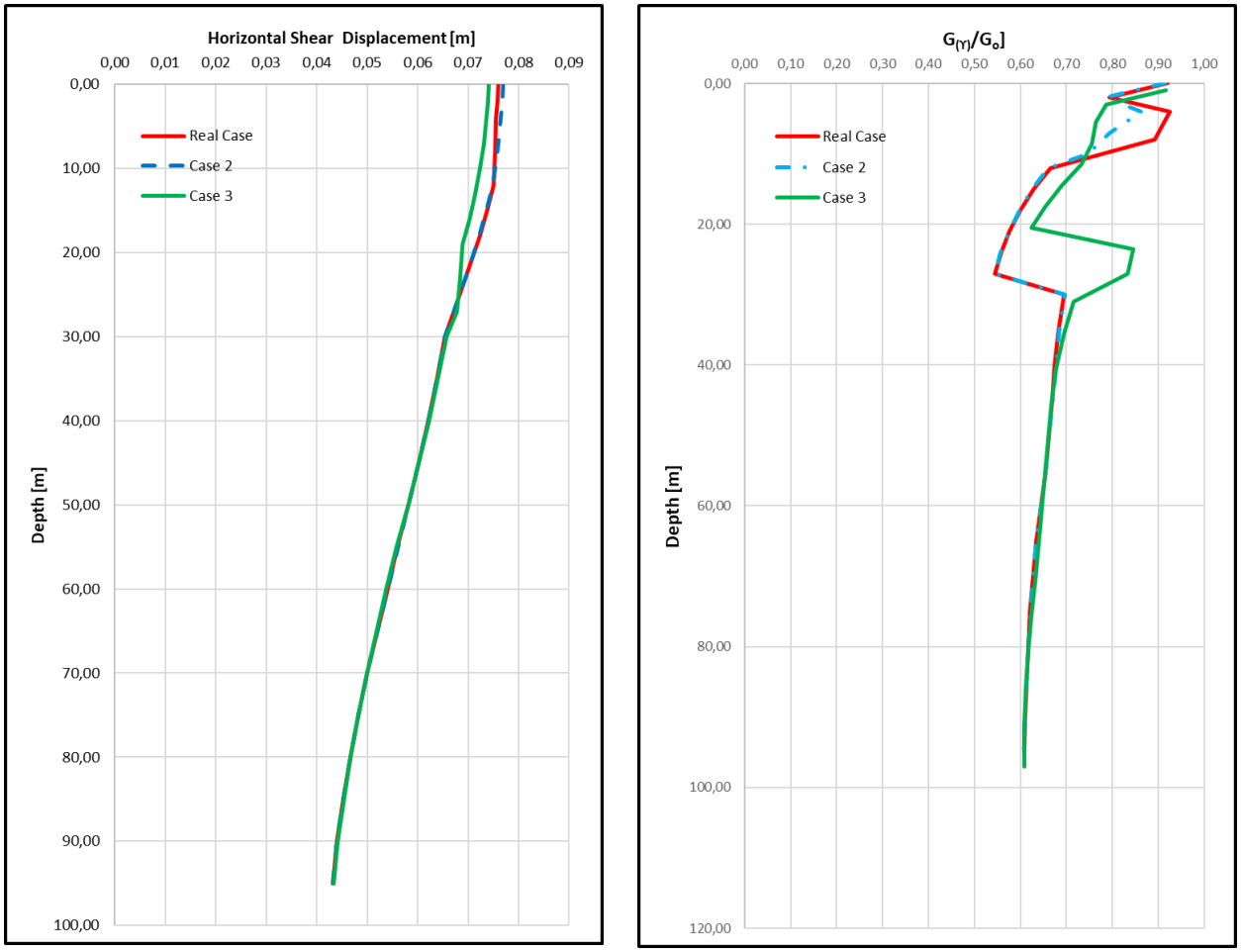

Figure 4-38 Comparison Horizontal Displacement and $G_{(\gamma)}/G_0$ in Cases

As a result, there is 3 methods to compute shear deformation due to seismic action for tunnel project. One of them is suitable just shallow tunnel till 20m depth from surface level. Other methods are suitable both shallow and deep tunnel. Simplified method for deep and shallow tunnel is the most conservative solution. SSR analysis is evident to more accurate solution and the more precise solution. In section have heterogeneous formation and multi-level tunnels like metro station tunnel and reduction tunnel. SSR analysis is recommended as it offers to read in many levels' precise values. In contrary, simplified method is invented for homogeneous and just a tunnel therefore it doesn't offer appliable solution.

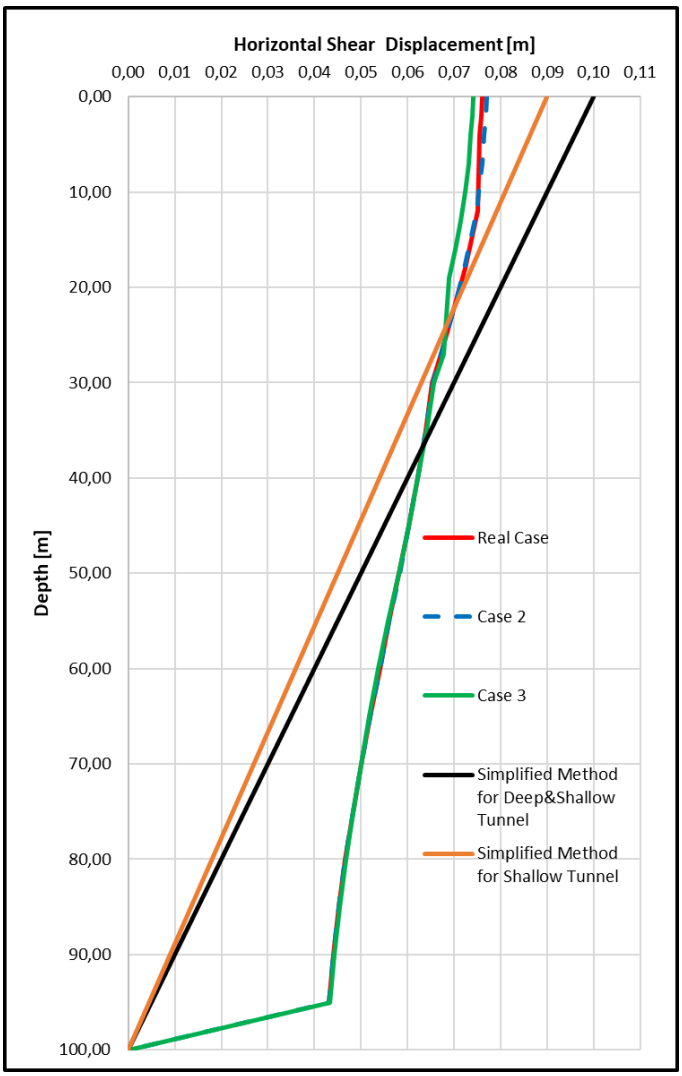

Figure 4-39 4.2 Comparison Free Field Shear Deformation – Each Methods and Cases

In addition, Impact of the L1669 lava formation can be observed apparently. Specially where located under a bit lower level, It reduced shear deformation upper part radically.

Chapter 5

5 Analysis, Results and Discussion

5.1 Static and Seismic Analysis

5.1.1 Static Analysis

The segmental section of the tunnel whose geometry was already described in details in Chapter Numerical Modelling of The Excavation Tunnel - Static Model2.3, was modelled for semplicity as an equivalent continuous concrete ring in the numerical analyses, adopting an equivalent inertia of the lining section, Ieq (Table 5-1), defined as proposed by Muir Wood (1975), by the following equation (4) :

Tunnel lining characteristics			BASE
Lining inner diameter	D_{inn}	m	9,60
Segment thickness	t_s	m	0,32
Segment length	L_s	m	1,50
Nr of segments	N_s	m	7,00
1/3 Key-Segment?	KS	-	NO
Lining outer diameter	D_{out}	m	10,24
Segment weight	W_s	kN	58
Segment inertia	I_s	m^4	0,00273
Segment axial stiffness	EA	MN/m	11611
Segment bending stiffness	EI	MNm^2/m	99
Lining stiffness (Muir-Wood, 1975, JSCE, 1989)			**BASE**
Joint width	t_j	m	0,3875
Joint inertia	I_j	m^4	0,00485
I Muir -Wood inertia	I_{eq}	m^4	0,00574
Effective ratio of bending rigidity	η	-	2,10
Transfer ratio of bending moment	ξ	-	-1,10
Equivalent bending stiffness	EI_{eq}	MNm^2/m	208
Eq. ring thickness	$t_{s,eq}$	m	0,464
Eq. Young's modulus	E_{eq}	kPa	25,0
	PLAXIS	**RESUME**	
Axial stiffness	EA	kN/m	11610560
Bending stiffness	EI	kNm^2/m	208280
Linear weight segment	w_c	kNm/m^3	8,6
Eq. gamma ring	γ_{eq}	kN/m^3	18,62
Poisson Ratio	v_c	-	0,2

Table 5-1 Tunnel Lining Characteristic

The finite element mesh of soil and the tunnel, created using Plaxis 2D, (Figure 4.11). Lateral boundary is set up 10D=96m distance and total height of the model is 100m. For the static analysis, the lateral boundary conditions included fixed displacements horizontally at the vertical sides of the model and fixed displacements in both directions at the bottom. Displacements along the upper surface were left unrestricted.

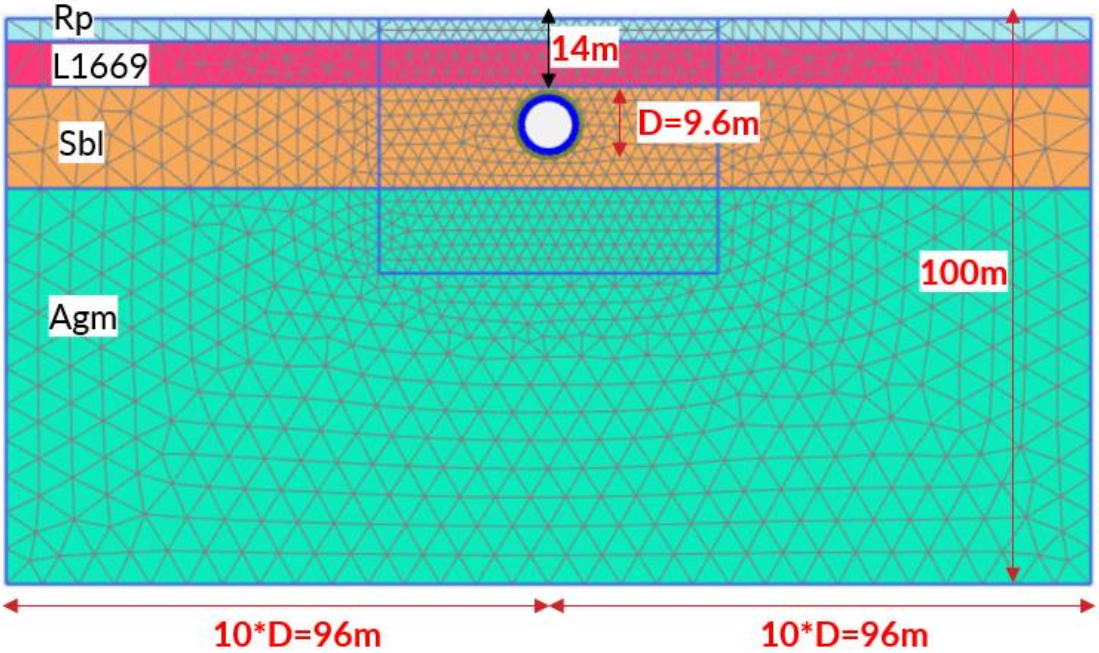

Figure 5-1 Plaxis 2D FE numerical static excavation model

An interface between the segmental lining and soil is introduced, with a reducing factor R= 0.7 applied to reduce strength and stiffness of the interface material, compared to the surrounding soil. Stress relaxation coefficient λ is accepted equal to 0.3.

Mohr-Coulomb soil model is used. Geotechnical parameters are summarized in Table 3-8

The excavation is simulated through three phases:

- 1st Phase: Generation of the initial lithostatic stress field.
- 2nd Phase: 30% Stress relaxation.
- 3rd Phase: Activation segmental lining and Interface.

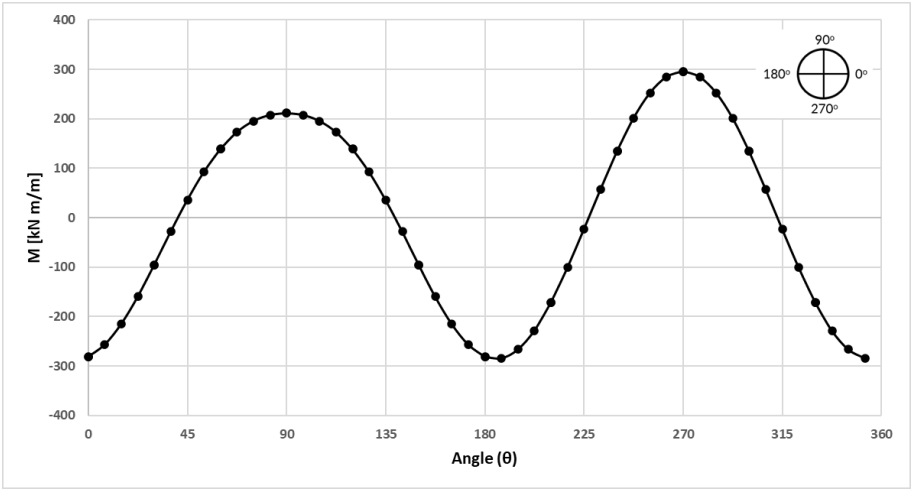

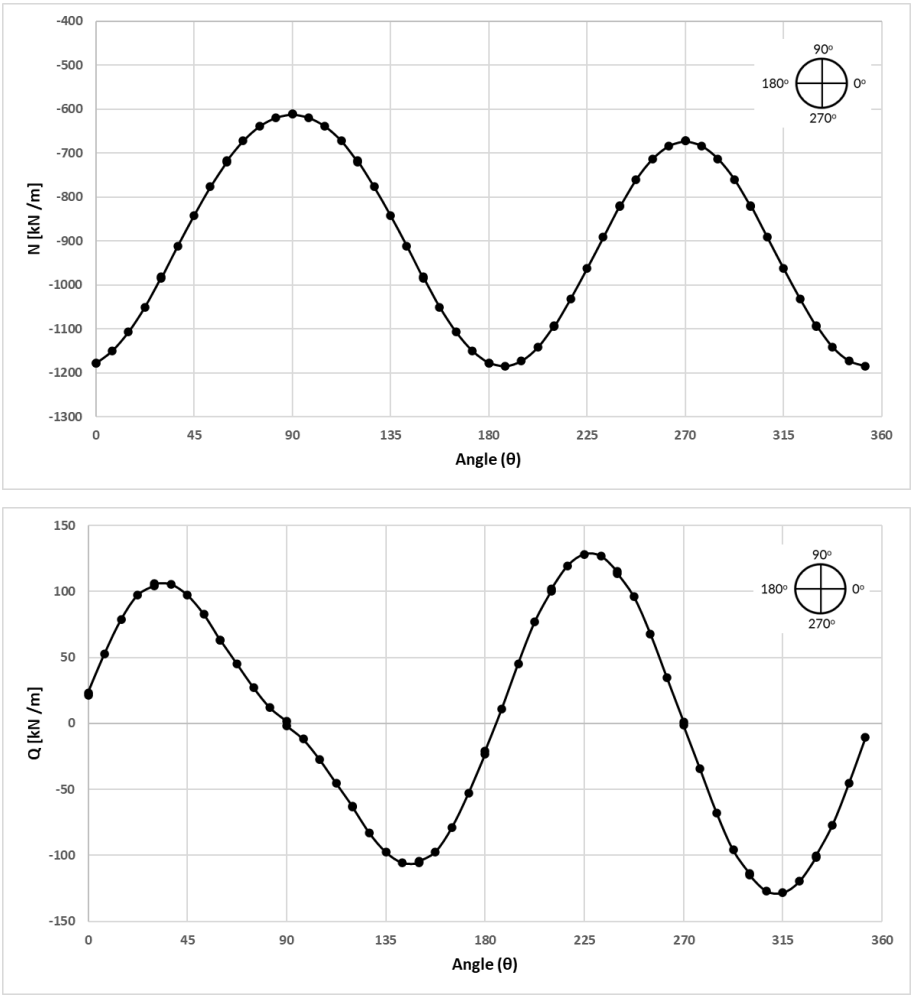

Figure 5-2 Static internal forces in the tunnel lining.

5.1.2 Seismic Analysis

5.1.2.1 Analytical Analysis Results

Lining parameters which are defined in Table 5-1, is used for computation. Calculation in Table 5-2, is followed steps are definein Chapter 2.6.1.

Input			
Deformazione al taglio indotta dal sisma		γ_{max}	0,00100 -
Modulo di deformazione al taglio iniziale		G_m	146000 kPa
Effective Young modulus of ground		E_m	379600 kPa
Coefficiente di Poisson del terreno		ν_s	0 -
Summary of the analysis and results			
Full- slip condition (Penzien, 2000)			
a^n - Penzien (2000) Full-Slip Condition	Eq. 44	a^n	0,058
R^n Penzien (2000)	Eq. 43	R^n	2,65
Δd^n lining Penzien (2000)	Eq. 39	ΔD^n_{lining}	0,013
Flexural moment	Eq. 42	M	**173,6** kNm/m
Axial force	Eq. 40	T	**35,0** kN/m
Shear force	Eq. 41	V	**-70,0** kN/m
No- slip condition (Penzien, 2000)			
Coefficient of lining-soil racking ratio	Eq. 38	a	0,066
Lining-soil racking ratio	Eq. 43	R	2,63
Lining diametric deflection	Eq. 34	ΔD_{lining}	0,013 m
Flexural moment	Eq. 37	M	**172,4** kNm/m
Axial force	Eq. 35	T	**69,5** kN/m
Shear force	Eq. 36	V	**-139,0** kN/m
Full- slip condition (Wang,1993)			
Parametro F Wang (1993) ,Flexibility ratio	Eq. 25	F	27,37
Rigidity K1 Wang (1993) , Lining response coefficient	Eq. 33	K1	0,1450
Flexural moment	Eq. 32	M	**173,6** kNm/m
Axial force	Eq. 31	T	**35,0** kN/m
No- slip condition (Wang,1993)			
Compressibility ratio ©	Eq. 24	C	0,29938
Rigidity K2 Wang (1993), Lining trust response coefficient	Eq. 28	K2	1,13
Flexural moment	Eq. 27	M*	**173,6** kNm/m
Axial force	Eq. 26	T	**819,6** kN/m

Table 5-2 Resutl of the Analytical Solution Wang,1993 and Penzien,2000

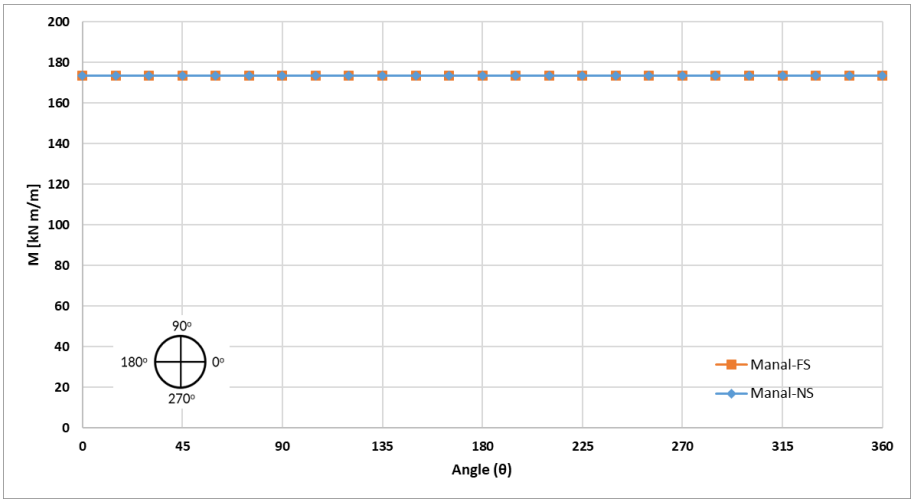

Figure 5-3 Seismic Bending Moment in the tunnel lining – Wang , 1993 – Analytical Approach

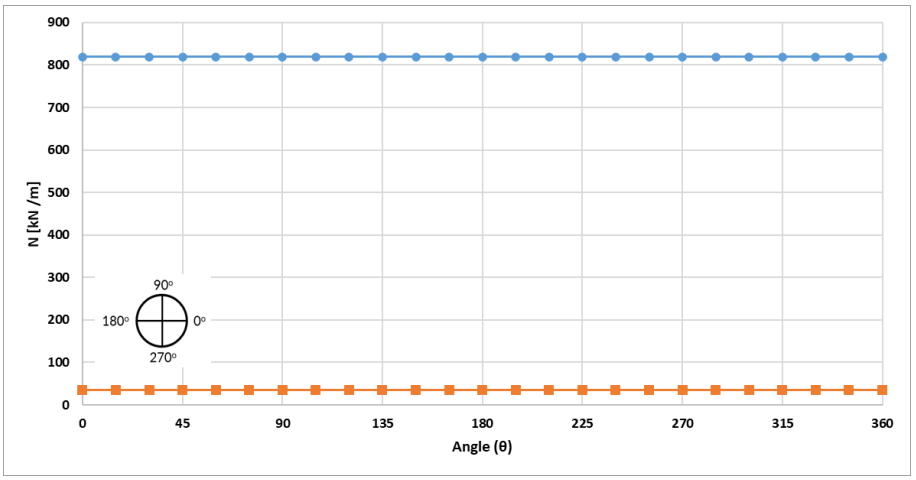

Figure 5-4 Seismic Axial forces in the tunnel lining – Wang , 1993 – Analytical Approach

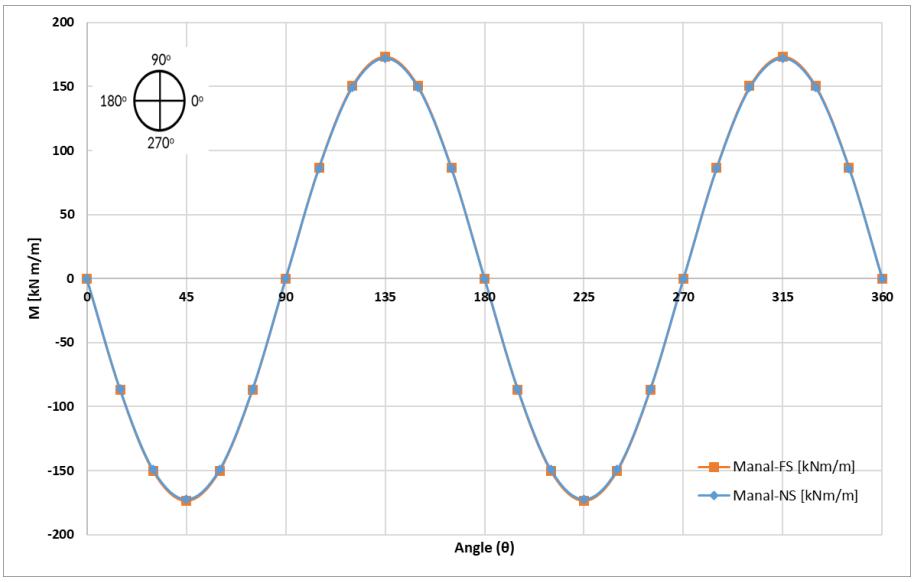

Figure 5-5 Figure 5-6 Seismic bending moment in the tunnel lining – Penzien, 1993- – Analytical Approach

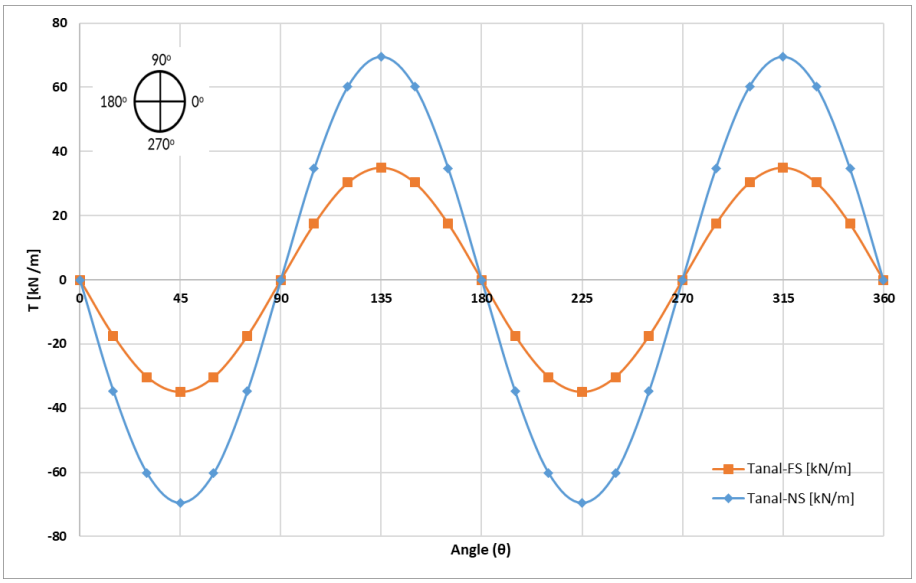

Figure 5-7 Seismic axial forces in the tunnel lining – Penzien, 1993- – Analytical Approach

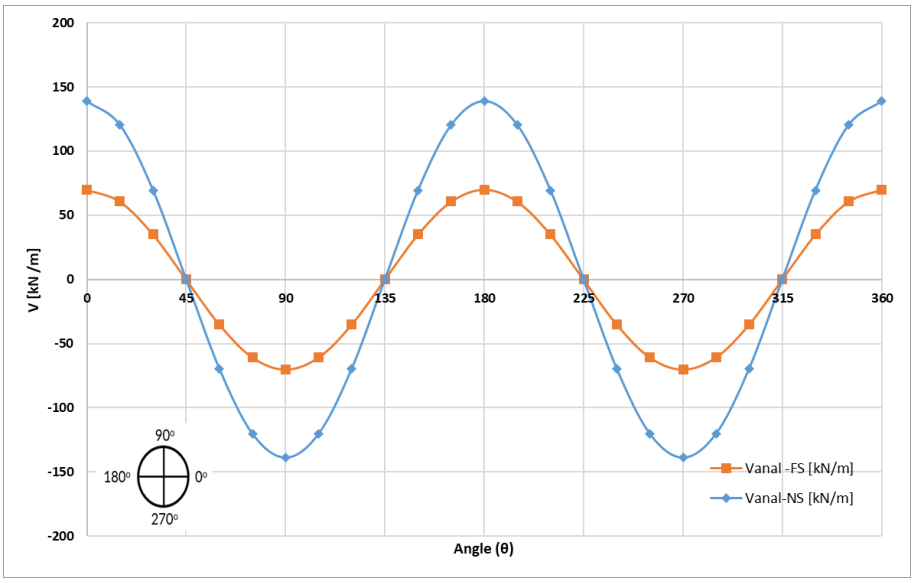

Figure 5-8 Seismic shear forces in the tunnel lining – Penzien, 1993- – Analytical Approach

5.1.2.2 Simplified Approach (Simplified Free Field Motion + Pseudo Static 2D Analysis)

The result of the simplified free-field seismic response analyses described in chapter 4.3. 0.1m horizontal displacement is described linearly both sides on the model, and uniformly at top of the model. Model boundary condition at y-direction fixed and x-direction prescribed. While bottom boundary is fixed both direction, top boundary is described free in y-direction and prescribed in x-direction. It is assumed that analyses cross-section is homogeneous.

Model condition

- $\Delta x_{max} = \gamma_{max} \cdot h_{mod} = 0.001 * 100m = 0.1m$
- Soil Model : Linear Eastic
- Soil Formation: Sbl
- $G_{(\Upsilon)}$ = 146 Mpa
- Analys Type: Full-Slip and Non-Slip conditons

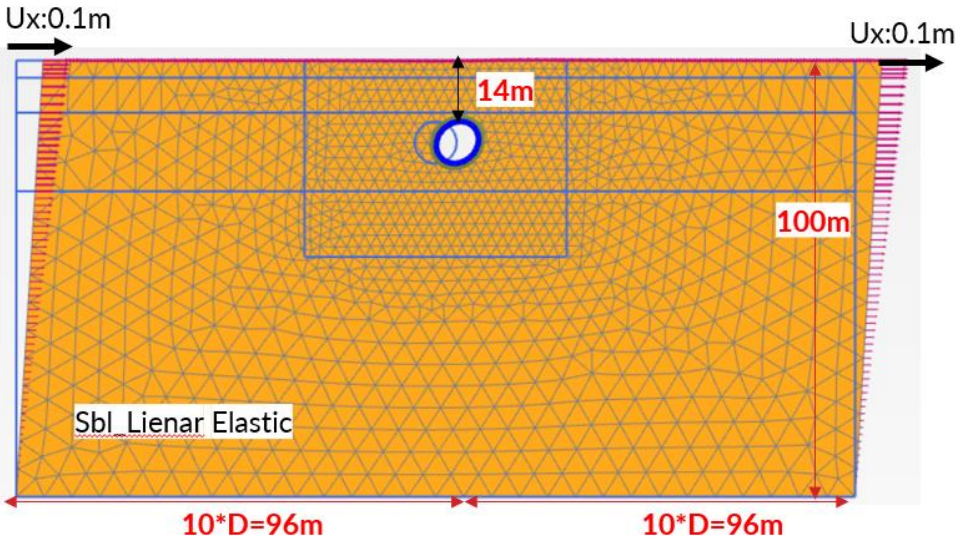

Figure 5-9 Mesh and boundary conditions of the FEM model – Simplified Approach

Seismic Actions on the Tunnel

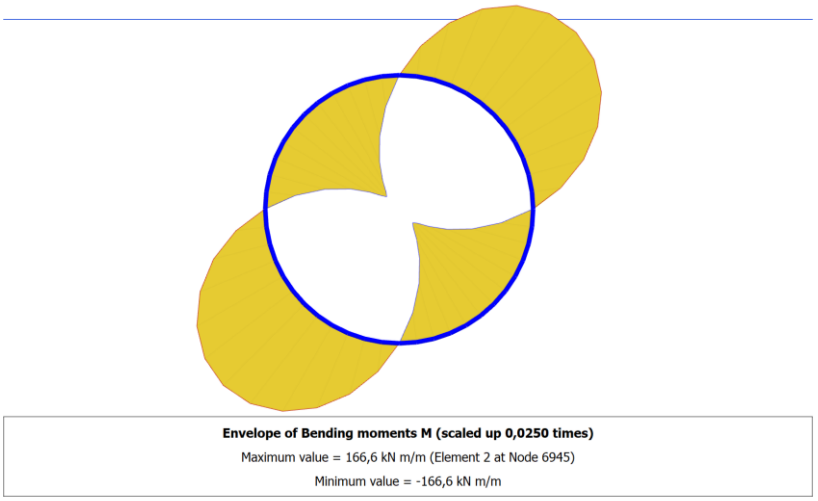

Figure 5-10 Envelope Bending Moment – Non-Slip Condition – Simplified Approach

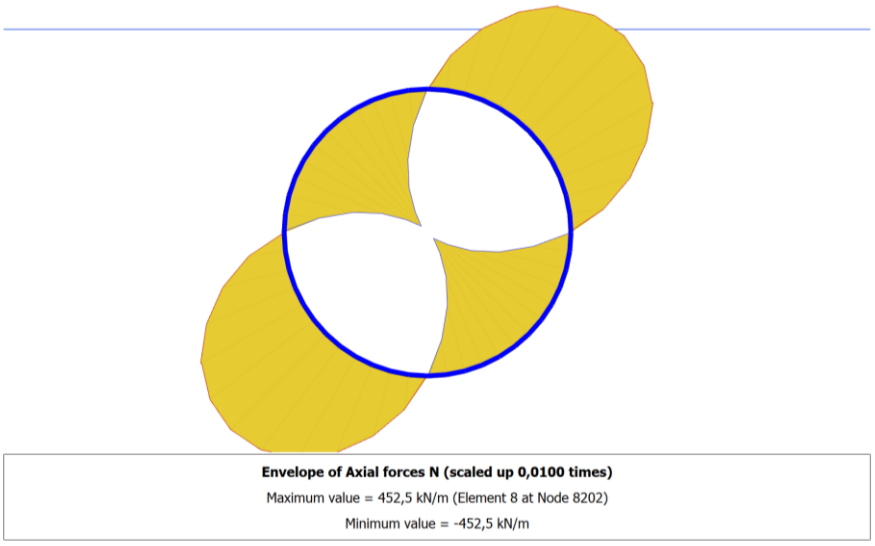

Figure 5-11 Envelope Bending Axial Force – Non-Slip Condition – Simplified Approach

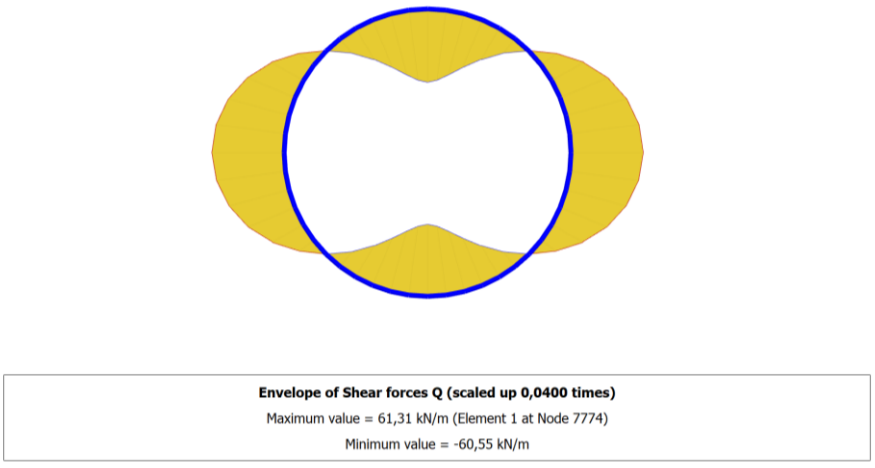

Figure 5-12 Envelope Shear Force – Non-Slip Condition – Simplified Approach

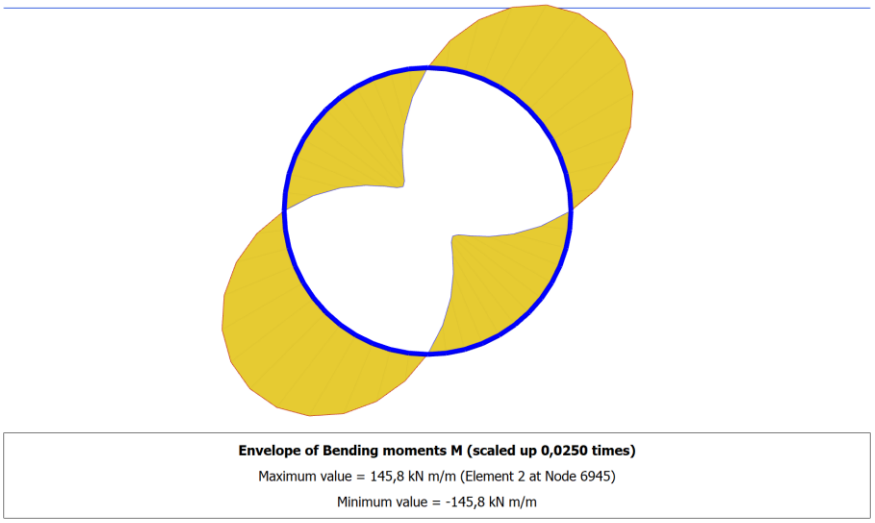

Figure 5-13 Envelope Bending Moment – Full-Slip Condition – Simplified Approach

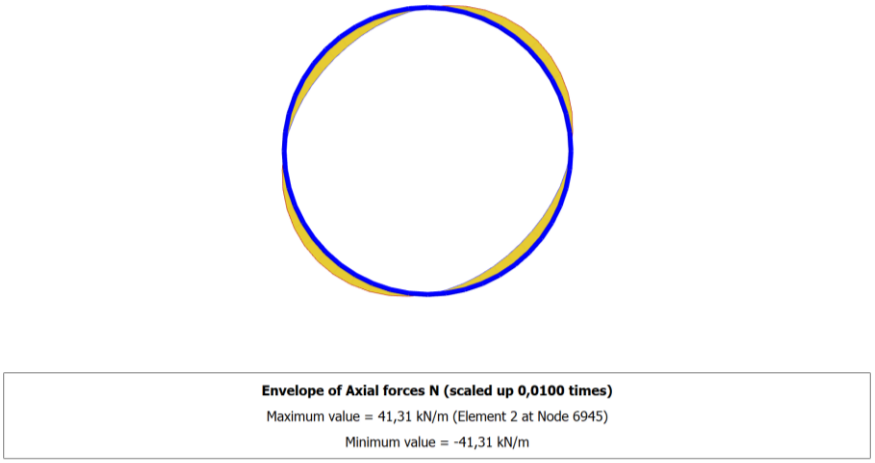

Figure 5-14 Envelope Axial Force – Full-Slip Condition – Simplified Approach

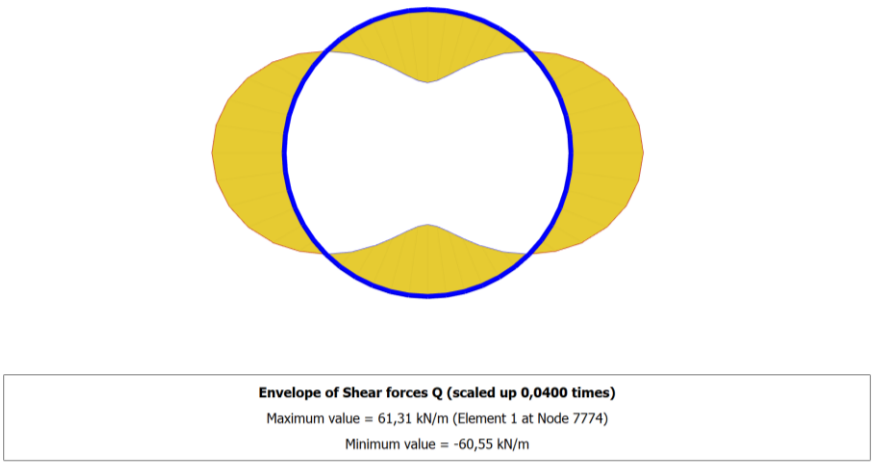

Figure 5-15 Envelope Shear Force – Full-Slip Condition – Simplified Approach

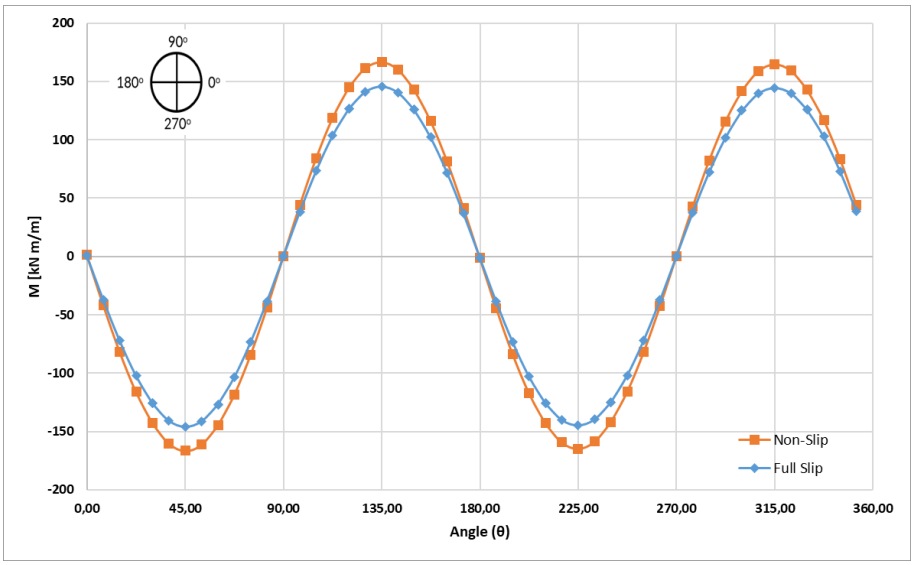

(a)

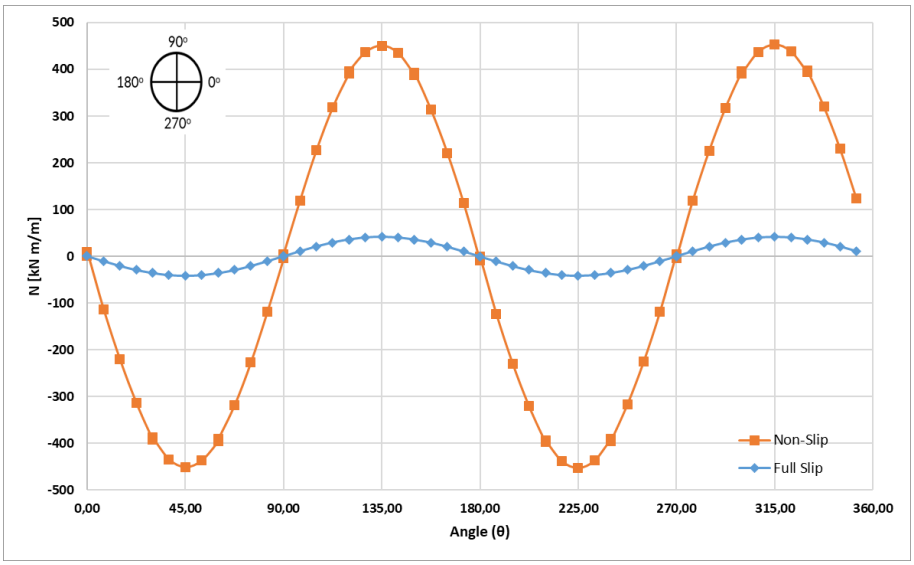

(b)

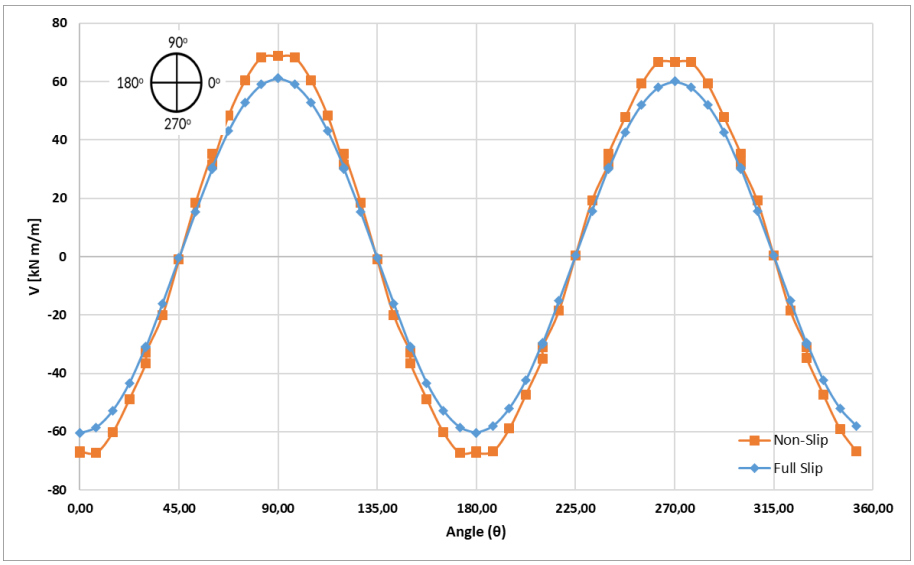

(c)

Figure 5-16 Comparison the action at the Full Slip and Non-Slip Condition a)Bending Moment kN.m/m , b) Axial Force kN/m and c)Shear Force kN/m

5.1.2.3 Uncoupled Approach (SSR + Pseudo static Analysis)

The result of the free-field seismic site response analyses described in 4.4. Average horizontal displacement in Figure 4-35 is described both sides on the model, and the average horizontal surface displacement is described at top of the model. Model boundary condition at y-direction fixed and x-direction prescribed. (Figure 5-17)While bottom boundary is fixed both direction, top boundary is described free in y-direction and prescribed in x-direction. All layer which has already been defined at Deepsoil, is defined on the model as linear elastically. $G_{(Y)}$ which is derived from SSR analysis (Figure 4-36), is defined on each layer (25 Layers)

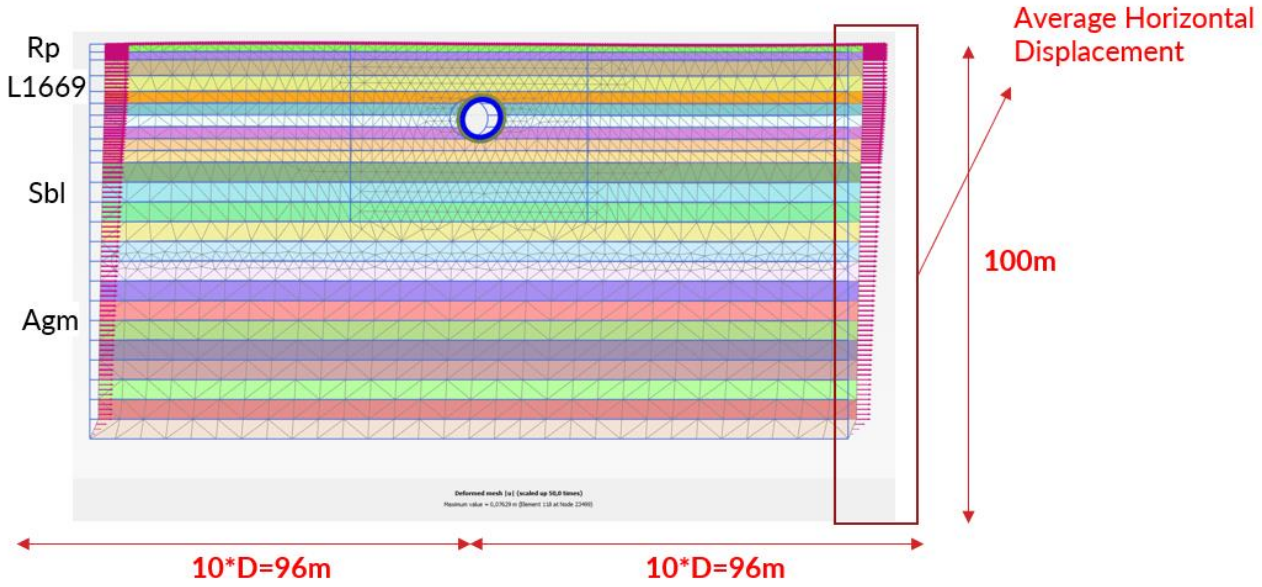

Figure 5-17 Mesh and boundary conditions of the FEM model – Uncoupled Approach

Seismic Actions on the Tunnel

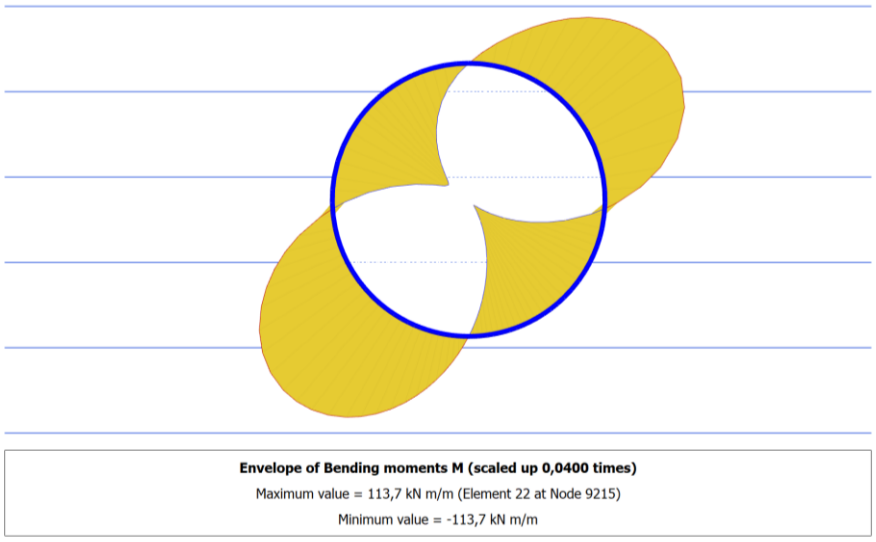

Figure 5-18 Envelope Bending Moment – Non -Slip Condition – Uncoupled Approach

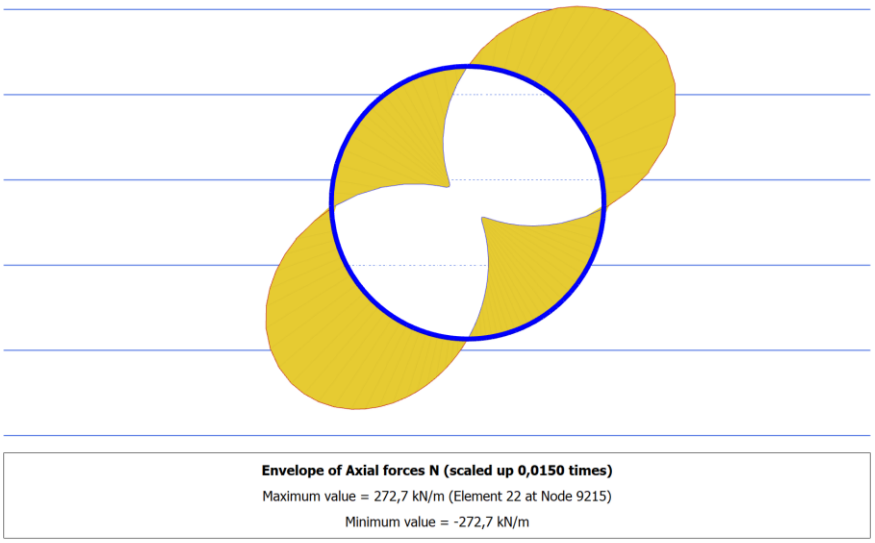

Figure 5-19 Envelope Axial Forces – Non-Slip Condition – Uncoupled Approach

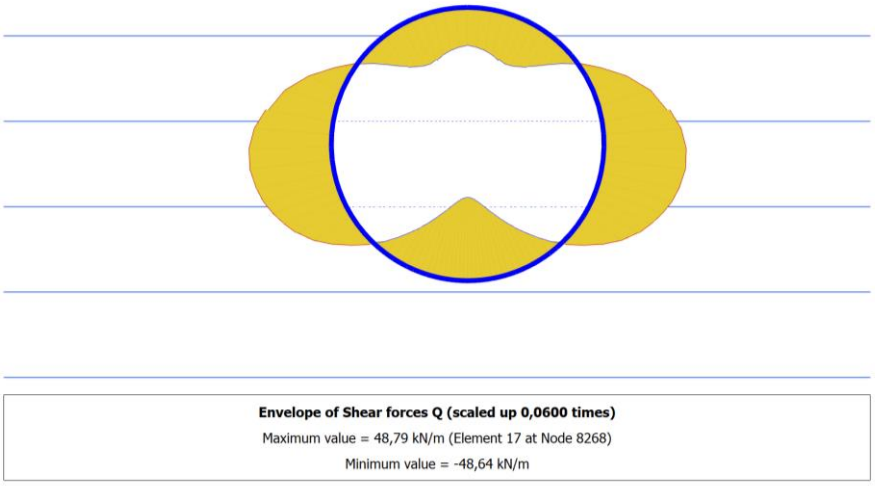

Figure 5-20 Envelope Shear Forces – Non-Slip Condition – Uncoupled Approach

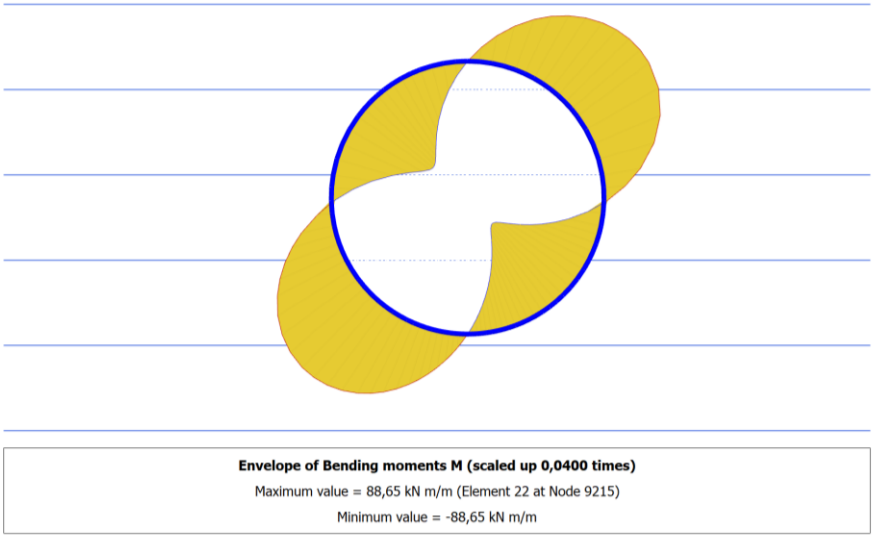

Figure 5-21 Envelope Bending Moment – Full -Slip Condition – Uncoupled Approach

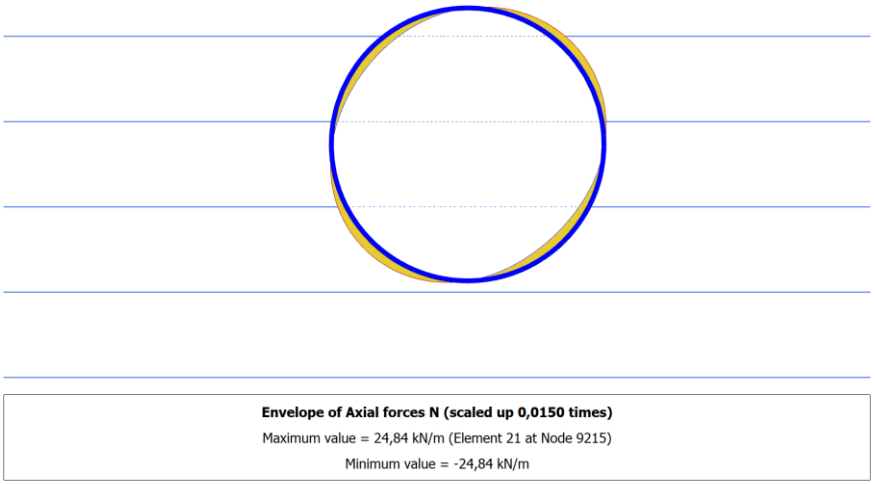

Figure 5-22 Envelope Axial Force – Full -Slip Condition – Uncoupled Approach

Figure 5-23 Envelope Shear Force – Full -Slip Condition – Uncoupled Approach

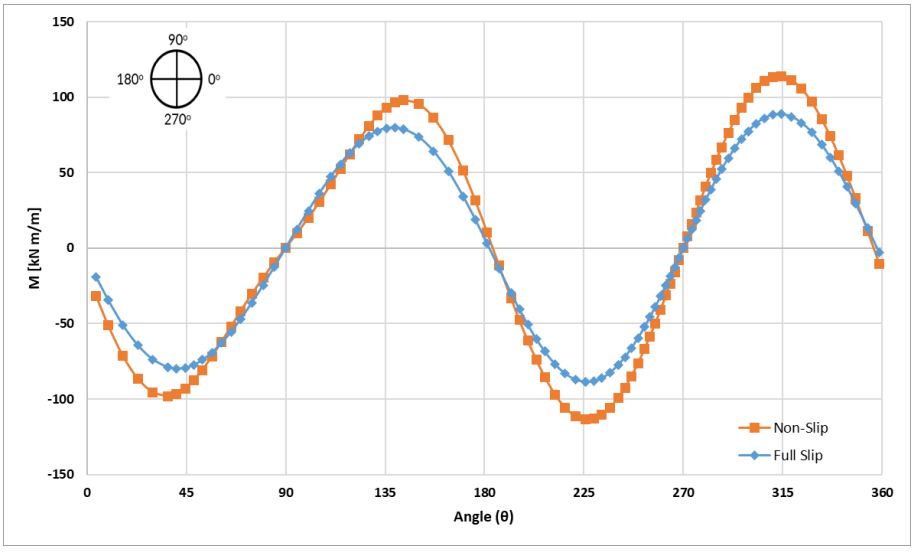

(a)

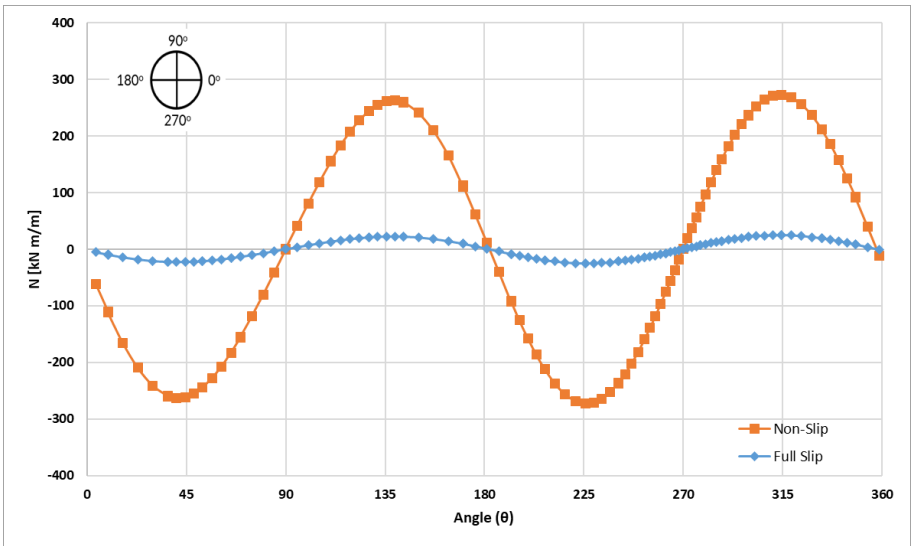

(b)

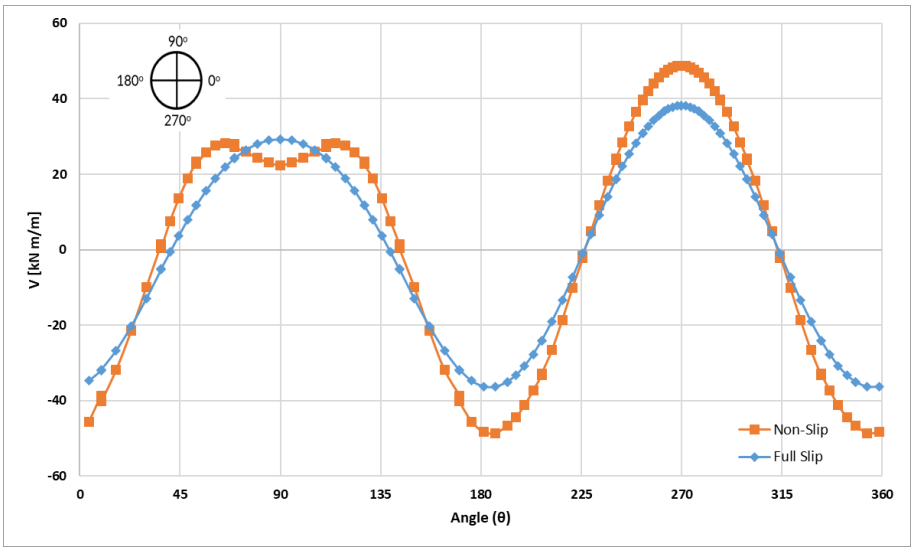

(c)

Figure 5-24 Comparison the action at the Full Slip and Non-Slip Condition a)Bending Moment kN.m/m , b) Axial Force kN/m and c)Shear Force kN/m

5.1.2.3.1 Impact of the L1669-Lave geological Unit

It is not uncommon for an 8m layer of rock to be located between ground formations. The reason for this is that the project area is a place where volcano movements are observed. This is a fact that affects the behavior of the lava layer in static and seismic conditions. For this reason, it should be examined in detail and measures should be taken regarding this heterogeneity. As explained in Chapter 4.4.6, 3 different 3 cases are considered to understand impact of L1669 formation on tunnel behavior under seismic actions, Obtained average horizontal displacement derived from SSR analysis are applied on models for each cases as explained previous chapter.

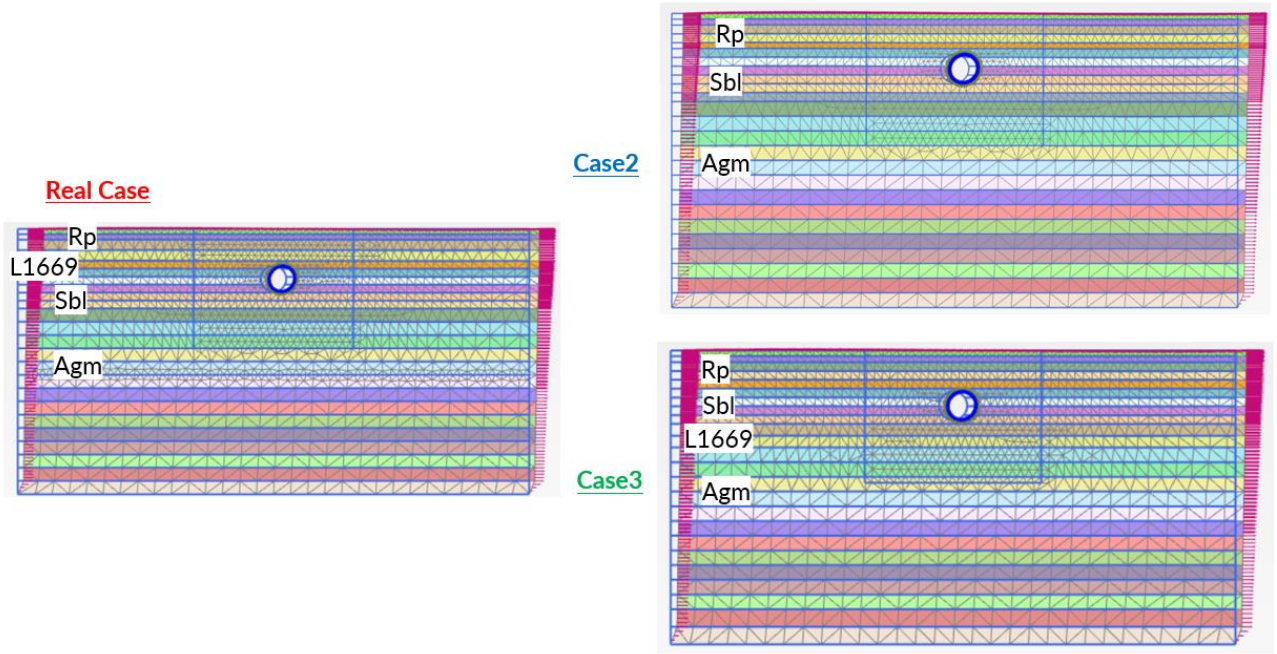

Figure 5-25 Mesh and boundary conditions of the FEM model of the Each Cases – Uncoupled Approach

In below, internal forces on tunnel lining are compared both full-slip and non-slip condition.

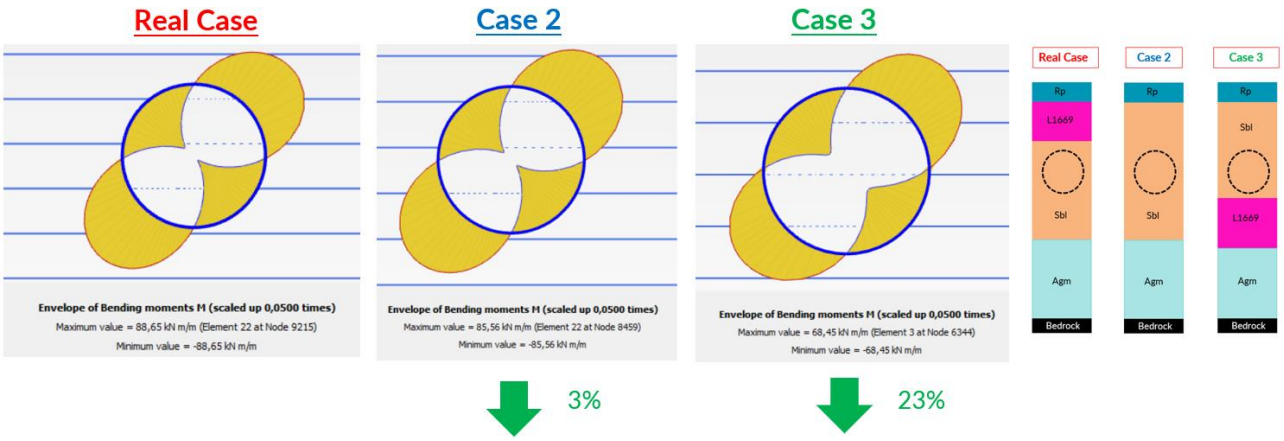

Figure 5-26 Envelope Bending Momen kNm/m – Full-Slip Condition

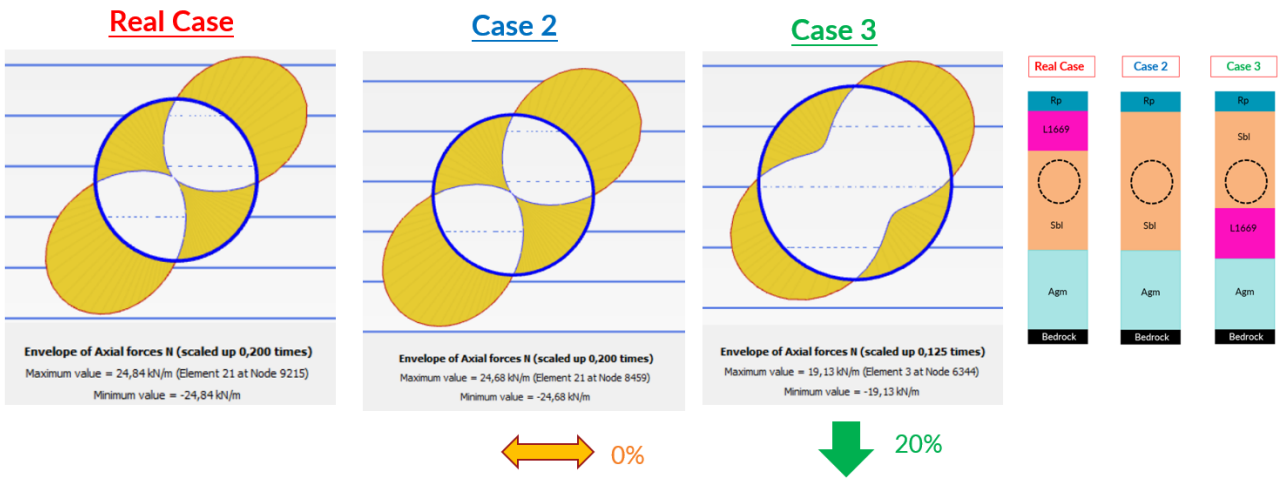

Figure 5-27 Envelope Axial Force kN /m – Full-Slip Condition

Figure 5-28 Envelope Bending Momen kNm/m – Non-Slip Condition

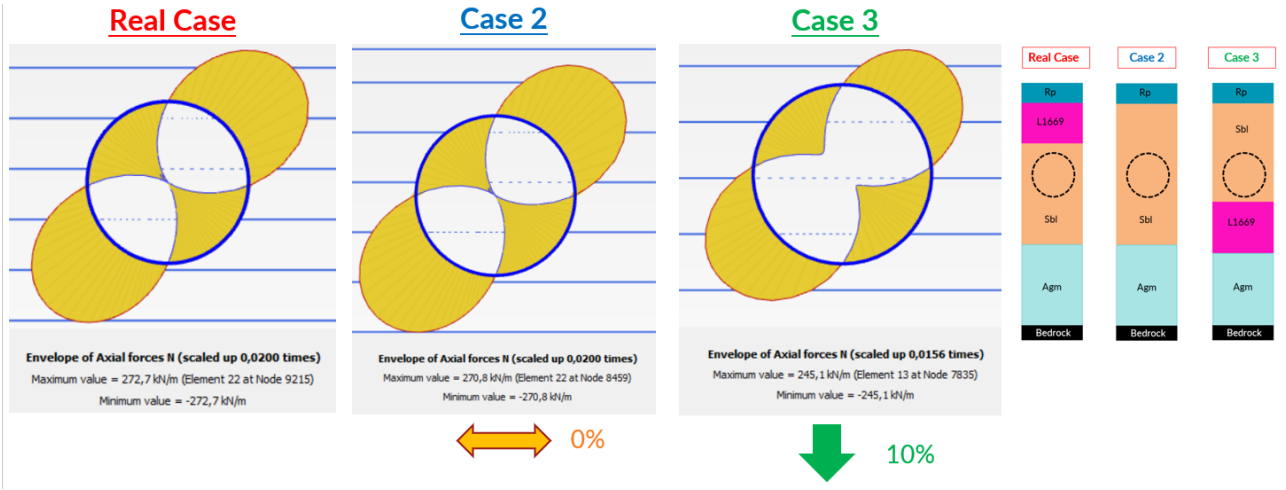

Figure 5-29 Envelope Axial Force kN /m – Non -Slip Condition

It has been proved that the real case is the most critical section after all. As a result of the analyses of the real case and Case 2, no difference is observed between the normal forces on the tunnel in both interface conditions, while a difference of 10% of the moment value is observed. On the contrary, in Case 3 where the lava layer is located under the tunnel, the moment value is 23% in full-slip condition and 30% in non-slip condition. Also, normal force was observed at 20% FS condition and 10% NS condition. When the lava layer is under the tunnel, it creates a barrier effect.

Presumably, if the effect on a building on the surface were to be observed, differences between Case 1 and Case 2 could be observed. However, since the lava layer is located on the tunnel in the real case, not much effect can be observed. Only the fact that the lava layer is on top shows a reflective feature, which makes it more critical than Case 2.

5.1.2.4 Coupled Approach (Non-Linear Analysis)

It's important to note that the identical finite element mesh, as illustrated in Figure 5-1 for static analysis, is initially fine-tuned for comprehensive dynamic analysis. As different from static model, 1m bedrocks has defined at the bottom of the model. The goal was to achieve a genuine free-field

condition at the lateral borders and minimize the impact of vertical boundaries, which were modeled using viscous dashpots in accordance with the recommendations of (Lysmer & Kuhlemeyer, 1969). Additionally, the mesh was discretized to ensure a dependable propagation of the maximum significant frequency of the input signal, leading to an average element size of 1.3m (Figure 5-30)

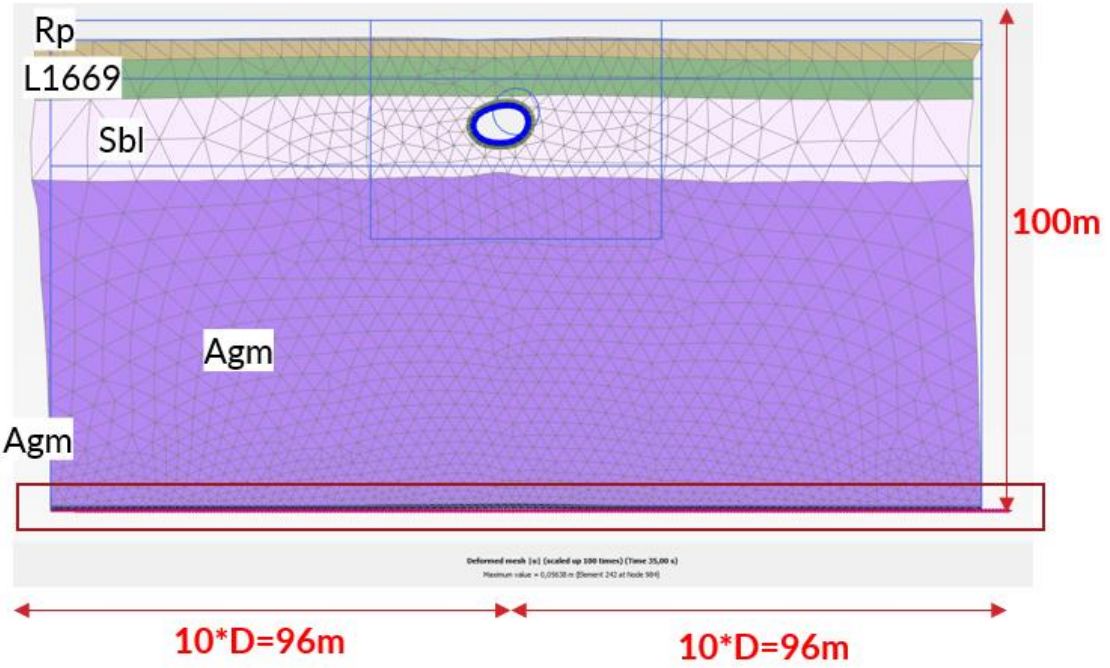

Figure 5-30 Mesh and boundary conditions of the numerical model for full-dynamic analysis of the tunnel

While Rp, Sbl and Agm soil formation are defined with HS Small Strain soil model, L1669 is defined as Mohr-Coulomb and Bedrock is defined Linear Elastic soil model.

General | Mechanical | Groundwater | Thermal | Interfaces | Initial

Property	Unit	Value
Stiffness		
E'_{ref}	kN/m²	3,914E6
v (nu)		0,2500
Alternatives		
G_{ref}	kN/m²	1,566E6
E_{oed}	kN/m²	4,697E6
Depth-dependency		
E'_{inc}	kN/m²/m	0,000
y_{ref}	m	0,000
Wave velocities		
V_s	m/s	800,0
V_p	m/s	1386

Figure 5-31 Bedrock Geotechnical Parameter – Linear Elastic

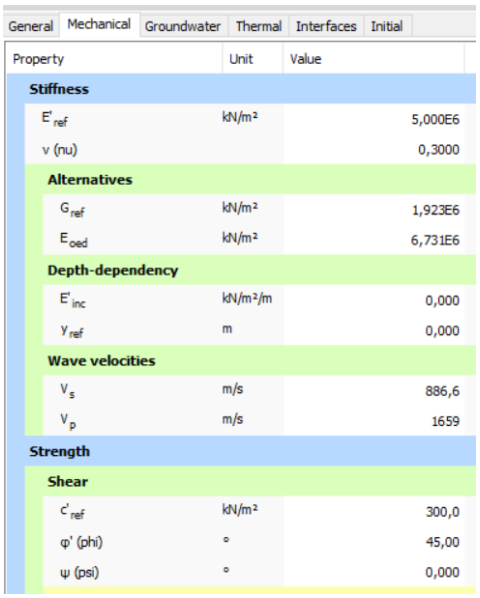

Figure 5-32 L1669 – Lava geotechnical Parameters – Mohr Coulomb

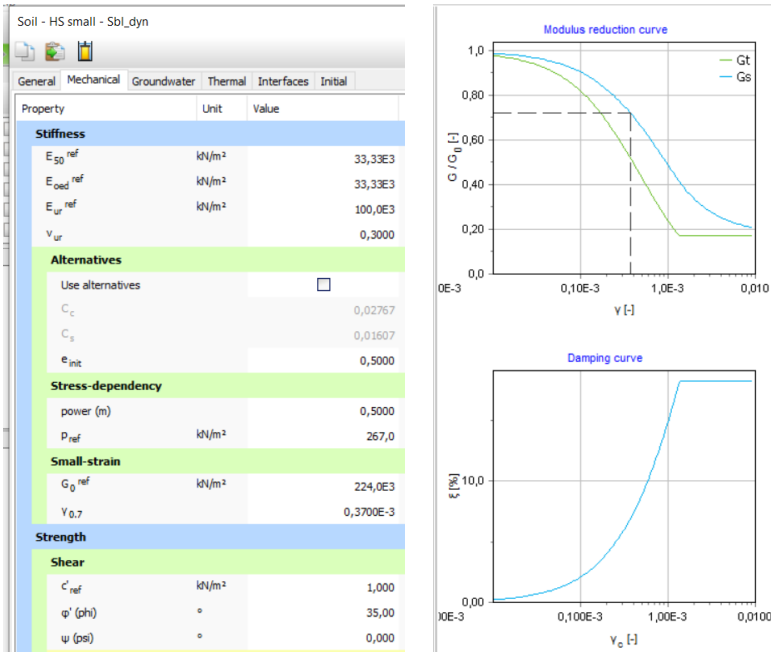

Figure 5-33 Sbl – Volcanic Sand Geotechnical Parameters – HS Small Strain

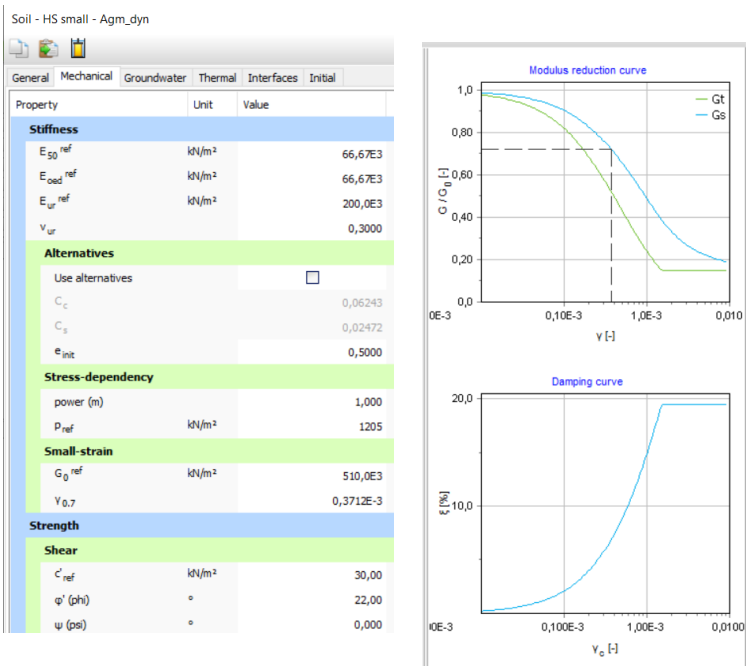

Figure 5-34 Agm – Sandy Silty Clay – HS Small Strain

The 7 selected input motions of earthquakes (Table 4-2) are applied at the rigid base of the model (rigid base means fix-end boundary, that is any downward-traveling waves in the soil will be completely reflected toward the ground surface by the rigid layer) as a time history of acceleration. Scale and duration of defined input motion are summarized in Table 5-3

No.	Earthquake Name	Scale	Duration(s)
EQ1	Irpinia (Italy)	4,89	76,20
EQ2	Umbria Marche (Italy)	6.15	36,00
EQ3	Central (Italy)	0,99	35,00
EQ4	Central (Italy)	1,39	62,00
EQ5	Fruli (Italy)	1.23	36,40
EQ6	Central Italy	0,45	45,00
EQ7	Irpinia (Italy)	4,08	76,20

Table 5-3 Input motions, scale, and Duration

An additional small-strain viscous damping was introduced in the dynamic calculation by means of the well-known Rayleigh formulation (*Park & Hashash 2004*), which considers a linear combination of the mass [M] and the stiffness [K] matrices as follows and it is explained at Chapter 2.6.4

The damping coefficients, α and β, are computed following to the 'double frequency approach' is defined at the Chapter 2.6.4 as target values the first natural frequency of the deposit and the main frequency of the input motion.

$$\xi = 0{,}5$$

$$w_i = 2\pi f = \frac{V_{s,av}}{4H} * 2H = \frac{446m/s}{4*100} = 1.115$$

$$w_j = n * w_i = 5*1.115 = 5.575$$

$$\alpha = 0{,}057$$

$$\beta = 0{,}00023$$

Rayleigh damping		
Input method		SDOF equivalent
Rayleigh α		0,05848
Rayleigh β		0,2375E-3
ξ_1	%	0,5000
ξ_2	%	0,5000
f_1	Hz	1,117
f_2	Hz	5,584

Table 5-4 Rayleigh Damping Coefficient in Plaxis 2D

Utilizing a non-linear soil constitutive model, the comprehensive dynamic analysis of the tunnel-subsoil system enabled the prediction of the internal forces' evolution in the lining. This analysis encompassed the stages of excavation, extending through the conclusion of the seismic shaking. Non-Linear analysis are performed just Non-Slip condition as it most critical and realistic.

Figure 5-35-Bending Moment, Figure 5-36-Normal Force and Figure 5-37 Shear Force show the distribution of the dynamic increment of the actions the actions force in tunnel section.

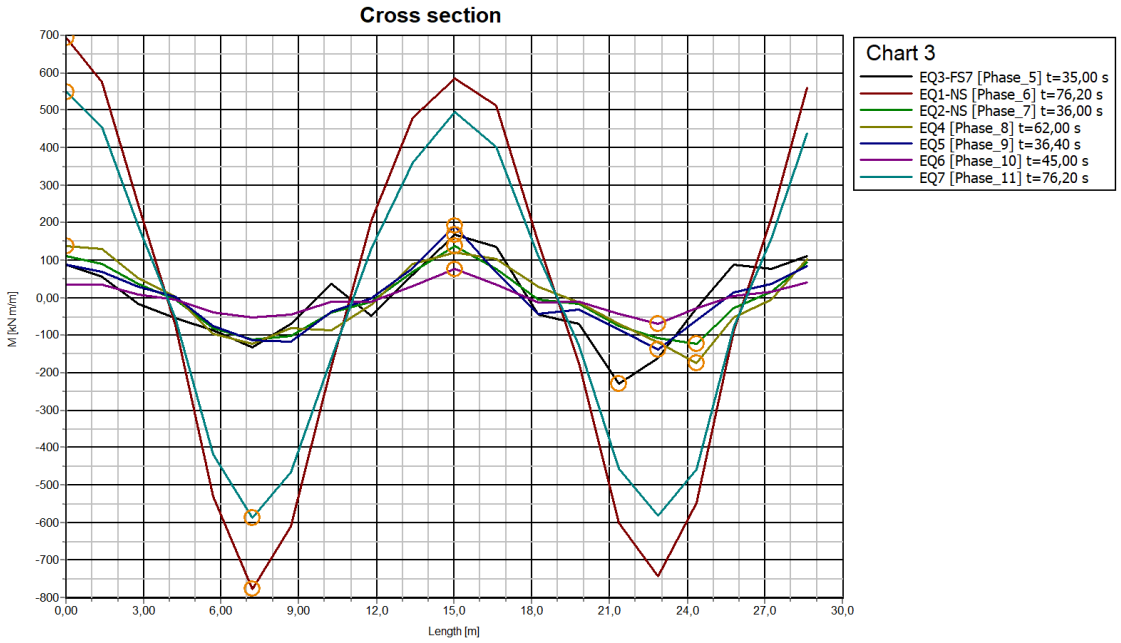

Figure 5-35 Bending Moment kNm/m of the Earthquakes – Coupled Approach

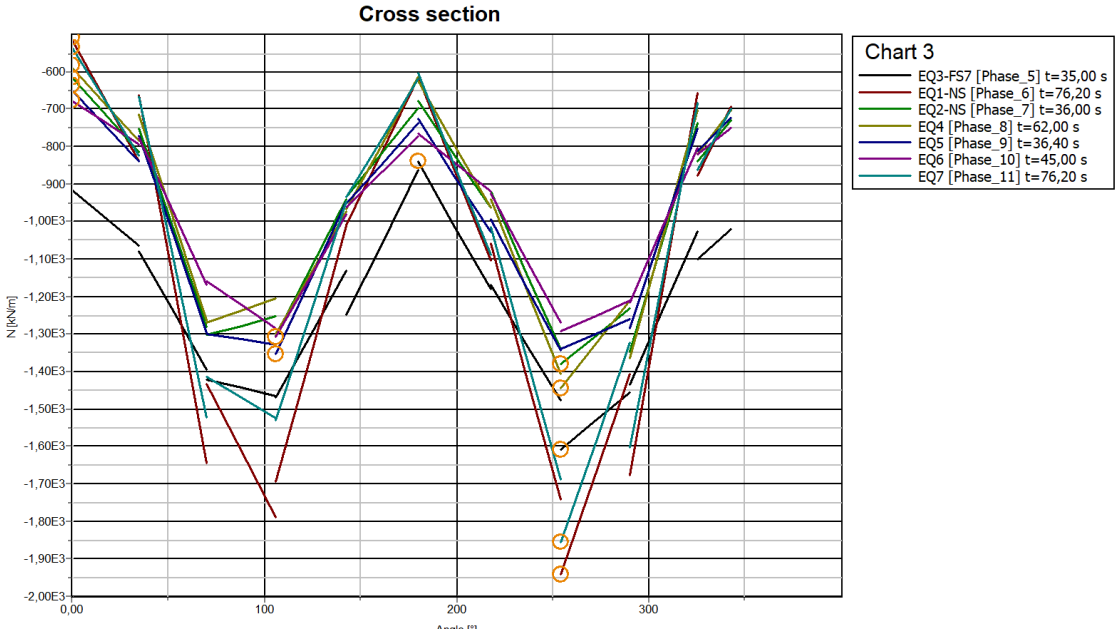

Figure 5-36 Normal Force kN/m of the Earthquakes – Coupled Approach

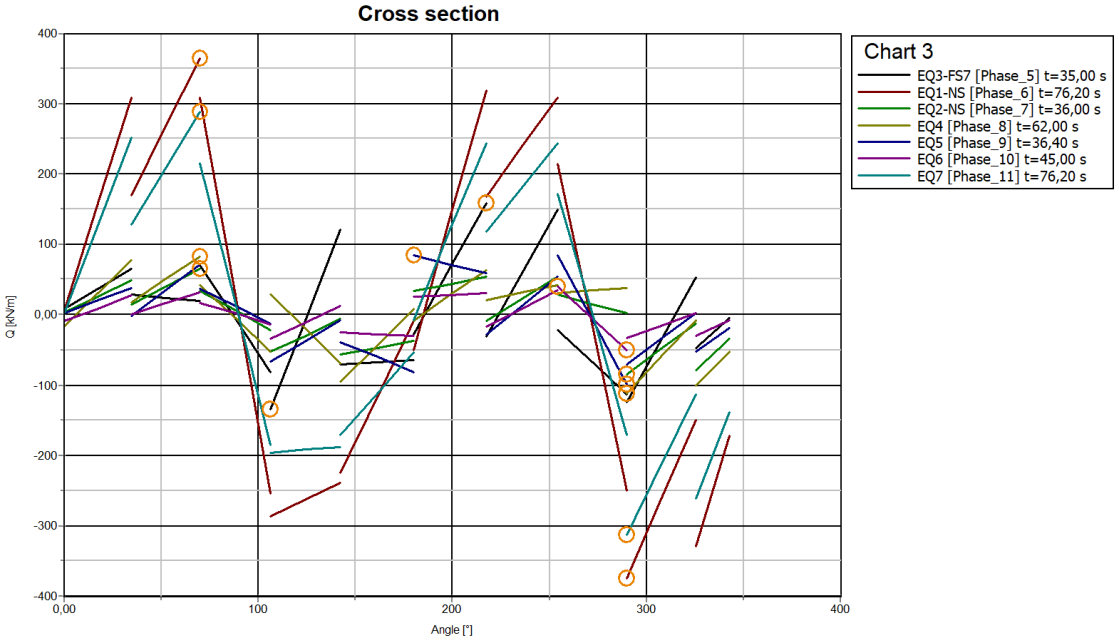

Figure 5-37 Shear Force kN/m of the Earthquakes – Coupled Approach

From the result, earthquakes Table 5-3 with high ground motion duration time and high scale factor cause unexpected internal forces on the tunnel lining and behavior. So, It is assumed that Earthquakes 1 and 7 don't represent reality. Another 5 Earthquakes (2,3,4,5,6) are evaluated to determine design internal action on lining. Average of the output are used for design values, and they are presented in below.

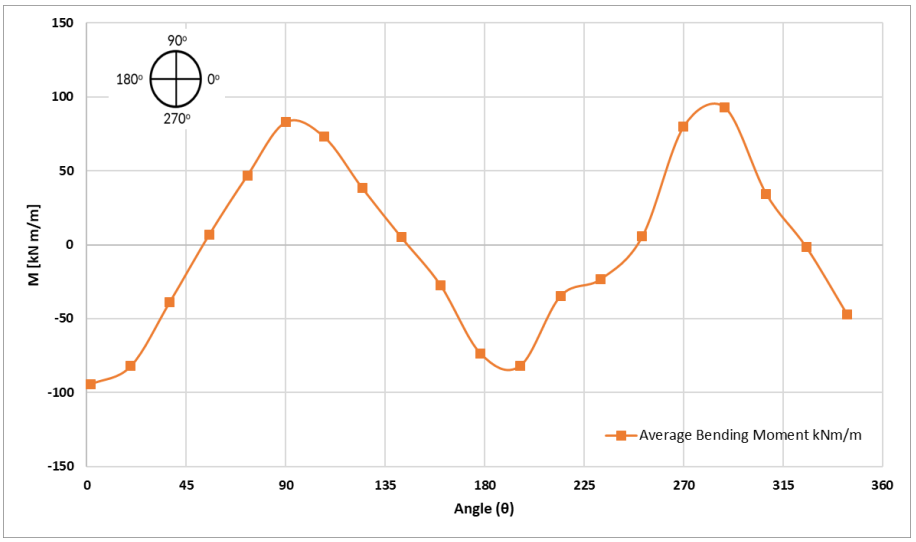

Figure 5-38 – Bending Moment kNm/m – Coupled Approach

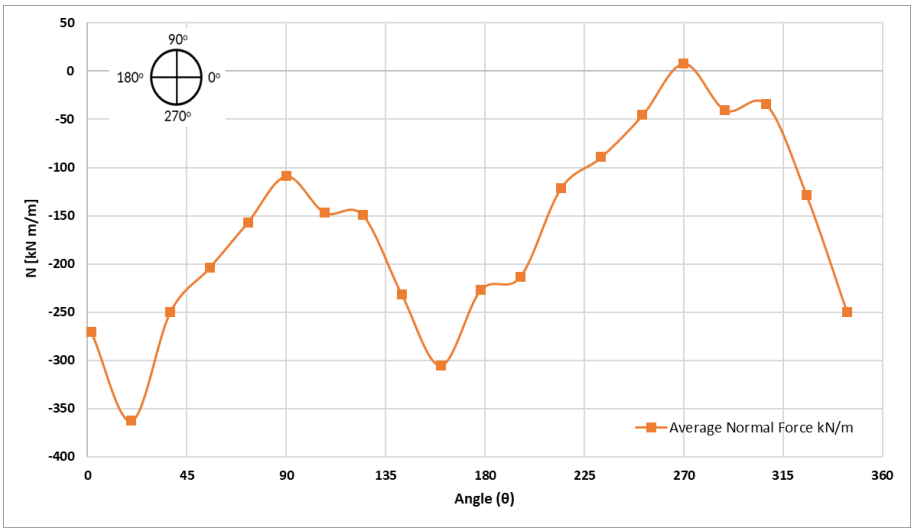

Figure 5-39 Axial Force kN/m – Coupled Approach

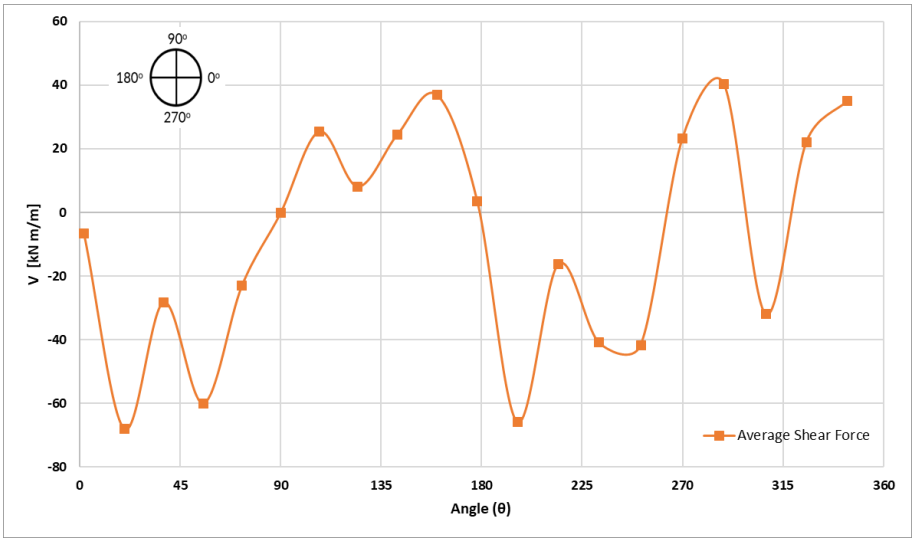

Figure 5-40 Shear Force kN/m – Coupled Approach

5.1.2.4.1 Impact of the L1669-Lave geological Unit

In this section, 2 of the 3 cases previously mentioned are evaluated. Since there is not a big difference between Case2 and the real case, only the real case and Case 3 are compared, 2 models are created as follows.

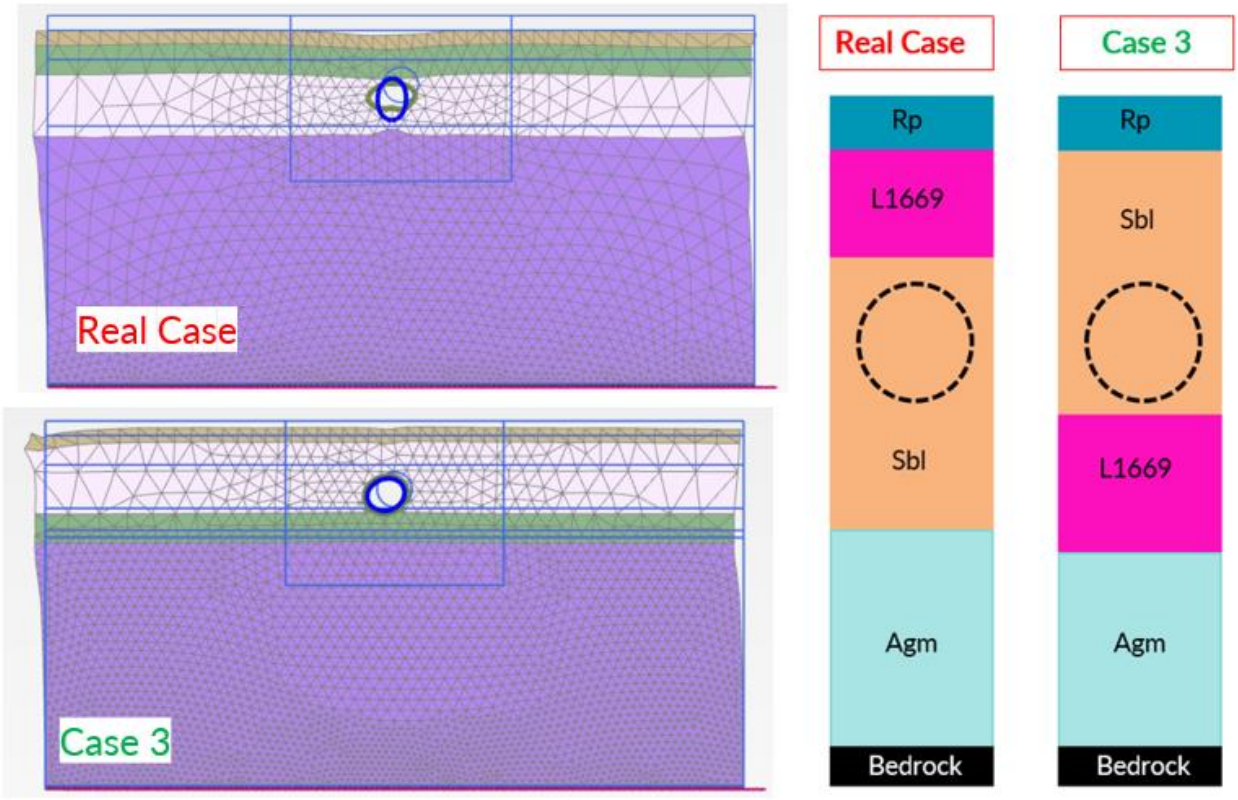

Figure 5-41 Mesh and boundary conditions of the FEM model of the Each Cases – Coupled Approach

As ground motion Earthquake-3 Central Italy which is 36 s ground motion duration time and 0.99 scale factor, are defined as ground motion on the model as it represents average of all favorable earthquakes.

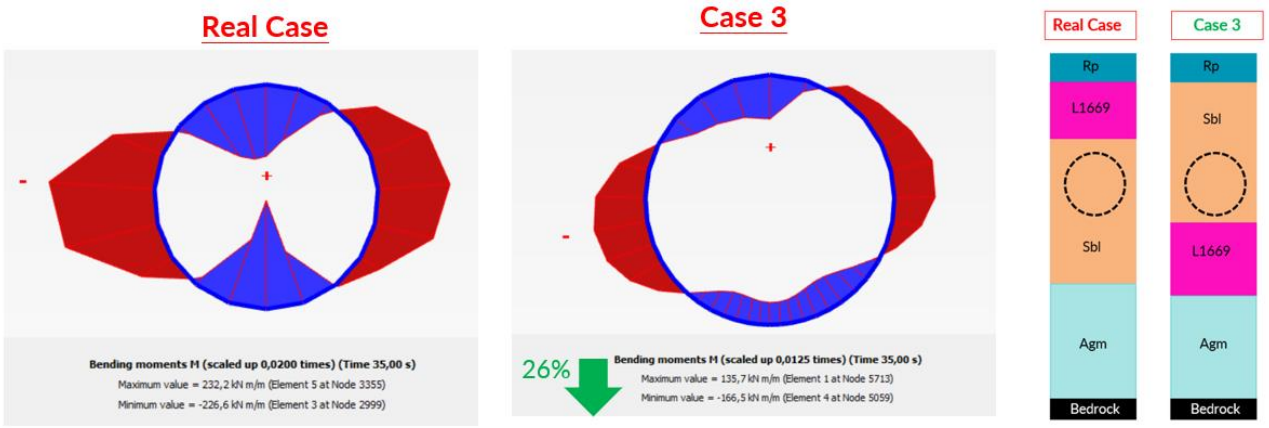

Figure 5-42 Bending Momens kNm/m – Non-Slip Condition – Coupled Approach

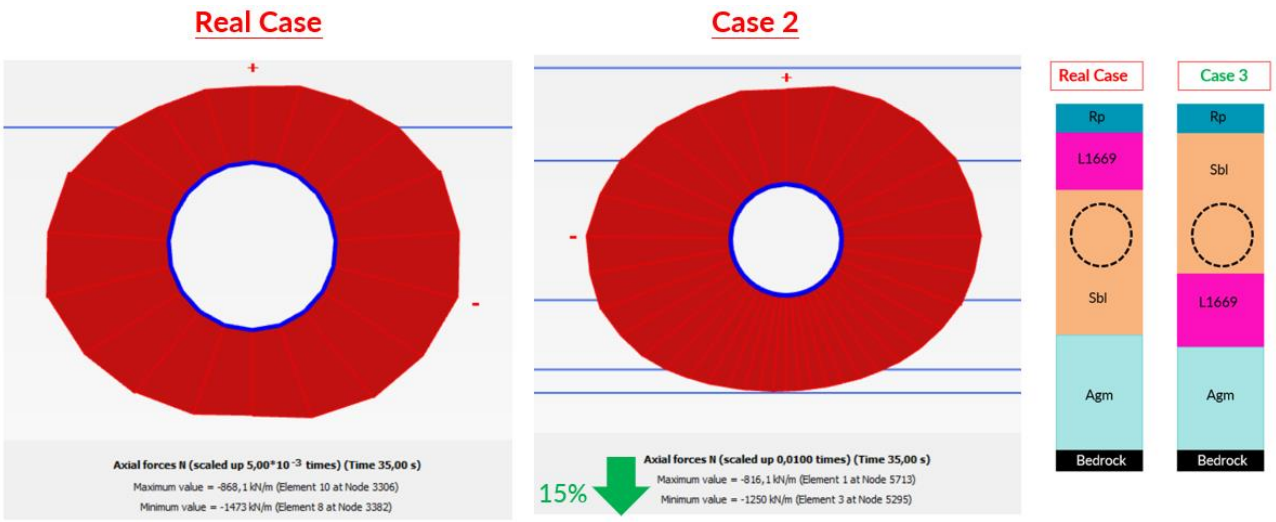

Figure 5-43 Axial Force kNm/m – Non-Slip Condition – Coupled Approach

The relationship between the real case and Case 3 is similar the uncoupled approach. As a result, while the lava layer in the formation is a barrier for the structure above it, it has a negative effect on the structure below it by showing reflective properties.

5.2 Results and Discussion

Internal forces in the tunnel lining due to seismic actions are derived from all approaches which are explained previous chapters, are presented in Table 5-5

Methods		Condition	M (kNm/m)	N (kN)
Analytical	Penzien,2000	Full-Slip	173,6	35
		Non-Slip	172,4	69,5
	Wang,1993	Full-Slip	173,6	35
		Non-Slip	173,6	819,6
Numerical	Simplified Pseudo-static	Full-Slip	145,8	41
		Non-Slip	166,6	452,5
	Uncoupled Approach	Full-Slip	88	25
		Non-Slip	113,7	272
	Coupled Approach	Non-Slip	94	362

Table 5-5 Internal Forces in Tunnel Lining due to Seismic Action Summary Table

While the highest action is derived from Wang,1993 Analytical method in non-slip condition, the lowest action is derived from uncoupled approach full-slip condition. Analytic and simplified numerical method, which assume homogeneous formation and linear shear displacement, lead to high internal forces. On the other hand, the uncoupled and coupled approach offer more realistic and accurate solutions because they consider each layer and perform calculations at bedrock depth using earthquake records.

Comparing the coupled and uncoupled approaches, the intrinsic forces obtained do not differ significantly. In the comparison under non-slip condition, the moment value is 20kNm/m higher in the uncoupled approach, while the normal force is 90kN/m higher in the coupled approach. this difference can be ignored when compared with simplified methods. Both approaches can be used for advanced engineering solutions.

Since coupled and uncoupled approaches are site-specific analyses, it is not logical to establish a general relationship between the approaches. However, tunnel projects run along a long line. Site-specific seismic analyses and dynamic analyses are time-consuming calculations. In this case, it would be appropriate to make a project-based correlation by performing sensitivity analyses as done in this thesis within the scope of the project to save time

Chapter 6

6 Conclusions

This thesis focused on the study of various aspects concerning the analysis of a tunnel in a seismic zone. Some literature examples have in fact highlighted how seismic events cause significant damage not only in elevated structures, but also in underground structures, even though they behave differently when subjected to dynamic loading.

By initially highlighting the main causes and aspects of damage to the structural parts of these types of structures, the paper aimed to expose different dynamic design methods, both analytical and numerical, trying to grasp the differences and highlight the most relevant aspects.

In particular, the design methodologies were applied to a case study concerning a metro tunnel built in the municipality of Catania, in the province of Sicilia, starting from the design considerations made previously by the technicians of the SYSTRA SWS design company, where this thesis was carried out. This design was adopted new design code.

The dynamic analysis of a tunnel, in fact, is nothing more than the final step in a design process that includes various phases, such as those of investigation, diagnosis and treatment, which make it possible to have both a general picture of the context within which the work will be built, but also the information necessary for the design of the structural interventions to be carried out in order to guarantee its stability.

Aim of this thesis is to clearly explain required input data for seismic analysis, to create methodology to follow step by step for fresh engineer, to update classical approaches according to new codes, to show and explain advanced solution for heterogenous – multilayer formations as a different classical method, and to give suggestion about approaches.

First, in the project to be carried out in a seismically active region, they should also carry out research for seismic design to obtain the dynamic parameters to be used in seismic design at the site investigation phase. Vs and G are the main parameters for seismic analysis. Therefore, depending on the depth of the tunnel, the appropriate geophysical method should be selected, and accurate measurements should be taken throughout the depth. In addition, resonant constant test and cyclic

torsional tests should be added to the laboratory test list to obtain decay curve. Bedrock depth should be determined especially for site specific seismic analyses.

Secondly, the use of the PHSA method to determine the design earthquake is an issue that the new regulations particularly emphasize. There are many databases depending on the national codes. Applications involving databases in accordance with the Italian codes have been defined and described step by step. The average earthquake magnitude and distance from the center, PGA, design target spectrum and natural accelerogram of the earthquake are determined. Applications made in this way are important in terms of standardization of designs. Especially for those who do not have in-depth knowledge of earthquake engineering, it prevents making a big mistake.

Thirdly, the determination of the free-field shear deformation is the most critical point of the calculation. In particular, the analytical method, the simplified method and the uncoupled approach are directly related to this. For Simplified free field shear deformation for shallow tunnels an update of the method in the literature has been introduced and it is suggested that the mobilized shear deformation modulus be considered in the calculations using the reduction coefficient recommended by EC8-2022. The results of 2 simplified methods and SSR analysis were compared. It is concluded that the amount of shear deformation resulting from SSR analysis is a more appropriate solution.

Using this information, it was then possible to create a numerical model was subjected to the various dynamic analyses considered. In particular, the differences between the simplified analyses, sometimes even analytical, and the somewhat more complex analyses, by means of numerical finite element modelling conducted, in this context, using the Plaxis 2D software, were examined.

In the last part of the thesis, the results obtained were analyzed and commented on, highlighting the differences between the various approaches, due to various factors, such as: type of analysis and relative complexity, and the presence of a possible stratigraphic cases. Taking all these cases into account, it was possible to compare the results, obtained from the different models, in terms of stresses and displacements, trying to identify the best solution for each circumstance.

While Coupled approach (Fully dynamic analysis) and Uncoupled approach (SSR + Pseudo static analysis) approach tend to estimate the dynamic effect of the earthquakes. Simplified numerical model and analytical approaches tend to overestimate the dynamic effect of the earthquake due to consider homogeneous geology and consider PGA and amplification factor.

The studies carried out could be continued to investigate three further aspects:

- Evaluate the effect of seismic stress in the longitudinal direction of the tunnel which can alter

the behavior of dynamic waves.

- There is lack of the literature to evaluate twin tunnel at the different level, tunnel-shaft connection, or reduction tunnels for applying simplified earthquake methods. It causes overdesign.
- A 3D numerical analysis can be carried out to analyze the changes in the geological formation along the route and to determine the exact influence of the thickness and location of the lava on the seismic behavior.

Bibliography

Abate, G., Grasso, S., & Massimino, M. R. (2023a). Effect of soil heterogeneity on seismic tunnel lining forces. *Soil Dynamics and Earthquake Engineering*, *168*. https://doi.org/10.1016/j.soildyn.2023.107849

Abate, G., Grasso, S., & Massimino, M. R. (2023b). Effect of soil heterogeneity on seismic tunnel lining forces. *Soil Dynamics and Earthquake Engineering*, *168*. https://doi.org/10.1016/j.soildyn.2023.107849

Abate, G., & Massimino, M. R. (2017). Numerical modelling of the seismic response of a tunnel–soil–aboveground building system in Catania (Italy). *Bulletin of Earthquake Engineering*, *15*(1), 469–491. https://doi.org/10.1007/s10518-016-9973-9

Bilotta, E., Lanzano, G., Madabhushi, S. P. G., & Silvestri, F. (2014). A numerical Round Robin on tunnels under seismic actions. *Acta Geotechnica*, *9*(4), 563–579. https://doi.org/10.1007/s11440-014-0330-3

Bilotta, E., Lanzano, G., Russo, G., Magistris, F. S. De, Aiello, V., Conte, E., Silvestri, F., & Valentino, M. (2007). Pseudostatic and Dynamic analyses of Tunnels in Transversal and Longitudinal Directions. *Proceedings of the 4th International Conference on Earthquake Geotechnical Engineering*, *1550*.

Bilotta, E., Lanzano, G., Russo, G., Santucci De Magistris, F., & Silvestri, F. (n.d.). *Methods for the seismic analysis of transverse section of circular tunnels in soft ground Méthodes pour l'analyse séismique de la section transversale des tunnels circulaires en terre*.

Cavallaro, A., Grasso, S., Cavallaro, A., & Maugeri, M. (n.d.). *Site Characterization at the Catania City, Italy*. https://www.researchgate.net/publication/258224847

Cavallaro, A., The results of 2 simplified methods and SSR analysis were compared. It is concluded that the amount of shear deformation resulting from SSR analysis is a more appropriate solution.& Maugeri, M. (2005). Non-linear behaviour of sandy soil for the city of Catania. *WIT Transactions on State-of-the-Art in Science and Engineering*, *8*.

Cavallaro, A., Maugeri, M., Lo Presti, D. C. F., & Pallara, O. (1999). Characterising shear modulus and damping from in situ and laboratory tests for the seismic area of Catania. *Pre-Failure Deformation Characteristics of Geomaterials*.

Cosentini, R. (2 C.E.). *Comportamento dinamico dei terreni Prove di laboratorio*.

Dean, A., Young, D. J., & Kramer, G. J. E. (2006). The use and performance of precast concrete tunnel linings in seismic areas. In *Proceedings of the IAEG 2006* (Issue 679).

Do, N. A., Dias, D., & Oreste, P. (2014). 2D seismic numerical analysis of segmental tunnel lining behaviour. *Bulletin of the New Zealand Society for Earthquake Engineering*, *47*(3). https://doi.org/10.5459/bnzsee.47.3.206-216

Dowding, C. H., & Rozan, A. (1978). Damage to rock tunnels from earthquake shaking. *Journal of the Geotechnical Engineering Division*, *104*(2), 175–191.

Eng. Marco Zucca. (n.d.). *Seismic analysis of Underground works and practice: The case of MetroLima*.

Eurocode8. (2022). *CEN/TC 250*.

Fabozzi, S., & Bilotta, E. (2016). Behaviour of a Segmental Tunnel Lining under Seismic Actions. *Procedia Engineering*, *158*. https://doi.org/10.1016/j.proeng.2016.08.434

Fabozzi, S., Bilotta, E., & Zollo, A. (2017). *Structural, geotechnical and seismic engineering Behaviour of segmental tunnel lining under static and dynamic loads*.

Foti, S., Aversa, S., Orazi, M., Silvestri, F., Lanzo, G., Rossi, C., & Pulelli, G. (2010). *La caratterizzazione geotecnica per la progettazione in zona sismica*.

Gokceoglu, C. (2023). Doğu Anadolu Fayının Yarattığı Son Büyük Depremler ve Tüneller Üzerindeki Etkisi. *Uluslararası Tünelcilik Sempozyumu*. https://doi.org/DOI:10.13140/RG.2.2.15008.15367

Grasso, S., Laurenzano, G., Maugeri, M., & Priolo, E. (2005). Seismic response in Catania by different methodologies. *Advances in Earthquake Engineering*, *14*, 63–79. https://doi.org/10.2495/1-84564-004-7/04

Hashash, Y. M. A., Hook, J. J., Schmidt, B., & I-Chiang Yao, J. (2001). Seismic design and analysis of underground structures. *Tunnelling and Underground Space Technology*, *16*(4). https://doi.org/10.1016/S0886-7798(01)00051-7

Hung, J., Monsess, J., Munfah, N., & Wisniewski, J. (2009). *FHWA Technical Manual for Design and Construction of Road Tunnel - Civil Elements*.

Iwasaki, T., Tatsuoka, F., & Takagi, Y. (1978). Shear moduli of sands under cyclic torsional shear loading. *Soils and Foundations*, *18*(1), 39–56.

Lai, C. G., Foti, S., Godio, A., Rix, G. J., Sambuelli, L., & Socco, L. V. (2000). Caratterizzazione geotecnica dei terreni mediante l'uso di tecniche geofisiche. *Rivista Italiana Di Geotecnica*, *34*(3), 99–118.

Lysmer, J., & Kuhlemeyer, R. L. (1969). Finite dynamic model for infinite media. *Journal of the Engineering Mechanics Division*, *95*(4), 859–877.

Muir Wood, A. M. (1975). The Circular Tunnel in Elastic Ground. *Geotechnique*, *25*(1). https://doi.org/10.1680/geot.1975.25.1.115

Newmark, N. M. (1968). Problem in wave propagation in soil and rock. *Proceedings of Int. Symp. Wave Propagation and Dynamic Properties of Earth Materials*, 7–26.

NTC. (2018). *GAZZETTA UFFICIALE DELLA REPUBBLICA ITALIANA DIREZIONE E REDAZIONE PRESSO IL MINISTERO DELLA GIUSTIZIA-UFFICIO PUBBLICAZIONE LEGGI E DECRETI-VIA ARENULA, 70-00186 ROMA AMMINISTRAZIONE PRESSO L'ISTITUTO POLIGRAFICO E ZECCA DELLO STATO-VIA SALARIA, 691-00138 ROMA-CENTRALINO 06-85081-LIBRERIA DELLO STATO Aggiornamento delle «Norme tecniche per le costruzioni»* (Vol. 20).

Owen, G. N. , S. R. E. (1981). *Earthquake engineering of large underground structures. Report no. FHWARD-80195. Federal Highway Administration and National Science Foundation*.

Penzien, J. (2000). *Seismically induced racking of tunnel linings*.

Penzien, J., & Wu, C. L. (1998). STRESSES IN LININGS OF BORED TUNNELS. In *EARTHQUAKE ENGINEERING AND STRUCTURAL DYNAMICS* (Vol. 27).

Power, M. S., Rosidi, D., & Kaneshiro, J. Y. (1998). Seismic vulnerability of tunnels and underground structures revisited. *North American Tunneling'98American Underground Construction Association*.

Priolo, E. (1999). 2-D spectral element simulations of destructive ground shaking in Catania (Italy). *Journal of Seismology*, *3*(3), 289–309. https://doi.org/10.1023/A:1009838325266

Rashiddel, A., Abedi, M., Dias, D., & Ramesh, A. (2024). Seismic analysis of segmental shallow tunnels adjacent to building foundations under soil liquefaction and its mitigation. *Soil Dynamics and Earthquake Engineering*, *178*. https://doi.org/10.1016/j.soildyn.2024.108479

Schnabel, P. B., Lysmer, J., & Bolton Seed, H. (1972). *A COMPUTER PROGRAM FOR EARTHQUAKE RESPONSE ANALYSIS OF HORIZONTALLY LAYERED SITES*.

Tsinidis, G., de Silva, F., Anastasopoulos, I., Bilotta, E., Bobet, A., Hashash, Y. M. A., He, C., Kampas, G., Knappett, J., Madabhushi, G., Nikitas, N., Pitilakis, K., Silvestri, F., Viggiani, G., & Fuentes, R. (2020). Seismic behaviour of tunnels: From experiments to analysis. *Tunnelling and Underground Space Technology*, *99*. https://doi.org/10.1016/j.tust.2020.103334

Wang, J. (1993). *Seismic Design of Tunnels A Simple State-of-the-Art Design Approach*.

Wang, J. H., Tanaka, H., Nakano, M., Sugiyama, H., Koizumi, A., & Chen, F. (n.d.). *INTERNATIONAL SOCIETY FOR SOIL MECHANICS AND GEOTECHNICAL ENGINEERING Transverse Seismic Analysis of Shield Tunnel Lining in Multi-Layered Soft Ground Using Different Methods*. https://www.issmge.org/publications/online-library

Yokota, K., Imai, T., & Konno, M. (1981). Dynamic deformation characteristics of soils determined by laboratory tests. *OYO Tec. Rep*, *3*, 13–37.